KRUPPEL-LIKE FACTOR 9 INHIBITS GLIOBLASTOMA STEMNESS THROUGH GLOBAL TRANSCRIPTION REPRESSION AND INHIBITION OF INTEGRIN ALPHA 6 AND CD151

By

Jessica Tilghman

A dissertation submitted to Johns Hopkins University in conformity with the requirements for the degree of Doctor of Philosophy

Baltimore, Maryland
October, 2015

Abstract

Glioblastoma (GBM) stem cells (GSCs) represent tumor-propagating cells with stem-like characteristics (stemness) that contribute disproportionately to GBM drug resistance and tumor recurrence. Understanding the mechanisms supporting GSC stemness is important for developing novel strategies that target tumor propagation to inhibit cancer progression and improve patient survival. Krüppel-like factor 9 (KLF9) has emerged as a regulator of cell differentiation, neural development, and oncogenesis; however, the molecular basis for KLF9's diverse contextual functions has been unclear. We establish for the first time a genome-wide map of KLF9-regulated targets in human glioblastoma stem-like cells, and show that KLF9 functions as a transcriptional repressor and thereby regulates multiple signaling pathways involved in oncogenesis and regulation of cancer stem-like phenotype. A detailed analysis of two novel KLF9 targets suggests that KLF9 inhibits glioma cell stemness by repressing expression of integrin α6 and CD151.

The expression of one candidate KLF9 target gene *ITGA6* coding for integrin α6 was verified to be downregulated by KLF9 in GSCs. ITGA6 transcription repression by KLF9 altered GBM neurosphere cell behavior as evidenced by reduced cell adhesion to and migration through membrane coated with the integrin α6 ligand laminin. Forced expression of integrin α6 partially rescued GBM neurosphere cells from the differentiating and adhesion/migration-inhibiting effects of KLF9.

Using GBM derived neurospheres, we identified cell surface tetraspanin family member CD151 as a novel regulator of GSC stemness and tumorigenicity. CD151 was found to be

overexpressed in GBM tumors and GBM neurospheres enriched in GSCs. Silencing CD151 inhibited neurosphere self-renewal and cell proliferation and attenuated expression of stem cell markers and drivers. Conversely, forced CD151 expression promoted neurosphere self-renewal, cell migration and expression of stemness-associated transcription factors. Additionally, targeting CD151 inhibited glioma angiogenesis and growth of GBM neurosphere derived xenografts. CD151 was found to form complexes with integrins α3, α6 and β1 in neurosphere cells and blocking the CD151-intgerin α3/α6 interaction impaired sphere formation, migration and phosphorylation of AKT, a marker of integrin signaling. These findings identify CD151 and its interactions with integrins α3 and α6 as potential therapeutic targets for depleting stem cell populations and stemness-driving mechanisms in GBM.

Thesis Advisor: Dr. John Laterra

Thesis Readers: Dr. John Laterra

Dr. Angelika Doetzlhofer

Acknowledgements

I would like to acknowledge my thesis advisor Johns Laterra for his support and direction with this project. I thank my colleagues in the laboratory; it was a pleasure to work alongside you during my thesis research. Gratitude goes to Mingyao Ying who was involved in many facets of this project and who assisted with the design and execution of some of these experiments. I would also like to thank Paula Schiapparelli for conducting some of the migration experiments, and Hongkai Ji and Yingying Wei for conducting the bioinformatics analyses.

I would like to acknowledge the following people who contributed to the project in one way or another: Han Sun, Shuli Xia, Yunqing Li, Hernando Lopez-Bertoni and Bachuchu Lal, Kathryn Wagner, Adam Moyer, Mary Blue, Mary Ann Wilson, Joseph Bressler, John Coulter, Paul Watkins, and Johnathan Pevsner.

Thanks to the faculty, staff and students in the Neuroscience Department, the Neuroscience graduate program and the faculty and staff at the Kennedy Krieger Research Institute. I would also like to express thanks to the Molecular Neuroscience Research.

I acknowledge the advice from the faculty who served on my thesis committee: Angelika Doetzlhofer, Alfredo Quinones-Hinojosa, Charles Eberhart and John Laterra. Thanks in particular to John Laterra and Angelika Doetzlhofer for comments on the thesis.

This project was supported by predoctoral awards from the National Science Foundation and Ford Foundation Fellowship. Portions of this work have been published previously and reprinted with permission from the Journal of Biological Chemistry. Other parts are being prepared for publication.

Table of Contents

Table of Figures

Chapter 1: Introduction

1.1 Glioblastoma Multiforme

Approximately 70% of malignant primary brain tumors are gliomas. The most common glioma is glioblastoma multiforme (GBM), which makes up 50-70% of malignant brain tumors. GBM, or glioblastoma, is a grade IV astrocytoma and is the most aggressive primary brain tumor (Alifieris & Trafalis, 2015). There are two clinical GBM subtypes: primary and secondary (Ahmed, Oborski, Hwang, Lieberman, & Mountz, 2014). A majority (95%) of GBMs are primary tumors, which arise *de novo*, within 3-6 months. These tumors are highly aggressive, invasive, and typically occur in older patients. Secondary GBMs are less common and evolve from the progression of lower-grade astrocytomas (over 10-15 years). These typically occur in patients less than 45 years old (Crespo et al., 2015). GBMs can be further divided into four molecular subtypes: classical, mesenchymal, proneural and neural. These subtypes are distinguished by different mutation and transcriptional patterns and can also differ in patient survival, patient age and sensitivity to treatment (Verhaak et al., 2010).

Each year, 2-3 cases of GBM per 100,000 adults and 1.1 to 3.3 cases per 100,000 children are reported in the United States and Europe. Males are more likely to develop the disease, with the incidence being 3 times higher in male children than female children (Urbanska, Sokolowska, Szmidt, & Sysa, 2014). Patients with GBM may experience headaches, vomiting, blurred vision, neurological deficits, memory loss, variations in personality or seizures (Alifieris & Trafalis, 2015). The current standard of treatment for newly diagnosed patients under 70 years of age is surgical resection followed by

radiotherapy and chemotherapy. Despite this aggressive treatment, recurrence is often seen. Patients with GBMs typically have a median survival time of only 12-15 months following treatment (Alifieris & Trafalis, 2015; Dolecek, Propp, Stroup, & Kruchko, 2012; McGirt et al., 2009).

GBMs are typically located in the cerebral hemispheres, the brain stem or the cerebellum (Figure 1.1). They are composed of a heterogeneous, anaplastic population of small abnormal shaped cells, that also display a high nuclear to cytoplasmic ratio (Urbanska et al., 2014). GBMs also display some degree of necrosis. Primary tumors typically have a large area of necrosis in the center of the tumor due to insufficient blood supply. Smaller irregularly shaped necrotic foci surrounded by hypercellular zones called pseudopalisades are found in both primary and secondary tumors. Additionally, GBM is one of the most highly vascularized tumors. The tumor vessels are highly permeable with abnormal endothelial walls and discontinuous pericyte coverage(Soda, Myskiw, Rommel, & Verma, 2013).

Activation of several signaling pathways is altered in GBM resulting in the support of brain tumor growth and progression. The three most prominent signaling pathways that are altered include growth factor tyrosine kinase receptor/Ras/phosphatidylinositol 3-kinase (PI3K)/ phosphatase and tensin homolog (PTEN)/Akt pathways (Alentorn et al., 2012; Dasari et al., 2010; Fan et al., 2002; P. H. Huang, Xu, & White, 2009; Koul, 2008; Patil et al., 2013; Rajasekhar et al., 2003), the P53 (Zawlik, Kita, et al., 2009) pathway and the RB tumor suppressor pathways (Cancer Genome Atlas Research, 2008) (Figure 1.2). In addition to genetic changes, epigenetic changes have also been associated with GBM. These include MGMT promoter

methylation (Zawlik, Vaccarella, et al., 2009), hypermethylation of CpG islands , and gene-specific and genome wide hypomethylation (Crespo et al., 2015).

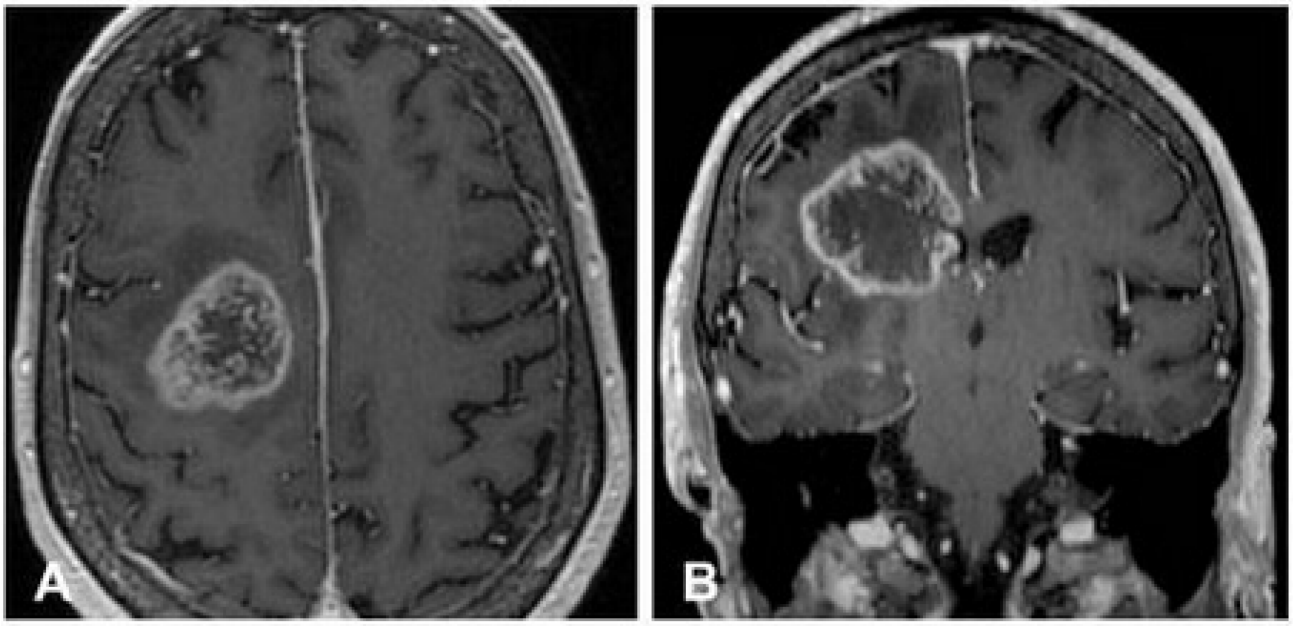

Figure 1.1 Preoperative (A) axial and (B) coronal post-contrast MR images of a 78-year-old female patient with a glioblastoma (Mabray, Barajas, & Cha, 2015).

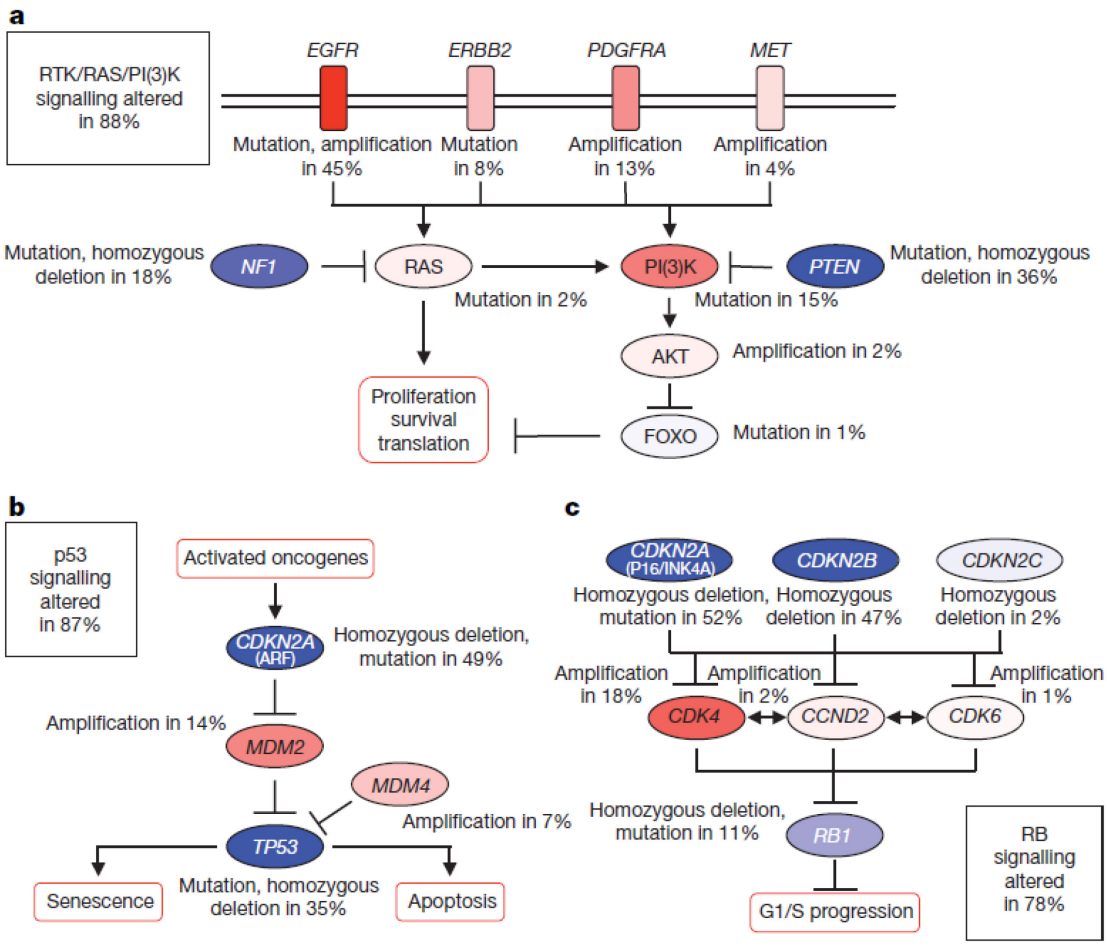

Figure 1.2 Frequent genetic alterations in three major signaling pathways in GBM. **(A-C)** Alterations for components of the **(A)** RTK/RAS/PI(3)K, **(B)** p53 and **(C)** RB signaling pathways are shown. Red indicates activating genetic alterations, with frequently altered genes shown in dark red. Blue indicates inactivating alterations, with genes with a higher percentage of alteration shown in dark blue. For each altered component of a particular pathway, the type of the alteration and the percentage of tumors affected are indicated. The boxes show the total percentages of glioblastomas with alterations in at least one known component gene of the pathway (Cancer Genome Atlas Research, 2008).

1.2 Cancer Stem Cells

Tumors consist of heterogeneous cells. There are two theories as to how this heterogeneity arises: the stochastic model and the cancer stem cell model (Figure 1.3). The stochastic model predicts that all cancer cells have the potential to form tumors, and the variability in their tumorigenicity is determined by stochastic intrinsic factors. The cancer stem cell model predicts that there is a minority population of cancer cells capable of propagating tumors. These cells give rise to the bulk of the tumor cells, which have limited tumorigenic potential and display a more differentiated phenotype (Nguyen, Vanner, Dirks, & Eaves, 2012).

Progression of several tumor types, including GBMs, is thought to be driven by cancer stem cells (CSCs). These highly tumorigenic cells display stem cell properties (i.e. stemness), including the ability to self-renew as spheres and the capacity to differentiate into the multiple lineages that make up the tumor population (Ajani, Song, Hochster, & Steinberg, 2015; Lobo, Shimono, Qian, & Clarke, 2007). Most importantly, CSCs efficiently propagate tumor xenografts that recapitulate the biological and histopathological characteristics of its original tumor when implanted orthotopically (Visvader & Lindeman, 2008). These cells use microenvironment-dependent and independent mechanisms to promote tumor angiogenesis, recurrence and resistance to cytotoxic therapies (Bao et al., 2006; L. Hu, McArthur, & Jaffe, 2010; Phillips, McBride, & Pajonk, 2006; Sarvi et al., 2014; Warrier, Pavanram, Raina, & Arvind, 2012; L. Zhang et al., 2012) and have a higher tendency to metastasize (Nakamura, Iinuma, Aoyagi, Shibuya, & Watanabe, 2010).

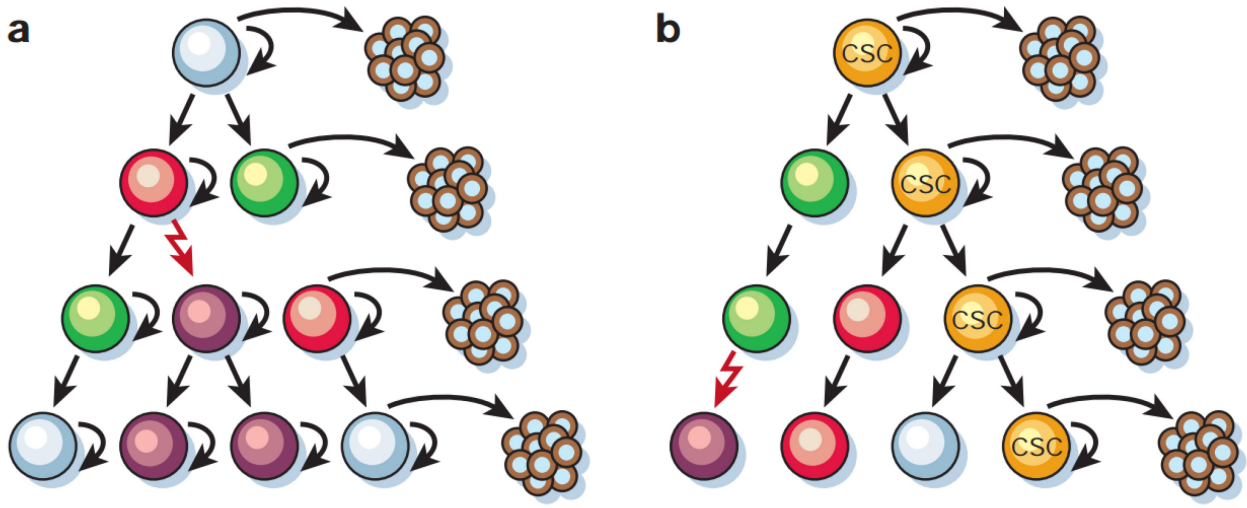

Figure 1.3. Models of cancer cell heterogeneity. (A) In the stochastic model, tumor cells have varying tumorigenic potential, which depends on stochastic intrinsic factors. **(B)** In the cancer stem cell model, only a subset of cancer cells (cancer stem cells) has the potential to give rise to other cancer stem cells and to cells with a more limited proliferative capacity (Reya, Morrison, Clarke & Weissman, 2001).

.

The History of Cancer Stem Cells

The idea of stem cells contributing to cancer development was initially formulated in 1907 by Max Askanazy. He developed the "embryonic rest hypothesis of cancer development" which postulates that cancers arise from embryo-like cells. The first evidence of stem cells arose in 1961 when Ernest McCulloch found that a subset of hematopoietic cells could give rise to colonies of cells following irradiation (Till & Mc, 1961). Evidence of CSCs was revealed soon after in a study by Bruce and Van Der Gaag (1963) that found that a subset of mouse lymphoma cells are able to form colonies in the spleen of mice. In 1971, Pierce and Wallace provided evidence of a cellular hierarchy in tumors that showed that only the undifferentiated cells give rise to the differentiated tumor cells in squamous cell carcinomas suggesting that tumor growth is dependent on undifferentiated cell proliferation. Hamburger and Salmon (1977) also found that only a minority of epithelial tumor cells could form colonies in vitro.

However, the first compelling evidence of cancer stem cells was provided in a study by Bonnet and Dick (1997) that identified and characterized a subset of cells capable of initiating human acute myeloid leukemia in mice with severe combined immunodeficiency (SCID). Since then, cancer stem cells have been discovered in several different cancers including breast, brain, colon, lung and liver (Al-Hajj, Wicha, Benito-Hernandez, Morrison, & Clarke, 2003; Ignatova et al., 2002; O'Brien, Pollett, Gallinger, & Dick, 2007).

The Cancer Stem Cell Niche

Both normal cells and cancer stem cells rely on a dynamic microenvironment detaining neighboring cells, proteins and other factors to support and maintain their

population. In the CSC niche, CSCs are anchored to the microenvironment through interactions between the extracellular matrix (ECM) and adhesion proteins on the cell surface. This interaction brings the CSCs in close proximity to factors released by the ECM that maintain the stem cell phenotype (Lu, Weaver, & Werb, 2012). The ECM also supports the CSC population by serving as a physical barrier for chemotherapeutics and migrating immune cells (Wong & Rustgi, 2013). Additionally, the mechanical properties of the ECM can influence stem cell characteristics and behavior. For example, a stiff ECM enhances hepatocellular carcinoma cell (HCC) proliferation by stimulating hepatocyte growth factor-dependent mitogenic signals through activation of extracellular signal-regulated kinase, protein kinase B (PKB/Akt), and signal transducer and activator of transcription 3 (Schrader et al., 2011).

In addition to the ECM, a variety of cells are recruited to the CSC microenvironment to sustain the stem cell population. One such cell, the mesenchymal stem cell (MSC), homes to the stem cell niche and releases cytokines that support CSC functions in several cancers including breast cancer and ovarian carcinoma. MSCs also promote tumorigenesis by supporting cell proliferation, metastasis and angiogenesis (Cuiffo & Karnoub, 2012). Endothelial cells also secrete factors that support stem cell self-renewal, proliferation and survival (Krishnamurthy et al., 2010; Xu, Wu, & Zhu, 2013). Tumor-associated macrophages (TAM) in the stem cell niche promote chemoresistance and metastasis in tumor cells, and may also promote angiogenesis and invasion (Solinas et al., 2010).

The tumor microenvironment also produces several cytokines and factors that promote CSC self-renewal, stimulate angiogenesis and recruit cells that support CSC

maintenance and tumor progression. For example, exogenous vascular endothelial growth factor (VEGF) stimulates glioblastoma stem cell (GSC) proliferation by activating VEGF receptor (VEGFR) 2 (Xu et al., 2013). Transforming growth factor β (TGF-β) induces epithelial–mesenchymal transition (EMT), a process that has been shown to enhance stemness characteristics and tumorigenicity in cancer cells, and tumor invasion and metastasis (Smith, Robin, & Ford, 2012; Ye et al., 2012).

There is increasing evidence that CSCs are supported by hypoxic tumor microenvironments as well. Hypoxia increases expression of hypoxia-induced factors (HIFs), which regulate several genes that regulate adaptation to low oxygen (J. W. Kim, Tchernyshyov, Semenza, & Dang, 2006). Additionally, HIFs have been shown to support GSC self-renewal, proliferation and survival (Z. Li et al., 2009). HIFs also support tumor angiogenesis and progression and enhance EMT phenotype (Gammon, Biddle, Heywood, Johannessen, & Mackenzie, 2013).

Cancer Stem Cell Markers and Regulators

While there is no one protein that is exclusively expressed in all CSCs, there are proteins that are highly expressed in CSCs, and isolation using these markers can enrich for CSCs. One of the most widely used cell surface markers for CSCs is CD133. It is present in several cancers including breast, prostate, pancreas, lung and glioblastoma (Grosse-Gehling et al., 2013). Other potential markers are drivers of cell stemness. OCT4, NANOG and SOX2 are three transcription factors involved in reprogramming somatic cells into induced pluripotent stem cells. In embryonic stem cells (ESCs), these transcription factors maintain stem cell self-renewal and pluripotency while also inhibiting differentiation (A. Liu, Yu, & Liu, 2013). These transcription factors are

upregulated in many cancers, particularly in poorly differentiated tumors, and have been shown to contribute to CSC regulation (Ben-Porath et al., 2008; Chiou et al., 2008). For example, NANOG promotes tumor formation and clonogenic capacity in prostate and colorectal CSCs and increases chemoresistance in breast cancer cell lines (Ibrahim et al., 2012; Jeter et al., 2011; J. Zhang et al., 2013). OCT4 increases tumorsphere formation, stem cell marker expression and tumorigenicity in mouse breast cancer cells (R. J. Kim & Nam, 2011). SOX2 was identified as a CSC marker in skin squamous cell carcinoma and medulloblastoma (Becher & Holland, 2014) and regulates self-renewal, chemoresistance and tumorigenicity in head and neck squamous cell carcinoma and melanoma-initiating cells (S. H. Lee et al., 2014; Santini et al., 2014).

Because CSCs and normal stem cells share phenotypic properties, it is not unexpected that they also share signaling pathways that maintain their stemness and regulate their tumor propagating capacity. These include the Notch (Lagadec et al., 2013; Suman, Das, & Damodaran, 2013), Wnt/β catenin (Clevers, Loh, & Nusse, 2014; Lobo et al., 2007), JAK/STAT (Bourguignon, Earle, Wong, Spevak, & Krueger, 2012; Kroon et al., 2013; L. Lin et al., 2011; Torres & Watt, 2008) and Sonic Hedgehog (SHH) pathways (Clement, Sanchez, de Tribolet, Radovanovic, & Ruiz i Altaba, 2007; F. T. Huang et al., 2012; Sims-Mourtada et al., 2006).

Culturing and Isolating Cancer Stem Cells

CSCs are grown in specialized cell culture conditions without serum and in the presence of growth factors. Traditionally, cancer stem cells, specifically GSCs, were grown as adherent cultures in the presence of serum. However, unlike in GBM patients, these cells were not invasive in xenograft models. These cells also expressed a high level

of differentiation markers. In 1992, Reynolds and Weiss discovered that neural stem cells (NSCs) could be expanded as free-floating neurospheres in specialized, serum-free culture medium containing specific growth factors. Soon after, it was discovered that cell isolates from GBMs also form spheres consisting of stem and non-stem cells in similar medium conditions Ignatova et al. (2002).

Glioblastoma Stem Cells

Glioblastoma stem cells (GSCs), or GBM-propagating cells, were first identified by Ignatova et al. (2002) in a study that found that glial tumor cells could form colonies in anchorage and serum free conditions in the presence of growth factors. Similar to neural stem cells (NSCs), GSCs form neurospheres and have the ability to self-renew as spheres. Unlike NSCs, GSCs have several genetic alterations, are chemoresistant and radioresistant and can recapitulate the original tumor in in vivo xenografts (Goffart, Kroonen, & Rogister, 2013). Although a universal marker for GSCs has not been identified, CD133 is most commonly used. Several other candidates have been identified including A2B5, CD44, L1CAM, SSEA1, integrin α6, Musashi, Nestin, Nanog, Oct4 and Sox2 (Sundar, Hsieh, Manjila, Lathia, & Sloan, 2014).

The origin of GSCs is still relatively unknown. There are two hypotheses that are currently supported: the dedifferentiation hypothesis and the stem cell hypothesis. The dedifferentiation hypothesis proposes that mature astrocytes accumulate genetic alterations over time that promote anchorage independent growth, resistance to antigrowth signals and apoptosis and self-renewal, resulting in malignant transformation of these cells(Bachoo et al., 2002; Uhrbom et al., 2002).

The stem cell theory proposes that GSCs arise from NSCs and progenitor cells in the subventricular zone stem cell niche and other germinal zones in the brain (Goffart et al., 2013; Lee da, Gianino, & Gutmann, 2012). These cells have been shown to accumulate mutations leading to tumor formation (Y. Wang et al., 2009). NSCs are also preferentially targeted by human cytomegalovirus, a brain tumor promoter (Price et al., 2013). There is also evidence to suggest that oligodendrocyte progenitor cells (OPCs) could potentially give rise to malignant gliomas (Goffart et al., 2013; Lindberg, Kastemar, Olofsson, Smits, & Uhrbom, 2009).

GSCs primarily reside in the brain tumor perivascular niche (PVN), located along the border of the tumor vasculature. The PVN is made up of several tumor and non-tumor cells including pericytes, macrophages, astrocytes and endothelial cells. Pericytes support the integrity of the tumor vascular and may contribute to microvascular proliferation in the tumor (Bababeygy et al., 2008; Guo et al., 2003). Macrophages in the brain, or microglia, are recruited to the perivascular niche by GSCs to support tumor growth. These cells localize to the advancing edge, the perivascular niche and perinecrotic regions to promote cell motility, metastasis and angiogenesis, respectively (Lewis & Pollard, 2006). Astrocytes contribute to GSC regulation by secreting factors such as SHH and astrocyte elevated gene-1 to support GSC self-renewal, invasion and survival (Charles & Holland, 2010; Emdad et al., 2010). Endothelial cells provide nutrients, oxygen and diffusible factors, such as eNOS, that regulate stem cell self-renewal and proliferation (Charles & Holland, 2010). GSCs in turn support the perivascular niche by secreting high levels of VEGF which results in highly angiogenic tumors. GSCs also

induce endothelial cell proliferation, migration and tube formation (Charles & Holland, 2010).

Multiple signaling pathways are active and support the PVN, like the SHH signaling pathway. SHH expression localizes to the glioma PVN and correlates with glioma grade (Becher et al., 2008). Inhibition of SHH pathway members Gli1 and SMO has also been shown to reduce glioma cell proliferation, migration and invasion (Clement et al., 2007; K. Wang, Pan, Che, Cui, & Li, 2010). The PI3K/Akt pathway, in addition to contributing to tumor formation and growth, supports GSC drug resistance in the PVN (Hambardzumyan et al., 2008; Holland et al., 2000). Notch signaling in GSCs has also been shown to regulate PVN angiogenesis (Charles & Holland, 2010).

Another GSC niche in GBMs are perinecrotic regions within the tumor with activated HIF1α and HIF2α, the main mediators of the hypoxic response (Seidel et al., 2010). HIF proteins are stabilized in hypoxic conditions and bind to hypoxia responsive elements on promoters of genes involved in cell survival, motility, metabolism and angiogenesis. HIF1α promotes proliferation and survival of all cancer cells while HIF2α enhances transcription in GSCs to promote GSC self-renewal and tumorigenicity (Covello et al., 2006; Heddleston, Li, McLendon, Hjelmeland, & Rich, 2009; Z. Li et al., 2009; Seidel et al., 2010).

1.3 Krüppel-like Factors and KLF9

Krüppel-like Factors

The krüppel-like factors (KLFs) compose a family of transcription factors that bind to GC rich regions of DNA to activate or repress transcription. The first human KLF

was identified by Page et al. in 1987. The first mammalian *klf* gene was cloned soon after in 1993 (I. J. Miller & Bieker). Since then, 16 other mammalian KLFs have been identified and are designated KLF1-KLF17 (Suske, Bruford, & Philipsen, 2005).

KLFs have three highly conserved consecutive Cys_2-His_2 zinc fingers located near the carboxyl terminus of the protein that enables them to interact with GC-rich sequences in target gene promoters and enhancers (Pearson, Fleetwood, Eaton, Crossley, & Bao, 2008). However, they have unique amino-terminal sequences that permit the transcription factors to interact with specific binding partners (McConnell & Yang, 2010) (Figure 1.4). Through transcriptional regulation of a variety of genes, KLFs regulate numerous cellular processes including cell growth, proliferation and apoptosis (McConnell & Yang, 2010).

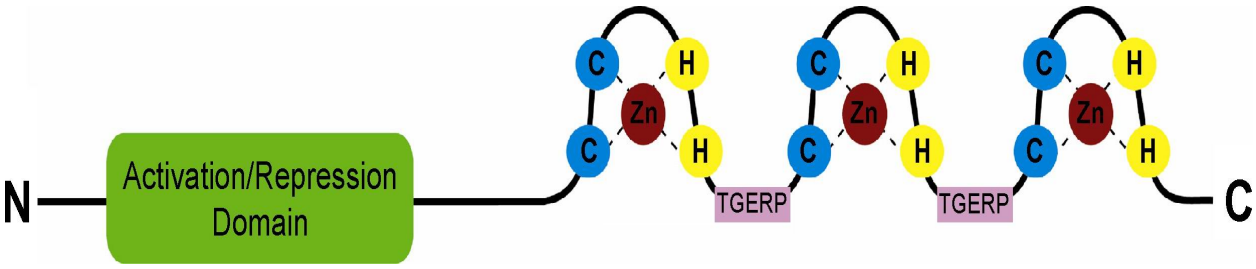

Figure 1.4 Structure of KLFs. KLFs consists of three C-terminal finger domains, each consisting of two cysteine and two histidine residues chelating one zinc ion. The zinc fingers are connected by a "TGERP"-like motif which assist DNA binding. The more variable activation/repression domain is found at the N-terminus of the molecule and determines the activating function of the transcription factor (Pearson, Fleetwood, Eaton, Crossley, & Bao, 2008).

KLFs are also involved in cell differentiation. For example, KLF1 supports erythropoiesis and regulates megakaryocyte-erythroid progenitor differentiation into erythrocytes (Drissen et al., 2005; McConnell & Yang, 2010). Several KLFs (KLFs 2, 3, 4, 5, 6, 7, 11, and 15) are involved in adipogenesis (McConnell & Yang, 2010). There is also evidence of KLF regulation of differentiation of cardiomyocytes, corneal epithelial cells and many other tissues (C. M. Carlson et al., 2006; Kuo et al., 1997; Nemer & Horb, 2007; Swamynathan et al., 2007).

Some KLFs support the self-renewal of stem cells. KLF4 is one of four transcription factors rigourously described by Yamanaka that, when ectopically expressed, reprogram somatic cells to pluripotent stem cells (Takahashi & Yamanaka, 2006; Wernig et al., 2007). Depletion of KLFs 2, 4 and 5 has also been shown to result in embryonic stem cell differentiation (Jiang et al., 2008).

KLFs may function as tumor suppressors and/or oncogenes depending on the cellular context. For example, KLF4 functions as a tumor suppressor by regulating cell cycle promoting genes in colon cancer (Rowland, Bernards, & Peeper, 2005). KLF6 functions as a tumor suppressor that is mutated in prostate and/or suppressed in many other cancers (McConnell & Yang, 2010; Narla et al., 2001). KLF8 expression is increased in many cancers and tissues and aberrant expression induces transformation (X. Wang & Zhao, 2007).

KLFs have also been implicated in CSCs. Most notable is KLF4. Knockdown of KLF4 in breast cancer cell lines reduces the cancer self-renewal capacity and the CSC population (F. Yu et al., 2011). KLF4 is also overexpressed in the CSC subpopulation in

colon cancer, and KLF4 silencing decreases the chemoresistance, invasion and tumorigenicity of these cells (Leng et al., 2013). Knockdown of KLF5 in ovarian CSCs increases the sensitivity of these cells to chemotherapeutics (Z. Dong, Yang, & Lai, 2013).

Krüppel-like Transcription Factor 9

KLF9 was isolated in 1992 from rat cDNA libraries (Imataka et al.). Its cDNA clone consists of 244 amino acids. (Ohe et al., 1993). KLF9's RNA was detected in every organ examined suggesting that it plays a fundamental role in cells. However, it was most abundant in the kidney, lung, brain and testis (Imataka et al., 1992). KLF9 binds to the basic transcription element (BTE) (Yanagida, Sogawa, Yasumoto, & Fujii-Kuriyama, 1990). Although it primarily functions as a transcriptional repressor, KLF9 has been shown to have both activating and repressive regulatory functions on gene transcription. However, this may depend on the number of GC boxes present. For example in monkey cell line CV-1, KLF9 functioned as a transcriptional repressor when BTE, a sequence consisting of a single GC box consensus sequence and part of the NF-1 binding sequence (Yanagida et al., 1990), but served as an activator when tandem repeats of the GC boxes were present (Imataka et al., 1992).

KLF9 regulates a variety of cellular functions, including survival and proliferation (Savignac et al., 2010; X. L. Zhang, Simmen, Michel, & Simmen, 2001; Zucker et al., 2014). However, it is best known for its role in steroid hormone signaling. KLF9 forms a complex with progesterone receptor (PR) B to promote transactivation of progresterone-responsive genes to ligand bound PR (D. Zhang et al., 2002). KLF9 also functions as a

negative regulator of estrogen receptor α signaling (Pabona, Velarde, Zeng, Simmen, & Simmen, 2009; Velarde, Zeng, McQuown, Simmen, & Simmen, 2007).

KLF9 has also been shown to regulate cell differentiation. For instance, KLF9 is upregulated following differentiation of dental follicle cells, preadipocytes and keratinocytes (Kimura & Fujimori, 2014; Morsczeck et al., 2009; Sporl et al., 2012). Mice null for KLF9 have shorter villi, inhibited cell proliferation and an alteration in the lineage determination in the intestines (Simmen et al., 2007).

KLF9 particularly influences differentiation in the central nervous system. KLF9 contributes to late phase maturation of dentate granule neurons, evidenced by the fact that loss of KLF9 inhibited late phase processes. Adult-born neurons in KLF9-null mice have fewer mature neurons and fewer neurons with complex dendritic trees (Scobie et al., 2009). Expression of KLF9 increases in the brain during tadpole metamorphosis and is expressed just outside of proliferative regions of the brain, supporting a role in neural cell differentiation (Hoopfer, Huang, & Denver, 2002). $KLF9^{-/-}$ mice also exhibit deficits in the rotating rod test and contextual freezing response behavioral tests compared to wildtype mice, which suggests deficits in the cerebellum, hippocampus and the amygdala, respectively (Morita et al., 2003).

Several studies point to KLF9 functioning as a tumor suppressor. KLF9 is downregulated in several cancers including colorectal cancer, non-small cell lung cancer, esophageal squamous cell carcinoma (ESSC), hepatocellular carcinoma, prostate cancer, endometrial and breast cancer (Kang, Lu, Xu, Hu, & Lai, 2008; Qiao et al., 2015; Tong, Liu, Wang, Zhang, & Liu, 2015). Forced expression of KLF9 inhibits cell growth, migration and metastasis of ESCC and HCC cells (Fu, Cheng, He, Liu, & Liu, 2014;

Qiao et al., 2015; Sun et al., 2014), delays tumor formation from HCC and prostate cancer cells and promotes regression of tumors established from HCC cells (P. Shen et al., 2014; Sun et al., 2014). However, KLF9 has been shown to promote tumor progression in ovarian cancer (Q. H. Zhang, Dou, Tang, Su, & Liu, 2015).

KLF9 and Glioma Stem Cells

KLF9 expression is downregulated in glioma cell lines and tissues, particularly grade III astrocytoma and GBM, compared to astrocyte cells and normal brain tissue, respectively (S. Huang et al., 2015). We previously showed that KLF9 expression is induced during forced differentiation of GSCs. Knockdown of KLF9 inhibits forced differentiation of GSCs while forced expression of KLF9 inhibits cell proliferation, sphere formation, invasion and tumor formation (Ying et al., 2011). Consistent with what we found, S. Huang et al. (2015) showed that knockdown of KLF9 increased glioma cell proliferation while its forced expression inhibited proliferation and glioma cell tumorigenicity. We found that KLF9 regulates GSC self-renewal in part by binding to the promoter of Notch1 and suppressing Notch signaling (Ying et al., 2011). However, other target genes and the molecular mechanism underlying KLF9's functional contribution to differentiation had yet to be comprehensively identified.

In the present study, we determined global KLF9 gene-binding and transcriptional signatures in human GBM-derived neurospheres using chromatin immunoprecipitation followed by high throughput deep sequencing (ChIP-Seq) and RNA-sequencing. This combined approach revealed a significant role for KLF9 in the regulation of several pathways involved in oncogenesis and stem cell biology, including the integrin signaling pathway. A more in depth analysis of proteins encoded by KLF9 gene targets integrin α6

and CD151 reveal novel mechanisms by which KLF9 regulates glioblastoma cell stemness.

1.4 Integrins and Integrin α6

Integrins

Integrins, a family of cell adhesion receptors, were discovered in multiple species and cell types and given various names in the 1980s (Hemler, Jacobson, & Strominger, 1985; Horwitz, Duggan, Greggs, Decker, & Buck, 1985; Knudsen, Horwitz, & Buck, 1985; Tamkun et al., 1986). It wasn't until the genes of these proteins were sequenced that they were found to be related (Hynes, 2004). Each integrin consists of a heterodimer between an α and β subunit that make up extracellular "headpiece" and "leg" regions, which pass through the membrane once, terminating in typically short cytoplasmic regions (Figure 1.5)(Springer & Dustin, 2012).

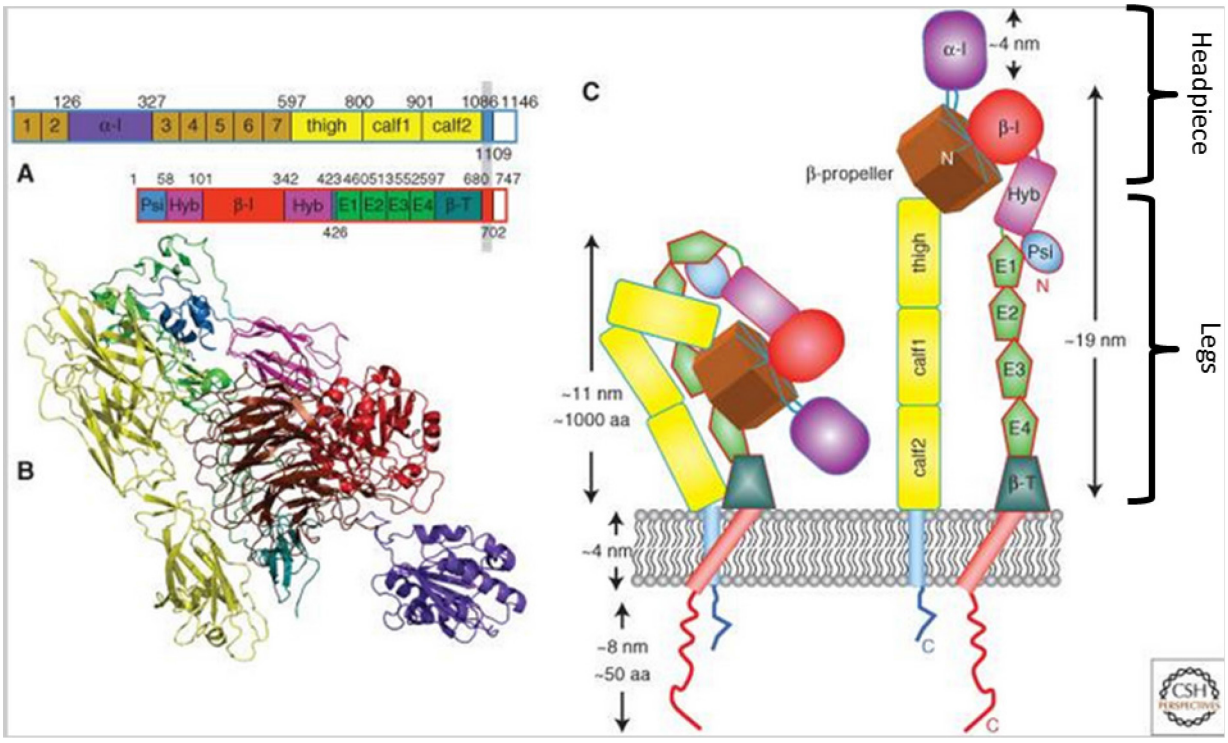

Figure 1.5. Integrin structure. (A) Domain structure and **(B)** bimolecular structure of αxβ2 using the same color coding; **(C)** cartoon representation of bent (inactive) and upright (activated) conformations (Campbell & Humphries, 2011).

Integrins are capable of bi-directional signaling. The main function of inside-out signaling is to promote the active integrin conformation to enhance binding to extracellular ligands. Ligand binding is facilitated by integrin binding proteins, talin and kindlins. These proteins promote integrin activation through strong interactions with the β integrin cytoplasmic tail (P. Hu & Luo, 2013). Exposure to ECM ligands stimulates integrin clustering to strengthen the high affinity integrin conformation. This increases ligand binding and triggers outside in signaling. Integrin clustering leads to the formation of small dynamic adhesions that can dissipate or develop into larger more stable focal adhesions. Both integrin α and β tails recruit focal adhesion kinase (FAK), integrin-linked kinase and Src family kinase, all of which facilitate the recruitment of other proteins to support the focal adhesion. Through this interaction with the ECM, integrins provide cells with information about the extracellular environment through downstream signaling leading to changes in cell behavior including cell shape, migration and survival (P. Hu & Luo, 2013).

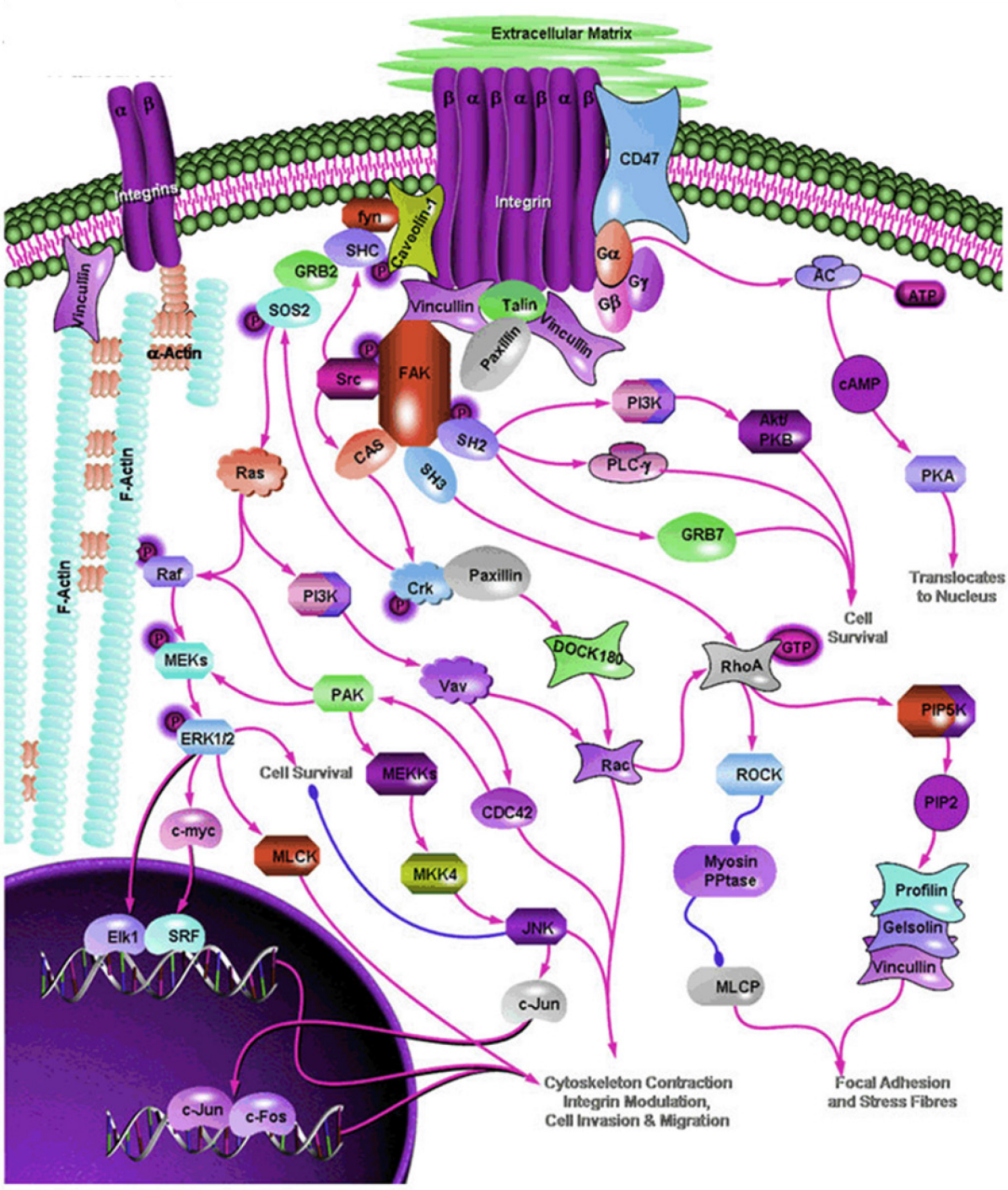

Figure 1.6. Integrin signaling pathway (www.SABiosciences.com).

Integrins are the primary cell surface receptors for adhesion to the ECM and activate intracellular signal transduction to regulate cellular processes such as cytoskeletal rearrangement, cell polarity, motility and gene expression in response to changes in the extracellular environment (Figure 1.6). These receptors have several ligands, including major ECM constituents laminin, fibronectin, and collagen (Johnson, Lu, Denessiouk, Heino, & Gullberg, 2009). In addition to ECM proteins, integrins can also interact with cell surface receptors on adjacent cells through interactions with membrane bound adhesion proteins like vascular or intracellular- cell adhesion molecules (VCAM and ICAM) (Prowse, Chong, Gray, & Munro, 2011).

Integrins detect and convey mechanical forces at the cell-matrix interface to the cell's interior where it is converted into biochemical signals, a process known as mechanotransduction. Integrins then link to the cytoskeleton in order to transmit the force throughout the cell and reinforce cell adhesion to resist the forces. The receptors reinforce cell adhesion by recruiting signaling proteins to form large complexes with the cytoskeleton called focal adhesions (DeMali, Sun, & Bui, 2014).

Mounting evidence is revealing the integrin signaling pathway to be a major player in stem cell regulation. Multiple integrins have been identified as potential stem cell markers, with integrin α6 being most notable (Seguin, Desgrosellier, Weis, & Cheresh, 2015). Integrins are believed to contribute to stem cell self-renewal largely by anchoring the cells to the stem cell niche where the cells can receive short range signals from the microenvironment and other cells to promote self-renewal. Integrins regulate downstream signaling of FAK and PI3K as well as facilitate EGFR, Notch and other signaling pathways involved in self-renewal and proliferation (L. S. Campos, Decker,

Taylor, & Skarnes, 2006). The receptors may also influence the polarity of cells to promote the retention of stem cells in the niche following cell division (Seguin et al., 2015).

Integrins have been implicated in tumor progression as well, the most notable receptors being integrins αvβ3, αvβ5, αvβ6, α5β1, α6β4, and α4β1. These receptors influence tumor maintenance by promoting cancer cell survival through interaction with the ECM (Desgrosellier & Cheresh, 2010). In addition to promoting tumor cell migration and drug resistance, integrins influence tumor progression by regulating host tissue angiogenesis and immune response to cancer (Brooks, Clark, & Cheresh, 1994; Friedlander et al., 1995; Garmy-Susini et al., 2005; Taverna et al., 2004). Many integrins are also upregulated in cancer stem cells and potentiate the CSC phenotype (Luo et al., 2009; Samanna, Wei, Ego-Osuala, & Chellaiah, 2006).

Integrin α6

One integrin of particular interest in CSC regulation is integrin α6. Integrin α6 was identified in the late 1980s in a heterodimer with integrin β1 in platelet lysate (Hemler, Crouse, Takada, & Sonnenberg, 1988). Similar to other integrins, the integrin α6 subunit has a large extracellular domain (991 residues), a short transmembrane domain (23 amino acids) and a short cytoplasmic domain (36 amino acids). Integrin α6 has two splice variants: integrin α6A and α6B (Hogervorst, Kuikman, van Kessel, & Sonnenberg, 1991). The α6A is 18 residues shorter than the α6B variant and is capable of being phosphorylated. However, both can heterodimerize with both integrin α6 binding partners and interact with laminin. Integrin α6 forms complexes with integrin β1 or β4 to regulate cell adhesion to laminin in the basement membrane (Aumailley, Timpl, &

Sonnenberg, 1990; Jones, Kurpakus, Cooper, & Quaranta, 1991; E. C. Lee, Lotz, Steele, & Mercurio, 1992).

Integrin α6 is expressed in almost every tissue in the adult human. It is most highly expressed in the epithelia of various tissues, with the strongest expression in those cells adjacent to the basement membrane. While integrin α6 expression is high in nerve cells of the developing embryo, it is mainly expressed only in the peripheral neurons and weakly in cerebellum neuron cell bodies in the adult suggesting that it may aid in cell migration and axonal growth during development (Terpe, Stark, Ruiz, & Imhof, 1994).

Integrin α6 is overexpressed in numerous cancers including pancreatic, liver, prostate, breast and brain cancer and can be associated with poorer clinical outcome (Begum et al., 1995; Chung, Bachelder, Lipscomb, Shaw, & Mercurio, 2002; Colombel et al., 2012; Kwon et al., 2013; Martin & Jiang, 2014). Integrin α6 supports several different oncogenic activities including cancer cell migration, metastasis, proliferation and survival (Colombel et al., 2012; Kwon et al., 2013; Martin & Jiang, 2014) (Chung et al., 2002).

Integrin α6 is also highly expressed in stem cells and even serves as a marker for many stem cells including prostate cells, HSCs and MSCs (Notta et al., 2011; Yamamoto et al., 2012; K. R. Yu et al., 2012). Integrin α6 supports these cells by anchoring them to the stem cell niche and directly activating mechanisms to potentiate the stem cell phenotype. For example NSCs located closest to the brain vasculature express the highest level of integrin α6β1 while those furthest away have lower expression; Blocking the integrin α6β1 receptor with an integrin antibody in vitro also reduces adhesion of NSCs to endothelial monolayer (Q. Shen et al., 2008). Integrin α6 expression promotes sphere

and colony formation in mouse and human prostate cells (Lawson, Xin, Lukacs, Cheng, & Witte, 2007; Mulholland et al., 2009). Integrin α6 is also enriched in tumor-propagating cell populations in various cancers including breast, cervical, prostate, colon and brain cancer (GBM) (Bragado et al., 2012; Cariati et al., 2008; Haraguchi et al., 2013; Lathia et al., 2010; Lopez, Poitevin, Mendoza-Martinez, Perez-Plasencia, & Garcia-Carranca, 2012; Yamamoto et al., 2012). Its expression promotes self-renewal and tumorigenicity in CSCs (Cariati et al., 2008; Fukamachi et al., 2013; Haraguchi et al., 2013; Lopez et al., 2012; To et al., 2010).

Integrin α6 has been shown to enrich for GSCs and regulate some GSC characteristics. In a 2010 study, Lathia et al. (2010) showed that Integrin α6 is upregulated and coexpressed with Olig2 and CD133 in GSCs compared to non-stem glioma cells. GSCs positive for integrin α6 were more proliferative and had a greater capacity to form spheres than integrin α6- cells regardless of CD133 expression. Integrin α6 + cells glioma cells also formed tumors more often and in a shorter time frame than those with low integrin α6 expression, suggesting that integrin α6 contributes to glioma formation.

Here, we demonstrate KLF9 regulates glioblastoma cell stemness in part by inhibiting integrin α6 expression and downstream functions. KLF9 may also influence integrin signaling by downregulation of integrin-binding partner and integrin signaling facilitator tetraspanin CD151.

1.5 Tetraspanins and CD151

Tetraspanins

Tetraspanins, or the transmembrane 4 superfamily, consist of 33 transmembrane proteins in mammals. These proteins have four transmembrane domains, consisting of one small extracellular loop (EC1) and one large extracellular loop (LEL or EC2), and two typically short (less than 20 amino acids) cytoplasmic N- and C- terminals (Charrin et al., 2009) (Figure 1.7). Tetraspanins are small proteins between 20 and 30 kDa or 204-355 amino acids. The small extracellular loop consists of fewer than 30 amino acids, while the larger extracellular loop has between 76-131 residues (Charrin et al., 2009). These proteins are defined by several structural characteristics in the extracellular loops and transmembrane domains including disulfide bonds, a CCG motif and posttranslational modifications (such as palmitoylation and N-glycosylation). Most tetraspanins are expressed in most or all cell types and localize to the cell membrane. However, a subset are also expressed in exosomes (Charrin et al., 2009).

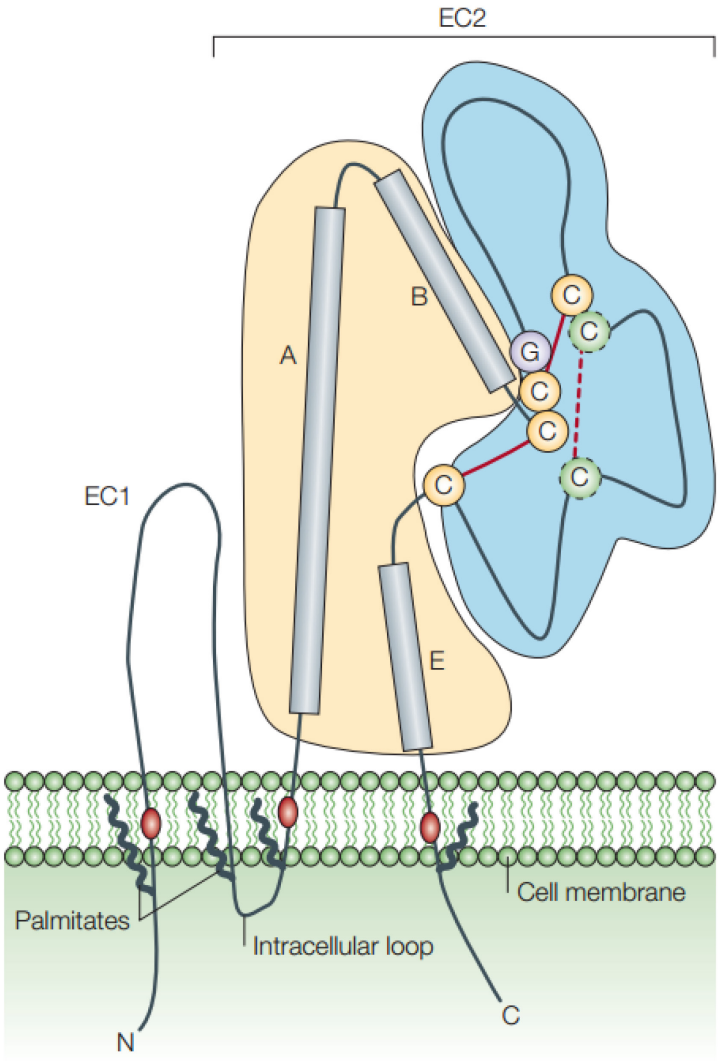

Figure 1.7. Structure of Tetraspanins. Tetraspanins are four transmembrane domain proteins with one small extracellular loop (EC1) and one large extracellular loop (EC2), and two typically short cytoplasmic N- and C- terminals. Tetraspanins also harbor disulfide bonds and a CCG motif in the EC2 and display posttranslational modifications (such as palmitoylation proximal to the transmembrane domains (Hemler, 2005).

Tetraspanins associate with multiple cell surface receptors and each other, forming specific membrane domains known as tetraspanin-enriched microdomains (TEMs). Although the total composition of TEMs is still unknown, it is apparent that TEMs consist of interactions between tetraspansins and several adhesion molecules (integrins and immunoglobulins), transmembrane receptors, enzymes and each other. Some tetraspanins (CD9 and CD82) also interact with gangliosides to stabilize interactions with integrins and c-Met. There are several orders of interaction, which can be detected using different detergents. The TEM links tetraspanins to several signaling pathways. Due to these interactions, tetraspanins influence several processes including oocyte fertilization, immune cell and platelet functions and wound healing (Charrin et al., 2009).

Tetraspanins have also been shown to contribute to tumor growth and metastasis. Tetraspanin 8 is upregulated in many cancers (Anami et al., 2015; Berthier-Vergnes et al., 2011; Gesierich et al., 2005; Hemler, 2014; Kanetaka et al., 2001) and promotes cancer cell migration and tumor growth (Ailane et al., 2014; Anami et al., 2015; Claas et al., 1998; Greco et al., 2010; Kanetaka et al., 2001). CD37 is exclusively expressed in mature B cells (Robak & Robak, 2014; Schwartz-Albiez, Dorken, Hofmann, & Moldenhauer, 1988) and is typically overexpressed in B cell malignancies (Robak & Robak, 2014). Targeting CD37 with antibodies induces apoptosis in lymphoma cells and leukemia cells and can be more potent than current standards of treatment (Heider et al., 2011).

Tetraspanins also play a major role in the maintenance of stem cells. Many biomarkers for mesenchymal stem cells (MSCs) are tetraspanins (CD63, CD81 and

CD82) (Al-Nbaheen et al., 2013; D'Ippolito et al., 2004; H. J. Lee, Choi, Min, & Park, 2009) . Tetraspanin CD9 is abundantly expressed in mouse and human embryonic stem cells and maintains the undifferentiated state in mouse ESCs (Cui et al., 2004; Harkness et al., 2008; Nagano et al., 2005; Oka et al., 2002). CD81 is expressed in pancreatic stem cells (Lin et al., 2006) and regulates haemopoietic stem cell proliferation through regulation of the AKT pathway (K. K. Lin et al., 2011).

CD82 and CD9 also support cancer stem cells. CD82 expression is high in leukemia stem cell-like AML cells (CD34+/CD38-) and blocking its expression inhibits colony formation, cell adhesion and AML cell engraftment in vivo (Bonardi et al., 2013; Nishioka et al., 2013). In cell lines established from malignant mesothelioma, CD9 is highly expressed with other stem cell markers. $CD9^{high}$ cells form more spheroid colonies and generate significantly larger xenograft tumors as well (Ghani et al., 2011).

CD151

Tetraspanin CD151, previously known as platelet endothelial tetraspanin antigen-3 (PETA-3) and SF-HT-activated gene 1 (SFA-1) protein, was identified by a monoclonal antibody raised against AML in 1991 (Ashman et al.). It was later cloned and characterized by Fitter et al. (1995) and Hasegawa et al. (1996), independently. CD151 has one open reading frame that is 253 amino acids (759 bp) long with a molecular weight of 28kDa (Fitter et al., 1995; Hasegawa et al., 1996). In its mature glycosylated form, CD151 has a molecular weight of 32kDa and is seen as a doublet in SDS-PAGE protein gels (Sincock et al., 1999b). Multiple splice variants have also been described for this protein. CD151 also has multiple modification sites including a potential N-glycosylation site located between the third and fourth transmembrane domains and at

least four intracellular palmitoylation sites proximal to the transmembrane domains that support CD151's association with other tetraspanins (Fitter, Tetaz, Berndt, & Ashman, 1995; Hasegawa, Utsunomiya, Kishimoto, Yanagisawa, & Fujita, 1996; X. Yang et al., 2002).

CD151 is expressed in virtually every tissue in normal healthy adults, particularly in the epithelium. It is highly expressed in vascular endothelium in multiple tissues, including specialized endothelium (capillaries of the blood–brain barrier, glomeruli, etc). This suggests that it may play a major role in vascular integrity (Sincock, Mayrhofer, & Ashman, 1997). CD151 expression is also high in heart, lung, pancreas and prostate tissues (Fitter et al., 1995). A very small amount has been detected in brain tissue, despite the high expression of CD151 in brain vasculature (Fitter et al., 1995; Sincock et al., 1997).

Because CD151 forms multiple secondary interactions with cell surface proteins in the tetraspanin-enriched microdomain (TEM), CD151 promotes several cellular processes including cell adhesion (Garcia-Lopez, Barreiro, Garcia-Diez, Sanchez-Madrid, & Penas, 2005; Geary et al., 2008; Palmer et al., 2014), migration (Fei et al., 2012; Peng et al., 2013; Sincock et al., 1999b; W. Yang et al., 2012), proliferation (Geary et al., 2008; W. F. Liu et al., 2011; Novitskaya, Romanska, Dawoud, Jones, & Berditchevski, 2010; Peng et al., 2013; W. Yang et al., 2012; Zheng & Liu, 2007a, 2007b; Zuo et al., 2010), wound healing (Cowin et al., 2006; Wright et al., 2004) and vessel formation (W. F. Liu et al., 2011; Peng et al., 2013; Sincock et al., 1999b; Zheng & Liu, 2007a, 2007b; Zuo et al., 2010). CD151 influences these processes through

activation of many signaling pathways including PI3K/Akt and Ras/Raf/MEK/ERK pathways (W. F. Liu et al., 2011; Zheng & Liu, 2007b; Zuo et al., 2010).

CD151 primarily complexes with laminin-binding integrins in the TEM. CD151 directly interacts with the α integrin subunits (α3, α6 and α7) through the extracellular loop (Hasegawa et al., 2007). Through these interaction, CD151 facilitates outside in integrin signaling and enhances integrin-regulated cellular processes including proliferation and cell migration and adhesion to laminin (Fei et al., 2012; W. F. Liu et al., 2011; Sterk et al., 2000; W. Yang et al., 2012; Zuo et al., 2010).

Integrin α3 and α6 form strong (Triton X-100 resistant) associations with CD151 at extracellular site $QRD^{194\text{-}196}$ (Kazarov, Yang, Stipp, Sehgal, & Hemler, 2002). Integrin α7 also appears to form a weaker bond with CD151 at this site (Sterk et al., 2002). This interaction is critical for CD151-integrin association and integrin signaling. Mutation of site $QRD^{194\text{-}6}$ to $AAA^{194\text{-}196}$ decreased the association between CD151 with integrin α3 and integrin α6 (W. F. Liu et al., 2011; W. Yang et al., 2012) and reduced CD151's ability to promote proliferation, migration and invasion in endothelial and cancer cells (Fei et al., 2012; W. F. Liu et al., 2011; Zuo et al., 2010). The mutation also prevented activation of integrin signaling pathway proteins FAK, PI3K, Akt, eNOS, ERK1/2, cdc42 and Rac1 by forced CD151 expression (W. F. Liu et al., 2011). CD151 also interacts with tetraspanins CD9 and CD81 in regions of cell-cell contact and has been shown to associate with GTPases when CD151 is overexpressed (Blumenthal et al., 2012; Hong, Jeoung, Ha, Kim, & Lee, 2012).

CD151 is highly expressed in several cancers, including gastric, endometrial, liver, breast, prostate (Detchokul, Newell, Williams, & Frauman, 2014; Devbhandari et

al., 2011; Voss et al., 2011; X. H. Yang et al., 2008; Y. M. Yang et al., 2013). Its aberrant expression is associated with multiple oncogenic activities such as metastasis and angiogenesis (Deng et al., 2012; Devbhandari et al., 2011).

CD151 has also been implicated in the progression of high grade glial tumors, including GBM. *CD151* mRNA levels are consistently upregulated in clinical GBM samples (Bredel et al., 2005). Patients with CD151-high glial tumors exhibit shorter progression free survival (PFS) and overall survival (OS) (D. Lee et al., 2013). The expression of CD151 is also correlated with MGMT promoter methylation status, and its predictive potential was improved when combined with MGMT promoter methylation to determine OS probability of patients with newly diagnosed GBMs (D. Lee et al., 2013). CD151 is also highly expressed in glioblastoma with an oligodendroglial component (GBMO), a subgroup of GBMs that display oligodendroglial phenotype in various areas throughout the tumor (Ha, Kang, Do, & Suh, 2013).

Functional analysis of gene expression in glioma tumor samples revealed an association of CD151 with glioblastoma cell invasion (Bredel et al., 2005). This association is supported by Rao Malla et al. (2013) who showed that downregulation of CD151 and blocking CD151 interaction with integrin α3β1 via silencing of cell surface proteins uPAR and Cathepsin reduced glioma cell adhesion and invasion on laminin.

Not much is known about the role of CD151 in stem cells. There is data suggesting that it is associated with less differentiated states in chrondocytes. For example, CD151 is highly expressed in MSCs (Diaz-Romero, Nesic, Grogan, Heini, & Mainil-Varlet, 2008; H. J. Lee et al., 2009), and the percentage of CD151+ cells decreases significantly during MSC differentiation (H. J. Lee et al., 2009). CD151 is also

highly expressed in less differentiated cells in oral squamous cell carcinoma tumors. (Romanska et al., 2013). Ablation of CD151 in $CD24^{Hi}CD49f^{Low}$ mammary cells, a subpopulation of luminal cells enriched in stem and progenitor cells, also increased the differentiation potential of progenitor cells and proliferative cells (Yin et al., 2014).

Very few studies have investigated the role of CD151 in CSCs. CD151 is highly expressed in prostate tumor-propagating cells and enhances sphere formation and tumor initiation (Rajasekhar, Studer, Gerald, Socci, & Scher, 2011). CD151 is also consistently expressed in several CD133+ tumorigenic colon cancer cell lines (Gemei, Di Noto, Mirabelli, & Del Vecchio, 2013).

We investigated the expression and function of CD151, whose gene is also downregulated by KLF9, in tumor-initiating GSCs using human GBM–derived neurosphere cultures. CD151 was found to be highly expressed in glial tumors and GSC lines. CD151 silencing in GSCs blocked self-renewal, migration, xenograft growth and vessel formation. CD151 knockdown also increased apoptosis in vivo. CD151 overexpression enhanced GSC self-renewal and migration. CD151 associated with integrins α3, α6 and β1 in GSCs. Blocking CD151 interaction with integrins α3 and α6 inhibited sphere formation, migration and activation of downstream integrin signaling. Together, the results support a critical role for CD151 and CD151-integrin interaction in GSC maintenance, migration and tumor formation.

Chapter 2

Materials and Methods

Reagents

All reagents were purchased from Sigma-Aldrich (St. Louis, MO, www.sigmaaldrich.com). Stock of all-trans retinoic acid (RA) was prepared in DMSO and diluted to 1μM in cell culture medium as a working concentration. Doxycycline (Dox) was diluted to a concentration of 0.5 μg/ml in cell culture medium as a working concentration. In all the experiments, the final DMSO concentration was <0.1% and DMSO also had no demonstrable effect on neurosphere cultures. Laminin was diluted to 10 μg/ml as a working concentration.

Cell Culture

The human glioblastoma neurosphere lines GBM1a (0913) and GBM1b (0627) were originally derived, characterized, and shown to be enriched in GSCs by Vescovi and colleagues (Galli et al., 2004). The enrichment of GSCs in these neurosphere lines have since been validated by multiple other investigators (Y. Li et al., 2011; Ying et al., 2011). The 1123 (M1123) and 146 (P146) neurosphere lines were derived from high grade glioma patients and kindly provided by Dr. Nakano (Ohio State University). Primary GBM neurospheres JHH612 (612) were derived from clinical GBM specimens at Johns Hopkins University using the methods and culture conditions described by Galli et al. (2004). Neurospheres were cultured and maintained in serum-free medium supplemented with epidermal growth factor (EGF) and fibroblast growth factor (FGF), and incubated in

a humidified incubator containing 5% CO2/95% air at 37 °C and passaged every 4–5 days by mechanical dissociation as described by Vescovi et al. and others (Galli et al., 2004; Sun et al., 2009; Vescovi et al., 1999). To induce differentiation, cells were grown in medium containing 1% fetal bovine serum (FBS) or 1μM retinoic acid (RA) (Galli et al., 2004; Ying et al., 2011). Primary GBM neurospheres 551 (JHH551) and 612 (JHH612) were derived directly from clinical GBM specimens obtained at Johns Hopkins Hospital using the same methods and culture conditions as described by Galli et al. (2004). Primary neurospheres were used at less than 10 passages. All human materials were obtained and used in compliance with the Johns Hopkins Institutional Review Boards.

Lentiviral Cell Transfection

The sequences for CD151 shRNA lentiviral vectors (TRCN0000300360, TRCN0000300331; Sigma-Aldrich; V3THS_308057; Thermo Scientific, Hudson, NH, www.thermoscientific.com) are listed below. N-terminal 3xFLAG-tagged KLF9 and CD151 were constructed with high-fidelity polymerase chain reaction (PCR; Roche, Basel, Switzerland, www.roche-appliedscience.com) and cloned into pTRIPZ vector (Thermo Scientific, Hudson, NH, www.thermoscientific.com) and/or pLEX vector (Thermo Scientific) using *AgeI* and *MluI* restriction sites. ITGA6 was also cloned into pLEX vector with *AgeI* and *Mlul*. Lentiviral packaging followed second generation lentivirus packaging protocol using psPAX2 and pMD2.G vectors (Addgene, Cambridge, MA, www.addgene.org). Glioma cells were infected with lentivirus at a multiplicity of infection of 5 and selected with puromycin (1 μg/ml) for stable cell lines. Transdux

(System Biosciences, Mountain View, CA, http://www.systembio.com) was used for improving lentivirus infection efficiency.

CD151 shRNA sequences

CD151 shRNA 1	CCGGGCTGGAGATCATCGCTGGTATCTCG AGATACCAGCGATGATCTCCAGCTTTTTG
CD151 shRNA 2	CCGGCCCTCAAGAGTGACTACATCACTCG AGTGATGTAGTCACTCTTGAGGGTTTTTG
Dox-inducible CD151 shRNA	CATGTTGTCTTCTTCTCGT

Neurosphere formation assays

Viable cells (2 x 10^3/well or 2 × 10^4/well) were cultured in 48-well or 6-well plates, respectively. After 7-14 days, neurospheres were fixed in medium with 1% agarose, stained with 1% Wright stain solution and counted by computer-assisted morphometry (MCID software, Cambridge, UK, www.mcid.co.uk) by measuring the number of neurospheres (>50 μm or >100 μm in diameter, as indicated) in three random fields per well.

Cell Adhesion Assay

Six well plates were coated with laminin at 37°C overnight and washed twice with phosphate buffered saline (PBS). Dissociated viable cells (1.0 ml) were plated at a density of 5 x 10^5/ml and incubated for 24 hours. Neurosphere cells expressing a Dox-inducible 3F-KLF9 transgene: Cells were then transfected ± lentivirus containing the ITGA6 transgene. After 24 hours, cells were treated ± Dox for 96 hours. Primary cells

were co-transfected with KLF9 and ITGA6 lentivirus. Neurosphere cells expressing a Dox-inducible 3F-CD151 transgene were treated ± Dox for 24 hours. The cells were then dissociated and plated (5 x 105/mL) on laminin coated six-well plates for 2-6 hours. Cells were stained with crystal violet (5 μg/μl) (Sigma-Aldrich) for 10 minutes. Crystal violet was dissolved with 2% SDS and quantified spectrophotometrically at 550 nm using a Spectra MAX 340pc (Molecular Devices, Sunnyvale, CA) plate reader. The results are shown as relative adhesion measured after subtracting the background absorbance from all values.

Cell Migration Assay

Cell migration assays were performed using 24mm transwell chambers with 8.0μm pore-size polycarbonate membranes (Corning Inc, Corning, NY, http://www.corning.com). The upper chambers were coated with laminin at 37°C overnight followed by washing with PBS 3 times. Dissociated neurosphere cells expressing a Dox-inducible 3F-KLF9 transgene were co-transfected with KLF9 and ITGA6 lentivirus. After 24 hours, cells were treated ± Dox for 48 hours in growth factor-free neurosphere culture medium. Primary cells were transfected with KLF9 lentivirus. GBM neurosphere lines were infected by CD151 shRNA lentivirus or incubated with anti-CD151 (integrin α3 binding site) antibody TS151r (Millipore) for 24 hours. Neurosphere cells expressing a Dox-inducible 3F-CD151 were treated ± Dox for 24 hours. The cells were then suspended in 1.5ml (1 x 10^6cells/well) of growth factor-free neurosphere culture medium and added to the upper chamber of the transwell. Minimum Essential Medium Eagle medium (2.6 ml) supplemented with 10% FBS was added to the

lower chamber. After 24 hours of incubation at 37°C, the transwell upper chamber surfaces were gently scrubbed with a cotton swab to remove non-invasive cells. Cells that had migrated through the filter were fixed with 4% paraformaldehyde and stained with Hoechst 33342 nucleic acid stain (Invitrogen, Carlsbad, CA, www.invitrogen.com). Migration was quantified by counting cells from eight random fields and averaged.

Migration of glioma cells was also quantified using a directional migration assay using a multi-well nanopatterned device, consisting of parallel nano-ridges/grooves of 400 nm in groove width, 400 nm in ridge width, and 500 nm in depth, constructed of transparent poly(urethane acrylate) (PUA), and fabricated using UV-assisted capillary lithography as previously described (D. H. Kim, Han, et al., 2009; D. H. Kim, Seo, et al., 2009). Prior to plating cells, nanogrooved substrata were coated with poly-D-ornithine (10 ug/ml concentration) for 15 minutes and laminin (3ug/cm2) overnight. These topographically patterned cell substrata, cause cells to align with and move along the direction of the nanogrooves. Cell migration was quantified using timelapse microscopy and a motorized inverted microscope (Olympus IX81) equipped with a Cascade 512B II CCD camera and temperature and gas controlling environmental chamber. Phase-contrast and epi-fluorescent cell images were automatically recorded under 4*1.6X objective using the Slidebook 4.1 (Intelligent Imaging Innovations, Denver, CO) for 10 hours at 10 minute intervals.

A custom-made MATLAB script was used to calculate cell speed using timelapse microscopy data as described previously (Abbadi et al., 2014; Garzon-Muvdi et al., 2012; Kondapalli et al., 2015; Q. Li et al., 2014). Average speeds of individual cells were

calculated from the total distance moved throughout the entire cell trajectory and the total time the cell was tracked.

Western Blot

Total cellular proteins were extracted with radioimmunoprecipitation assay buffer (Sigma-Aldrich) containing protease and phosphatase inhibitors (Calbiochem, Billerica, Massachusetts, www.calbiochem.com). The Subcellular Protein Fractionation Kit was used for membrane protein extraction (Thermo Scientific). SDS-PAGE was performed with 50 μg total cellular proteins using 4% to 12% gradient Tris-glycine gels (LI-COR Biosciences, Lincoln, NE, www.licor.com). Western blot analysis was performed using Quantitative Western Blot System, with secondary antibodies labeled by IRDye infrared dyes (LI-COR Biosciences). The primary antibodies were: anti-CD151, anti-Olig2, anti-FLAG (Santa Cruz), anti-Sox2, anti-pAkt, anti-tAkt, anti-integrin α3, anti-integrin α6, anti-integrin β1 (Cell Signaling), anti-pan Cadherin (Abcam, Cambridge, MA, www.abcam.com), anti-β-actin (Sigma-Aldrich), anti-FLAG-HRP (Sigma-Aldrich), anti-BMI1 (Cell Signaling), anti-Nestin (Santa Cruz) and anti-CD133 (Cell Signaling).

Immunoprecipitation

A total of 1 x 10^7 GBM1A 3F-CD151 cells were treated ± Dox for 48 hours. Cells were lysed in the immunoprecipitation buffer containing 1% Brij-O1, 20mM Tris HCl pH 8, 137mM NaCl, 2mM EDTA and protease and phosphatase inhibitors (Calbiochem) for 1 hour at 4°C on a rotating shaker. Mouse anti-FLAG M2 antibody (Sigma-Aldrich) or Protein A/G magnetic beads (Thermo Scientific) crosslinked with mouse IgG (served as the control) were added to the above cell lysate and incubated overnight at 4°C on a

rotating shaker. 3F-CD151 bound complexes were eluted using 3x FLAG peptide (Sigma-Aldrich). Immunoprecipitates were immunoblotted with primary antibodies or analyzed by tandem mass spectrometry (LC/MS/MS) by the Johns Hopkins University Mass Spectrometry and Proteomics Facility.

Immunofluorescence

Neurosphere cells were collected by cytospin onto glass slides and fixed with 4% paraformaldehyde. Cells were permeabilized by Triton X-100 and immunostained with anti-GFAP (Sigma-Aldrich), anti-β-actin (Sigma-Aldrich), anti-CD151 (Santa Cruz Biotechnology, Dallas, TX, www.scbt.com), anti-integrin α3 (Cell Signaling), anti-integrin α6 (Cell Signaling), and/or anti-integrin β1 (Cell Signaling) antibodies and Hoechst 33342 nucleic acid stain (Invitrogen) following the protocol from Cell Signaling. Secondary antibodies were conjugated with Alexa488 or Cyanine Cy3. Immunofluorescent images were captured and analyzed using Axiovision software (Zeiss, Thornwood, NY, www.zeiss.com).

Flow Cytometric Assay

Flow cytometric analysis was done on unfixed cells were stained with CD133/2(AC133)-PE (Miltenyi Biotec, Auburn, CA, www.miltenyibiotec.com), PE-CD151 (BD Biosciences, San Jose, CA, www.bdbiosciences.com) or ITGA6-FITC (CD49f; BD Pharmingen, Franklin Lakes, NJ, www.bdbiosciences.com) antibody following manufacturer's protocol using a FACSCalibur (Becton Dickinson, San Jose, CA, http://www.bd.com) with with CELLQuest Version 3.3 software (Becton

Dickinson). The cells were blocked with Fc receptor blocking reagent and incubated at 4°C with CD133/2 (AC133)-PE for 10 minutes or with PE-CD151 or ITGA6-FITC for 30 minutes. The cells were then washed and resuspended in PBS containing 0.5% BSA and 2 mM EDTA. Mouse IgG labeled with PE or FITC (Miltenyi Biotec) was used as control.

Tumor implantation and animal treatments

All animal protocols were approved by the Johns Hopkins School of Medicine Animal Care and Use Committee.

For subcutaneous (s.c.) xenografts, female athymic nude mice were injected s.c. in the flank with 5×10^6 viable neurosphere cells in 0.1 ml DMEM. When tumors reached about 50 mm^3, mice were randomly divided into groups for treatment. Dox was administered in animal feed. Tumor sizes were determined daily by measuring two dimensions (length [a] and width [b]) and volumes (V) were calculated using the formula $V = ab^2/2$ (Lal, Xia, Abounader, & Laterra, 2005).

For intracranial (i.c.) xenografts, SCID immunodeficient mice received 5,000 viable neurosphere cells (determined by trypan blue staining) in 2 μL Dulbecco's Modified Eagle Medium by stereotactic injection to the right caudate/putamen (AP = 0 mm, ML = −2.5 mm, DV = −3.0 mm). Mice were perfused with 4% paraformaldehyde at the indicated times and the brains were removed for histological analysis. Tumor sizes were quantified by measuring maximum tumor volume on hematoxylin and eosin–stained brain coronal sections using computer-assisted morphometry (MCID software).

Histology and immunohistochemistry

Laminin immunohistochemistry was performed using anti-laminin antibody to detect orthotopic xenograft vascularization (Ljubimova et al., 2004). The tumor blood vessels were quantified as total vessel area relative to tumor cross-sectional area, as previously described (Abounader et al., 2002). Activated caspase-3 immunohistochemistry was conducted using anti-cleaved caspase-3 (Cell Signaling Technology, Beverly, MA). Apoptotic indices were determined by computer assisted quantification of the number of positively stained cells per microscopic field as previously described (Abounader et al., 2002; Lal et al., 2005).

Quantitative real-time PCR

Total RNA was extracted using Rneasy Mini Kit (Qiagen, Venlo, Limburg, www.qiagen.com). After reverse transcription using MuLV reverse transcriptase (Applied Biosystems, Calsbad, CA, www.appliedbiosystems.com) and Oligo(dT) primer, quantitative real-time PCR (qRT-PCR) was performed using SYBR Green PCR Mix (Applied Biosystems) and IQ5 detection system (Bio-Rad, Hercules, CA, www.bio-rad.com). Primer sequences are listed below. Relative gene was normalized to 18S rRNA.

Primer sequences for quantitative real-time PCR. Fold enrichment was calculated using the following formula: 2^–(Ct Flag IP-Ct Mouse IgG IP). The percentage of input was calculated using 100 x 2^(adjusted input-Ct Flag IP), where the adjusted input = Ct Input – (log2 of dilution factor). Ct, threshold cycle.

Primer Name	Sequence (5'-3')
KLF9	AACTGCTTTTCCCCAGTGTG

	TCCCATCTCAAAGCCCATTA
RAP2A	TCTACAGCCTCGTCAACCAGCA TCTGCCTTCGCTGGACGATACT
CAMK2G	GACACGGTAACTCCTGAAGCCA TCCACAGTCTCCTGACGATGCA
CDC42	TGACAGATTACGACCGCTGAGTT GGAGTCTTTGGACAGTGGTGAG
MAPK3	TGGCAAGCACTACCTGGATCAG GCAGAGACTGTAGGTAGTTTCGG
PAK4	GATGATTCGGGACAACCTGCCA AGGAATGGGTGCTTCAGCAGCT
PIK3C2B	CCTCCTGAAACGAGCTGTGTCT CACAGTAAGGCTGCCAGCAGAT
PIK3R2	ATGGCACCTTCCTAGTCCGAGA CTCTGAGAAGCCATAGTGCCCA
RND2	GAGCTGTCCAAGCAGAGGCTTA GAGCACTCAACATAGGACACAGC
SOS1	GGAGATCAACCCTTGAGTGCAG TGCTCTACCCAGTGCCGACATA
SOS2	GGCATATCAGCAAACCAGGACAG CACTCCCTACAAGTTCAGACGG
CXCR4	CTCCTCTTTGTCATCACGCTTCC

	GGATGAGGACACTGCTGTAGAG
GNAQ	GATCAGAGCCATGGACACACTC GCAGACACCTTCTCCACATCAAC
ITGA6	CGAAACCAAGGTTCTGAGCCCA CTTGGATCTCCACTGAGGCAGT
ITGA9	TCAGGTCACAGAGAAGCTGCAG CACATGCTCACTGAGGCTGTAG
ARPC1B	CTCCTGTGACTTCAAGTGTCGG GGCTGAGAAACAGACGCCATGT
CAPN5	AGTGTGAGGGAGACAAAGTCCG CATCCTTCAGCACTCGGTGGTT
MAP3K11	CTGGATGGCTCCTGAGGTTATC CACAGCAAGGCAGTCAATGCCA
MYLK	GAGGTGCTTCAGAATGAGGACG GCATCAGTGACACCTGGCAACT
GIT1	CCGAGAGTTTGCCACCTTGATC ACGCTGTCGTAGTCGTGTTGGT
ADAM17	AACAGCGACTGCACGTTGAAGG CTGTGCAGTAGGACACGCCTTT
NOTCH1	GGTGAACTGCTCTGAGGAGATC GGATTGCAGTCGTCCACGTTGA
NOTCH3	TACTGGTAGCCACTGTGAGCAG

	CAGTTATCACCATTGTAGCCAGG
NUMBL	CTACGGCTGAATGAGCTGCCAT CAGAGCGTTGATGCTGTCACTG
DTX1	AGAATCCCGAGGATGTGGTTCG TCGTAGCCTGATGCTGTGACCA
APH1B	AGGTGAGACAGCACCCTCTATG GAGGAGAATCTCCATGAATGCCC
HES1	GGAAATGACAGTGAAGCACCTCC GAAGCGGGTCACCTCGTTCATG
HEY2	TGAGAAGACTTGTGCCAACTGCT CCCTGTTGCCTGAAGCATCTTC
RAC3	ACAAGGACACCATTGAGCGGCT CCTCGTCAAACACTGTCTTCAGG
CD151	GGAGAACCTGAAGGACACCATG CAGTCCTGTGAGTTGTTGCTGC
SOX2	GCTACAGCATGATGCAGGACCA TCTGCGAGCTGGTCATGGAGTT
OLIG2	ATGCACGACCTCAACATCGCCA ACCAGTCGCTTCATCTCCTCCA
BMI1	GGTACTTCATTGATGCCACAACC CTGGTCTTGTGAACTTGGACATC

RNA Isolation and RNA Sequencing

Total RNA was extracted using the RNeasy kit (Qiagen, Valencia, CA, www.qiagen.com) following the manufacturer's protocol. 4 µg total RNA was subjected to library preparation using Illumina TrueSeq RNA Sample Preparation Kit v2 (Illumina, San Diego, CA, www.illumina.com) following manufacturer's protocol. Indexed adapters were used in order to pool 4 cDNA libraries into one sequencing reaction. Libraries were quantified and quality control was assessed using an Agilent Bioanalyzer (Agilent Technologies, Santa Clara, CA, http://www.genomics.agilent.com/) to confirm that cDNA fragment sizes were between 200bp and 500bp in length. Sequencing was performed using Illumina HiSeq 2500 platform (Illumina).

RNA-Seq Analysis

The raw reads were aligned to reference human genome build hg18 using TopHat (Trapnell, Pachter, & Salzberg, 2009) with default parameters. See Figure 3.2C for the percentage of reads aligned. For each gene, the number of reads aligned to its exons were counted and summarized into gene level counts by R bioconductor package GenomicFeatures (M. Carlson et al.) based on UCSC refFlat table for hg18. Normalization between samples was carried out by R package edgeR (Robinson, McCarthy, & Smyth, 2010; Robinson & Oshlack, 2010), which controls sequencing depth and RNA composition effects, i.e. high expression of some genes in a sample may contribute a substantial proportion of total reads and thus undersample reads from other

genes. The consistency of RNA-Seq data for the two biological replicates was examined by scatter plot for $\log_2$ fold changes between the two cell lines for all genes and by heatmap for expression patterns for differentially expressed genes.

Reproducibility Plots for RNA-Seq Data

RPKM, namely reads per kilobase per million mapped reads, for each differentially expressed gene was calculated by R bioconductor package GenomicRanges (M. Carlson et al.).The heatmap (Figure 3.2D) was generated according to the count table with scaling across the samples for each gene. The $\log_2$ fold change, $\log_2$((IPRMKM+1)/(ControlRPKM+1)), for each gene in each cell line was calculated. The $\log_2$ fold change for KLF9-GBM1b is plotted against that of KLF9-GBM1a (Figure 3.2E).

KLF9 Target Gene Detection

Differential gene expression detection was carried out by R bioconductor package edgeR (Robinson et al., 2010) with tagwise dispersion at FDR 5%. A matched study design was used since the four samples came from two cell lines. The list of differentially expressed transcripts was further filtered if the absolute values of $\log_2$ fold changes for differentially expressed transcripts comparing the case vs control exceeded 0.8. KLF9 target genes were defined as differentially expressed transcripts with ≥1 KLF9-binding peak in the -20 kb to +10 kb window surrounding the transcription start sites (TSSs).

Chromatin Immunoprecipitation (ChIP) and ChIP Sequencing

A total of 5 x 10^6 KLF9-GBM1a and KLF9-GBM1b cells were treated with Dox for 48 hours and subjected to ChIP using MAGnify ChIP system (Invitrogen, Carlsbad, CA, www.invitrogen.com) following manufacturer's protocol. KLF9 bound DNA was immunoprecipitated using mouse anti-FLAG M2 antibody (Sigma-Aldrich) and Dynabeads Magnetic Beads (Life Technologies). Mouse IgG served as the control. ChIP-enriched DNA was purified using the minElute Reaction Cleanup kit (Qiagen, Valencia, CA) and used in semi-quantitative PCR and qPCR reactions with primer pairs and sequencing. 10ng ChIP-enriched DNA or input DNA was subjected to library preparation using ChIP-Seq DNA Sample Prep Kit (Illumina) following manufacturer's protocol. Quality control using an Agilent Bioanalyzer (Agilent Technologies) was performed to assure that ChIP-enriched and input DNA library had similar DNA size distribution patterns of between 150-250 bp in length. Sequencing was performed using Illumina HiSeq 2500 platform (Illumina).

Primer sequences for Chromatin Immunoprecipitation quantitative real-time PCR.

Primer Name	Sequence (5'-3')
RHOV KLF9 Binding Site	CTCTGACTGAATGGGTCCAG TGCCTGCCTTTCCTCCTCC
CAMK2G KLF9 Binding Site	GAGAGCGAGGGAGGGAGG GCGAGGGCGGCTCCGGG
SOS1 KLF9 Binding Site	GAGGACGTGTGGAGGGACG CCTCAGGGCAGCCAGATTC
CXCR4 KLF9 Binding Site	GTCACATCTTGGCTAACTC

	GTTAATCACTGCCCCTC
ITGA6 BTE Site B	ACGTCGTGGCTTCCGGGCAGGTA GGAGACTCGCAGGCGTTTTATCAAG
MYLK KLF9 Binding Site	CTCAAACCACCCGCTCCAG GTGCAGGATAAGTGCGAGG
NOTCH1 KLF9 Binding Site	GAGAGGCTGGGCTCGGGACG GAGGCACTAGTGAGGCTC
NUMBL KLF9 Binding Site	GATGGTGCGGGATGCACG CGGGGTCTTCAGGCCAAG
ITGA6 KLF9 Binding Site/BTE Site A	CCAGAGCCGGCGGGTAAGGTG CGAGGCTGCCGCGCTGCTGCTA
ITGA6 No BTE Site 1	GCTTTATGAGTATCTTGGCACAGTA GGGGCGGTTGGAGGGAAAATGG
ITGA6 No BTE Site 2	GACTGGCTGATCCTCCTTTAGA ATTTTTGTCATTGCCCCTCACTTT
NOTCH1 BTE Site	CGGGTCCCTCCTCCCCGGAG CCTCCCGCGGCCGAGGCACT
NOTCH1 No KLF9 Binding Site	CAGCTGGGCCCTCGTGTTTC CCTGGCCTGGCGCTCTTCCT
RAP2A KLF9 Binding Site	GATCTGGGCGTGGAGGCGCG GGCAACTGAGGGAGCAGC
RND2 KLF9 Binding Site	CTGGACCCCGGCTCTGAG

	CAACACCGGCATCTC
PSEN2 KLF9 Binding Site	CCTCTGGCCACGGTCCCTTC GAAGTGGGGACGCAGTGAG
HEY2 KLF9 Binding Site	CTGGCCCAGCCAATCGCGAG CTAGCGGCTCTTTCCCAC
ITGA9 KLF9 Binding Site	GAAGTGCGCGCAGGGCTCAC GGGCGCTGAAGGCGAGCACA
ARPC1B KLF9 Binding Site	CGACGTCTGCGCGGGTACC GACTCTGGGCAGTCGACGCG
GIT1 KLF9 Binding Site	GCTTCTGCAGGAAGCGGCGC CCCACGCGGAAAGTGAAGGG
Random Genomic Region 1	GTCTGTACTCCCAGCTACTC GACAGAGCAAGACTCCATC
Random Genomic Region 2	GTGTCAAAGCTCGGAACTG GGTGCCAGGTGATCCCAAC
Random Genomic Region 3	CTGCACTTGGCCAATATTTC CTTTGCTGACCCATTTTATTC
Random Genomic Region 4	CTAAGGCCACACAGCTAG CTATTAGAACCCCGAGATC
Random Genomic Region 5	CGTGAGCCAATTTCCCAAC GTTTCTCCCTACTTTGTC
Random Genomic Region 6	CATCTACACCTGCGGTCTTG

	GAGGCACCCTTGAGTTAG
Random Genomic Region 7	CTTAGGAATAAATTTAAC CATTGGGATTTTAATAG
Random Genomic Region 8	GTGTATGTATAAAGAATG CTTGTTAAACTTTTATAG
Random Genomic Region 9	GACTGGTTCATTCACTGCTC CACTTCCCTACCCGAAAC
Random Genomic Region 10	CTAATGTGCGATCAAGGTTAAG GAGTAGCTGGGATTACAG

Peak Calling

The 50 bp long raw KLF9 ChIP-Seq reads were aligned to the reference human genome build hg18 using Bowtie (Langmead, Trapnell, Pop, & Salzberg, 2009) allowing at most two mismatches in the first 28 bp "seed" bases. See Figure 3.3E for the percentage of reads aligned. KLF9 binding sites were called using CisGenome (Ji et al., 2008) with default settings by comparing the two IP samples against the two control samples. At false discovery rate (FDR) (Benjamini, Drai, Elmer, Kafkafi, & Golani, 2001)of 1%, 3,1261 binding peaks were identified.

Reproducibility Plots for ChIP-Seq Data

The number of reads aligned to the peak regions by each of the four ChIP samples was counted by R bioconductor package GenomicRanges (M. Carlson et al.) and then

normalized for the library size for each sample. In the resulting count table, each column represents a peak region and each row corresponds to a sample. For each peak region, its normalized counts in a given sample was further subtracted by its mean normalized counts across samples and then divided by its standard deviation, which gave the scaled binding intensity. The heatmap (Figure 3.3F) shows the scaled binding intensities for each peak in each sample. As shown in the heatmap, the two control samples from both cell lines are clustered together and the two IP samples are clustered together by hierarchical clustering with complete linkage. After correcting for library size, the $\log_2$ IP intensity, $\log_2$(IPreads+1), for each peak in both cell lines was also calculated. The $\log_2$ IP intensity for cell line KLF9-GBM1b is plotted against that of cell line KLF9-GBM1a (Figure 3.3G, correlation= 0.8750). Both the heatmap and the scatter plot demonstrate that the IP intensities at KLF9 binding peaks were consistent for both biological replicates.

De novo Motif Discovery

The 150 bp long sequences centered at the peak summits for the top ranked 500 peaks were extracted and fed as the input for de novo motif discovery algorithm of CisGenome. Ten motifs of varying length with mean motif length being 12 were searched simultaneously. To obtain the truly KLF9 enriched motifs, the occurrence rate of motif in the 150 bp long sequences centered at the peak summits for all peaks was compared with its occurrence rate in control genomic regions. The control regions were randomly chosen to match the GC content and distributional properties of ChIP-Seq peak regions (Ji, Vokes, & Wong, 2006). Of all the motifs, only one motif has an enrichment score

exceeding 5 (with value= 5.446253) and it was selected as the binding motif for KLF9. See Figure 3.3J.

ChIP-Seq Peak List Annotation and RNA-Seq Target Gene List Generation

Figure 3.3I displays the peak distribution within the neighborhood of gene transcription start sites (TSS). Each identified peak was annotated by the closest gene satisfying the condition that the peak locates within the (-20 kb to 10 kb) neighborhood of the gene's TSS according to UCSC refLocus table for hg18. Each peak was classified as up regulated region, down regulated region, non-differentially expressed region and not-annotated region according to the differential expression status of its corresponding gene. On the other hand, for the gene list, each gene was annotated as whether it has KLF9 binding peaks within its (-20 kb to 10 kb) neighborhood of TSS and whether its binding peaks contain motif sequences or not. For all the 24,524 transcripts and 18,275 genes in the refLocus table, 16,030 transcripts and 11,995 genes have KLF9 binding peaks within their (-20 kb to 10 kb) neighborhoods of TSS.

Pathway Analyses

Canonical pathway analysis was performed using Ingenuity Pathway Analysis (IPA, http://www.ingenuity.com). The significance of association between KLF9 targets and a canonical pathway was measured using the ratio between the number of KLF9 targets in the pathway and the total number of molecules in the pathway database. A Fisher's exact test was performed to determine the association between KLF9 targets and canonical pathways.

Other Statistical Methods

Cell response data (excluding ChIP-Seq and RNA-Seq as described above) were analyzed using Prizm software (GraphPad, La Jolla, CA, www.graphpad.com). Statistical differences were evaluated by ANOVA followed by Student's t test and the Tukey multiple comparison tests as appropriate. All data are represented as mean value ± SEM. All results reported are representative of at least three independent replications.

Chapter 3

KLF9 Regulates a Transcriptional Network in GBM

3.1 KLF9 expression and Glioblastoma Cell Stemness

We previously found that induction of endogenous KLF9 expression associates with and is required for GBM neurosphere cell responses to forced differentiation and that enforced KLF9 expression inhibits GBM cell stemness and suppress the activity of Notch signaling, a known stemness-supporting pathway (Ying et al., 2011). In order to identify whole genome KLF9 targets linked to neurosphere cell stemness inhibition, we first established appropriate GBM neurosphere cell models and KLF9 induction conditions. The magnitude change in endogenous KLF9 expression was quantified in GBM-derived neurospheres following exposure to two inducers of GSC differentiation, retinoic acid (RA) and serum following EGF/FGF withdrawal (B. Campos et al., 2010; Galli et al., 2004; Pollard et al., 2009; Ying et al., 2011). These differentiating conditions induced a 10-12 fold increase in KLF9 expression concurrent with increased cell expression of the neuronal marker β-tubulin III (TUJ1) and the astroglial marker glial fibrillary acidic protein (GFAP) (Figure 3.1 A-B). Two human GBM neurosphere lines were engineered to express a Dox-inducible 3xFLAG-tagged KLF9 transgene (designated KLF9-GBM1a and KLF9-GBM1b) (Figure 3.1C), and Dox treatment for 48 hours induced KLF9 mRNA expression ~28-fold, comparable to the magnitude of endogenous KLF9 induction in response to RA and serum treatment (Figure 3.1D). KLF9 protein levels plateaued by 2 days of Dox treatment and quickly diminished 12-24 hours

after Dox withdrawal (Figure 3.1E). We examined the effects of 3xFLAG-KLF9 induction on the expression of molecular markers and drivers of GBM cell stemness. The percentage of CD133-positive cells in KLF9-GBM1a and KLF9-GBM1b neurospheres was reduced from 59.3% to 36.9% and from 64.0% to 41.6%, respectively, following KLF9 induction (Figure 3.1F). BMI1, Nestin, Olig2 and Sox2 expression levels also decreased in response to KLF9 induction (Figure 3.1G).

Figure 3.1. KLF9 is induced by forced differentiation by either RA or serum in GBM-derived neurospheres and reduces stem cell marker expression. (A) GBM1b cells were treated with either RA (1μM) or 1% FBS for 48hours. Expression of KLF9 was analyzed using quantitative real-time polymerase chain reaction (qRT-PCR). KLF9 expression is induced by FBS and RA. **(B)** GBM1b cells were cultured in neurosphere medium with 1% fetal bovine serum (FBS). FBS induces GFAP and TUJ1 expression as shown by immunofluorescence staining of control neurospheres and adherent serum-treated cells. **(C)** Schematic representation of the 3FLAG-tagged KLF9 construct. 3FLAG-tagged KLF9 ectopic expression vector was constructed using pTRIPZ vector (Open Biosystems) as described in Methods. TRE: tet-inducible promoter. UBC: human ubiquitin C promoter driving rtTA3 expression of rtTA3 and IRES-puro. rtTA3: reverse tet-transactivator. IRES: internal ribosome entry site. Puro': mammalian selectable marker. **(D)** Stable GBM1b cells established from cells infected with lentivirus containing Dox-inducible 3FLAG-tagged KLF9 (KLF9-GBM1b) were treated ± Dox for 48 hours. Expression of KLF9 was analyzed using qRT-PCR to show KLF9 expression is induced by Dox. **(E)** KLF9-GBM1b cells were treated ± Dox for 6 days and then passaged into Dox free medium for 2 days. Whole cell lysate was collected from cells on the days indicated and analyzed by immunoblot staining with anti-FLAG antibody demonstrating that KLF9 expression returns to baseline expression quickly following Dox withdrawal. **(F)** Stable GBM1a cells engineered to express a Dox-inducible N-terminal FLAG-tagged KLF9 (KLF9-GBM1a) and KLF9-GBM1b cells were treated ± Dox for 6 days and analyzed by flow cytometry using CD133 antibodies and isotope IgG control. A representative histogram and quantification of CD133+ cells are shown. **(G)**

GBM neurospheres were treated ± Dox for 6 days. Whole cell lysate was collected from the cells and analyzed using immunoblot staining. KLF9 reduces the protein level of BMI, Nestin, Olig2 and Sox2.

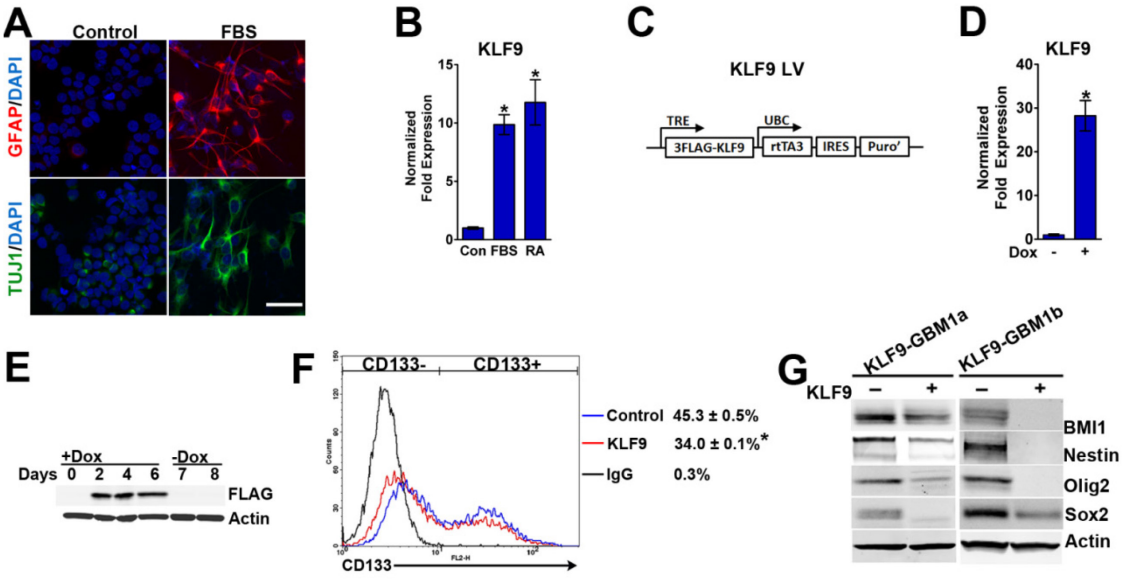
A
Control
FBS
GFAP/DAPI
TUJ1/DAPI
B
KLF9
Normalized Fold Expression
Con FBS RA
C
KLF9 LV
TRE
UBC
3FLAG-KLF9
rtTA3
IRES
Puro'
D
KLF9
Normalized Fold Expression
Dox - +
E
+Dox
-Dox
Days 0 2 4 6 7 8
FLAG
Actin
F
CD133-
CD133+
Control 45.3 ± 0.5%
KLF9 34.0 ± 0.1%*
IgG 0.3%
CD133
G
KLF9-GBM1a
KLF9-GBM1b
KLF9 – + – +
BMI1
Nestin
Olig2
Sox2
Actin

3.2 KLF9 Gene Binding and Gene Expression Signatures

A genome-wide analysis of KLF9 targets was performed by combining gene expression profiling and transcription factor binding site mapping in GBM neurospheres following KLF9 induction (strategy outlined in Figure 3.2A). KLF9-GBM1a and KLF9-GBM1b cells were treated ± Dox for 48 hours after which RNA was isolated, reverse transcribed to create cDNA libraries (Figure 3.2B) that were then subjected to deep sequencing. Over 16 million cDNA reads were generated for each of four samples representing two biological replicates (KLF9-GBM1a and KLF9-GBM1b) with or without KLF9 induction (Figure 3.2C). Consistency between the two RNA-Seq datasets was confirmed by heat map and scatter plot analyses (Figure 3.2D; Figure 3.2E). Of all the 24,524 RefSeq transcripts (18,275 genes), 1,550 transcripts (1,161 genes, 6.4%) were upregulated ($\log_2$ (Fold Change)) $\geq$ 0.8, Ying et al., 2014) and 2,843 transcripts (2,092 genes, 11.4%) were downregulated ($\log_2$ (Fold Change)) $\leq$ -0.8, Ying et al., 2014) in response to KLF9 induction (Figure 3.2F).

Genome-wide KLF9 binding sites were identified using ChIP-Seq in GBM neurospheres. Cellular chromatin bound by 3xFLAG-KLF9 was specifically precipitated using anti-FLAG antibody and the specific ChIP-enriched DNAs (150-250 bps in length) were further processed to produce libraries for ChIP-Seq (Figure 3.3A & B). The quality of the ChIP-Seq library was assessed using qPCR directed at Notch1 promoter elements previously found by us to bind KLF9 and mediate Notch1 suppression (Figure 3.3C-D) (Ying et al., 2011). Over 150 million reads were generated from ChIP-enriched DNA and input controls derived from two biological replicates (Figure 3.3E). Using CisGenome,

31,261 KLF9 binding peaks were called at a false discovery rate (FDR) of 1% (Ji et al., 2008) (Ying et al., 2014). The ChIP intensities within KLF9 binding peaks were consistent for both biological replicates as shown by heat map and scatter plot analyses (Figure 3.3F; Figure 3.3G). The majority of KLF9 binding sites were found to be located in intergenic regions (54.0%) and introns (35.9%), and binding sites localized less frequently to 5'- untranslated regions (7.3%), exons (10.9%) and 3' -untranslated regions (1.2%) (Figure 3.3H). KLF9-binding sites were found to be highly enriched around transcription start sites (TSSs) (Figure 3.3I). The top 500 KLF9 ChIP-Seq peaks as ranked by their FDR were used to perform de novo motif discovery analysis. The consensus sequence 5' G/A G/T GGG C/T G G/T GGCN 3' was identified as the most enriched KLF9 binding motif (Figure 3.3J). This motif closely resembles the motifs of two Sp1/KLF family members, KLF4 (5'-NGGG T/C G G/T GG-3') and Sp1 (5'-GGGGGNGGGG-3') (Figure 3.3K).

Figure 3.2. Identification of KLF9 gene expression and binding signatures by ChIP-Seq and RNA-Seq analyses. (A) Flow chart of analyses used to identify KLF9 gene targets. KLF9-GBM1a and KLF9-GBM1b cells were treated ± Dox to induce KLF9 expression for 48 hours. cDNA and ChIP DNA libraries obtained from the treated cells were analyzed by RNA-Seq and ChIP-Seq to reveal KLF9 binding peaks and differentially expressed transcripts following KLF9 induction, respectively. KLF9 targets, differentially expressed transcripts that are also bound by KLF9 following KLF9 induction, were determined by combing ChIP-Seq and RNA-Seq data. **(B)** KLF9-GBM1a and KLF9-GBM1b cells were treated ±Dox for 48 hours to induce KLF9 expression. RNA was collected, reverse transcribed and fragmented to create a cDNA library for RNA-Seq analysis. Fragment length was between 150bps and 500bps. **(C)** Total number of RNA-seq reads and the percentage of reads aligned to the hg18 using TopHat are shown for control samples from KLF9-GBM1a and KLF9-GBM1b cells (indicate as control A and control B, respectively) and samples treated with Dox for 48hours from KLF9-GBM1a and KLF9-GBM1b cells (indicated as KLF9 A and KLF9 B, respectively). **(D)** Heatmap of expression pattern for differentially expressed genes from RNA-Seq data. Reads per kilobase per million mapped reads (RPKM) for each differentially expressed gene was calculated by R bioconductor package GenomicRanges. In the count table, each column represents a peak region and each row corresponds to a sample. The heatmap was generated according to the count table with scaling across the samples for each gene. **(E)** RNA-Seq reproducibility scatter plot. The $\log_2$ (Fold Change) for each gene in each cell line was calculated. The $\log_2$ (Fold Change) for KLF9-GBM1b genes is plotted against that of KLF9-GBM1a genes. **(F)** Volcano plot of all genes

analyzed for differential expression. The $\log_2$ (Fold Change) between control and Dox-treated cells is plotted along the x axis. The false discovery rate (FDR) for each gene is plotted on the y axis ($-\log_2$ scale). Red indicates genes that have an FDR less than or equal to 0.05 and a $\log_2$ (fold change) greater than 0.8. The dashed horizontal line corresponds to FDR=0.05.

A

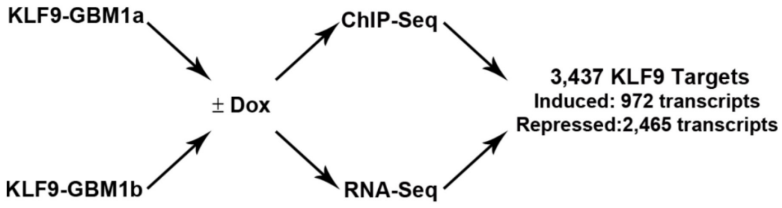

B

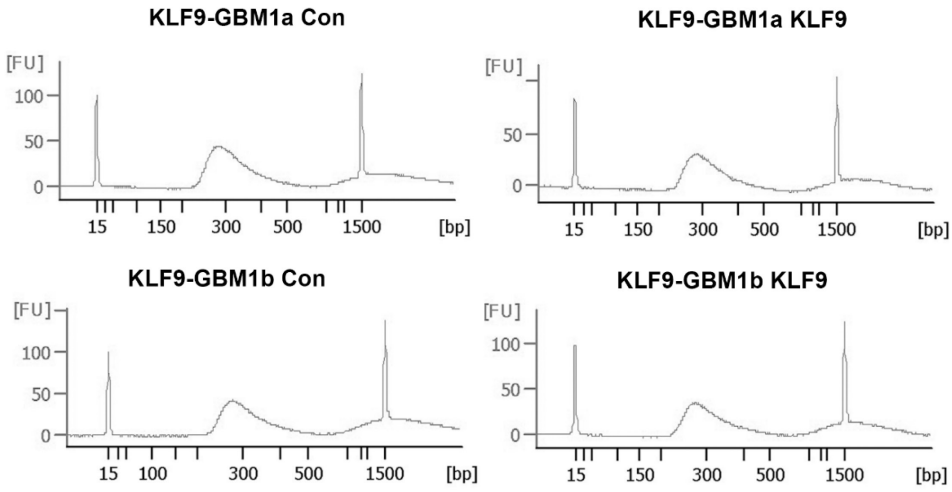

C

RNA-Seq

Sample	Total Reads	Percentage Aligned
Control KLF9-GBM1a	29,544,989	84.25%
Control KLF9-GBM1b	16,062,617	83.19%
KLF9 KLF9-GBM1a	33,853,911	83.41%
KLF9 KLF9-GBM1b	19,974,360	82.70%

D

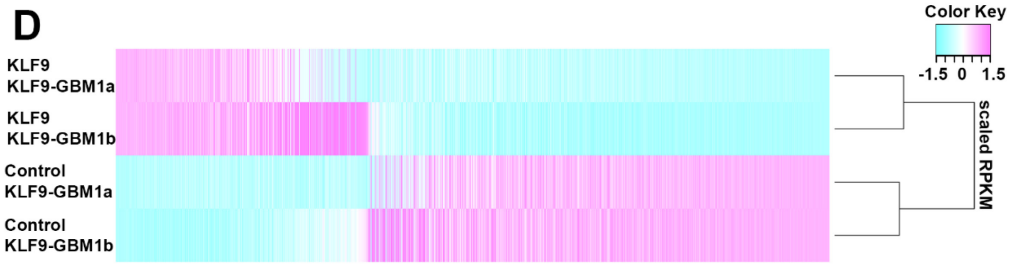

E

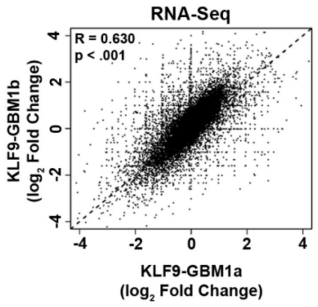

F

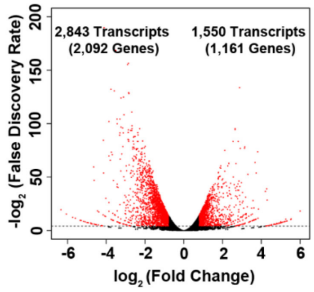

j

Figure 3.3. Identification of KLF9 gene expression and binding signatures by ChIP-Seq and RNA-Seq analyses. (A) KLF9-GBM1a cells were treated with Dox for 48 hours. anti-FLAG antibody but not nonimmune IgG specifically precipitated FLAG-tagged KLF9 from fragmented DNA-protein complexes. **(B)** KLF9-GBM1a cells were treated with ±Dox for 48 hours. DNA fragments precipitated had a length was between 150bps and 250bps. **(C)** Schematic of the human Notch1 promoter (-10,000 to +1 bp relative to the ATG site; BTE1: GGGGCGGGGC; BTE2: GGGGCGGAGC; Notch1 transcription start site: -262 bp). Segment A and B indicate the locations of amplified sequences used for analysis of chromatin immunoprecipitation as described in (D). **(D)** DNA fragments were precipitated with anti-FLAG antibody and analyzed with polymerase chain reaction (PCR) primer pairs designed to amplify BTE-free and BTE-containing Notch promoter sequences. anti-FLAG antibody coprecipitated BTE-containing (segment B) but not BTE-free (segments A) promoter regions. **(E)** Total number of ChIP-seq reads and the percentage of reads aligned to the hg18 using Bowtie are shown for control samples from KLF9-GBM1a and KLF9-GBM1b cells (indicate as control A and control B, respectively) and samples treated with Dox for 48hours from KLF9-GBM1a and KLF9-GBM1b cells (indicated as KLF9 A and KLF9 B, respectively). **(F)** Heatmap of IP intensities for identified peaks in KLF9 ChIP-Seq data. The number of reads aligned to the peak regions by each of the four ChIP samples was counted by R bioconductor package GenomicRanges and then normalized for the library size for each sample. In the count table, each column represents a peak region and each row corresponds to a sample. The heatmap was generated according to the count table with scaling across the samples for a given peak. The two control samples from both cell

lines are clustered together and the two IP samples are clustered together by hierarchical clustering with complete linkage. **(G)** ChIP-Seq reproducibility scatter plot. After correcting for library size, the $\log_2$ IP intensity for each peak in both cell lines was also calculated. The $\log_2$ IP intensity for cell line KLF9-GBM1b is plotted against that of cell line KLF9-GBM1a. **(H)** The genomic distribution of KLF9-binding sites relative to human genes shows that the majority of KLF9 binding peaks are located in intergenic regions and introns. **(I)** The peak frequency near known transcription start sites (TSS)s reveals that KLF9-binding sites are enriched around TSSs. **(J)** The KLF9-binding motif was discovered using a CisGenome de novo motif discovery algorithm. The enrichment score of the KLF9 binding motif, determined by dividing its occurrence frequency in randomly sampled genomic matched control sequences, is 5.45. **(K)** When compared to all know motifs in JASPAR (Bryne et al., 2008), KLF4 and Sp1 motifs are the most similar ones to our discovered KLF9 motif. The enrichment scores for the KLF4 and Sp1 motifs, determined by dividing its occurrence frequency in randomly sampled genomic matched control sequences, are 3.34 and 2.59 respectively. Abbreviations: BTE, basic transcription element; GBM, glioblastoma; IP, Immunoprecipitation KLF, Krüppel-like family of transcription factor, Sp, specificity protein, GBM, glioblastoma; IP, Immunoprecipitation; KLF, Krüppel-like family of transcription factor; TSS, Transcriptional Start Site; UTR, untranslated region.

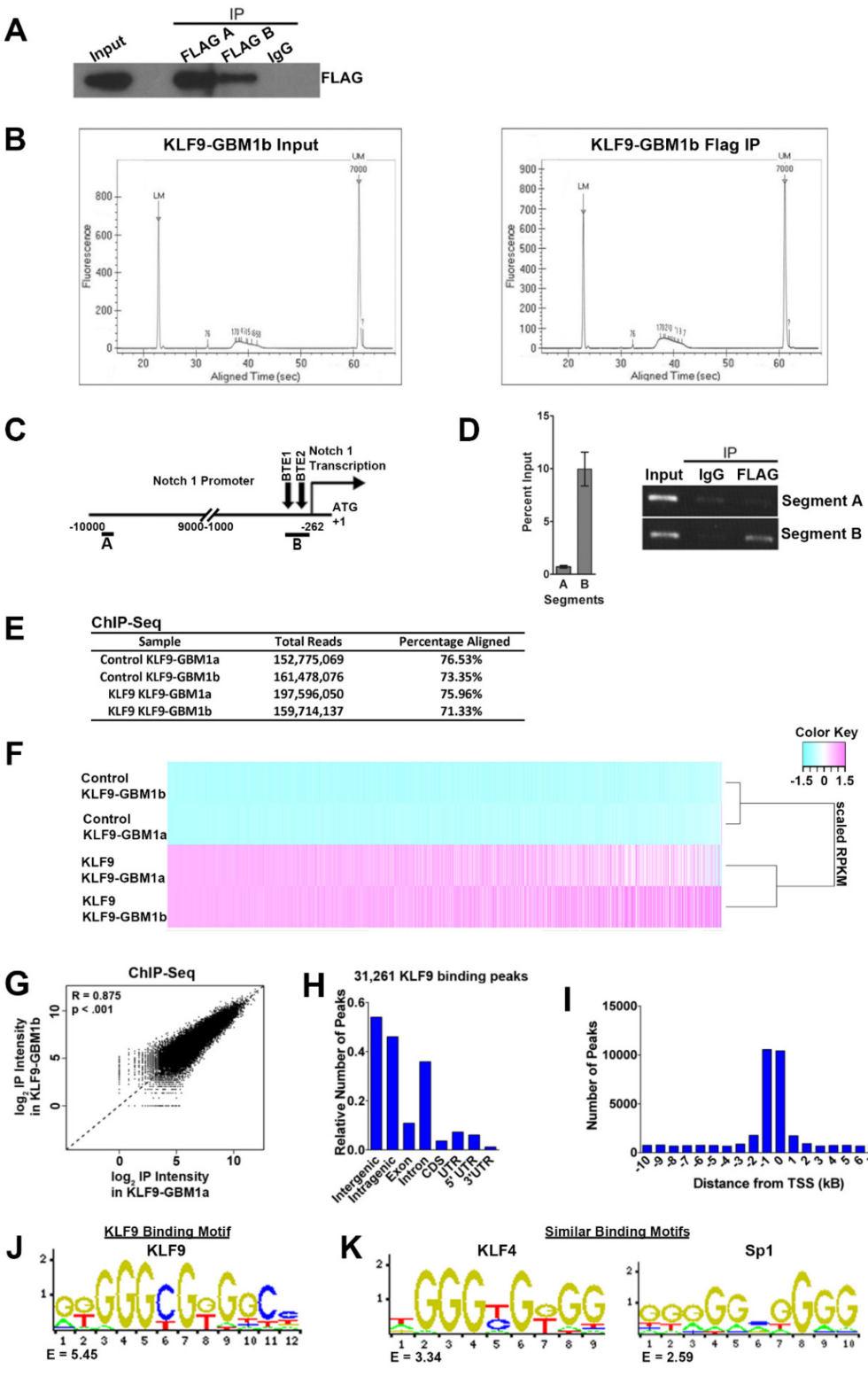
A
IP
Input
FLAG A
FLAG B
IgG
FLAG
B
KLF9-GBM1b Input
KLF9-GBM1b Flag IP
Fluorescence
Aligned Time (sec)
LM
UM
7000
C
Notch 1 Promoter
BTE1
BTE2
Notch 1 Transcription
ATG
+1
-10000
9000-1000
-262
A
B
D
Percent Input
Segments
IP
Input
IgG
FLAG
Segment A
Segment B
E
ChIP-Seq
Sample | Total Reads | Percentage Aligned
Control KLF9-GBM1a | 152,775,069 | 76.53%
Control KLF9-GBM1b | 161,478,076 | 73.35%
KLF9 KLF9-GBM1a | 197,596,050 | 75.96%
KLF9 KLF9-GBM1b | 159,714,137 | 71.33%
F
Color Key
-1.5 0 1.5
Control KLF9-GBM1b
Control KLF9-GBM1a
KLF9 KLF9-GBM1a
KLF9 KLF9-GBM1b
scaled RPKM
G
ChIP-Seq
R = 0.875
p < .001
log2 IP Intensity in KLF9-GBM1b
log2 IP Intensity in KLF9-GBM1a
H
31,261 KLF9 binding peaks
Relative Number of Peaks
Intergenic
Intragenic
Exon
Intron
CDS
5' UTR
3'UTR
I
Number of Peaks
Distance from TSS (kB)
J
KLF9 Binding Motif
KLF9
E = 5.45
K
Similar Binding Motifs
KLF4
E = 3.34
Sp1
E = 2.59

3.3 Analysis of KLF9-regulated Gene Targets

KLF9 ChIP-Seq and RNA-Seq datasets were combined to establish gene targets directly regulated by KLF9 (i.e. genes differentially expressed in response to KLF9 induction and having one or more KLF9-binding peaks within -20kb to +10kb of their TSSs). The expression of KLF9-bound and unbound genes is summarized in Figure 3.4A. Among the 2,843 transcripts downregulated by KLF9, 2,465 (86.7%) fulfilled these criteria. This number was significantly higher than random (i.e. the number of KLF9 bound transcripts found among 2,843 transcripts selected randomly 1,000 times from the genome; see Figure 3.4B, top panel, p-value =0). In contrast, among the 1,550 upregulated transcripts, only 972 (62.7%) were directly bound by KLF9, a number indistinguishable from that found in 1,000 randomly selected sets of 1,550 transcripts (Figure 3.4B, bottom panel). These results indicate that the predominant role of KLF9 is to serve as a transcriptional repressor. Therefore, we focused the functional analyses described below exclusively on the 2,465 KLF9 downregulated transcripts (Ying et al., 2014).

Gene function annotation and Ingenuity Pathway Enrichment Analysis (IPA) were performed using KLF9 downregulated transcripts, as described above (Thomas & Bonchev, 2010; Xia & Wishart, 2010). The top pathways enriched with KLF9 downregulated targets included those active in cancer regulation (e.g. molecular mechanisms of cancer, CXCR4 signaling, integrin signaling and notch signaling), stem cell pluripotency signaling (mouse embryonic stem cell pluripotency) and signaling in

neurons (axonal guidance signaling, CREB signaling in neurons and semaphorin signaling in neurons) (Figure 3.4C).

Figure 3.4. Analyses of KLF9-regulated gene targets. (A) The percentage of all genes that show differential expression following KLF9 induction and had one or more KLF9 binding peaks within +20 to-10 kb of their TSS. **(B)** The frequencies of KLF9 binding to 2,092 randomly selected down-regulated genes (top panel) or to 1,161 randomly selected up-regulated genes (bottom panel) were determined 1,000 times to generate null distributions (red bars). The dashed lines correspond to the number of KLF9 down-regulated or up-regulated genes identified by ChIP-Seq and RNA-Seq. Only the number of KLF9 down-regulated genes differs significantly from the null distribution. **(C)** Pathways enriched in KLF9 down-regulated gene targets determined by Ingenuity Pathway Analysis. Pathways are ranked by –log(pvalue) calculated by Fisher's exact test. The ratio was calculated by dividing the number of KLF9 targets genes in the pathway with the total number of genes in the pathway (ratio threshold, 0.05).GNRH, gonadotropin-releasing hormone; NFAT, nuclear factor of activated T cells; CREB, cAMP-response element-binding protein.

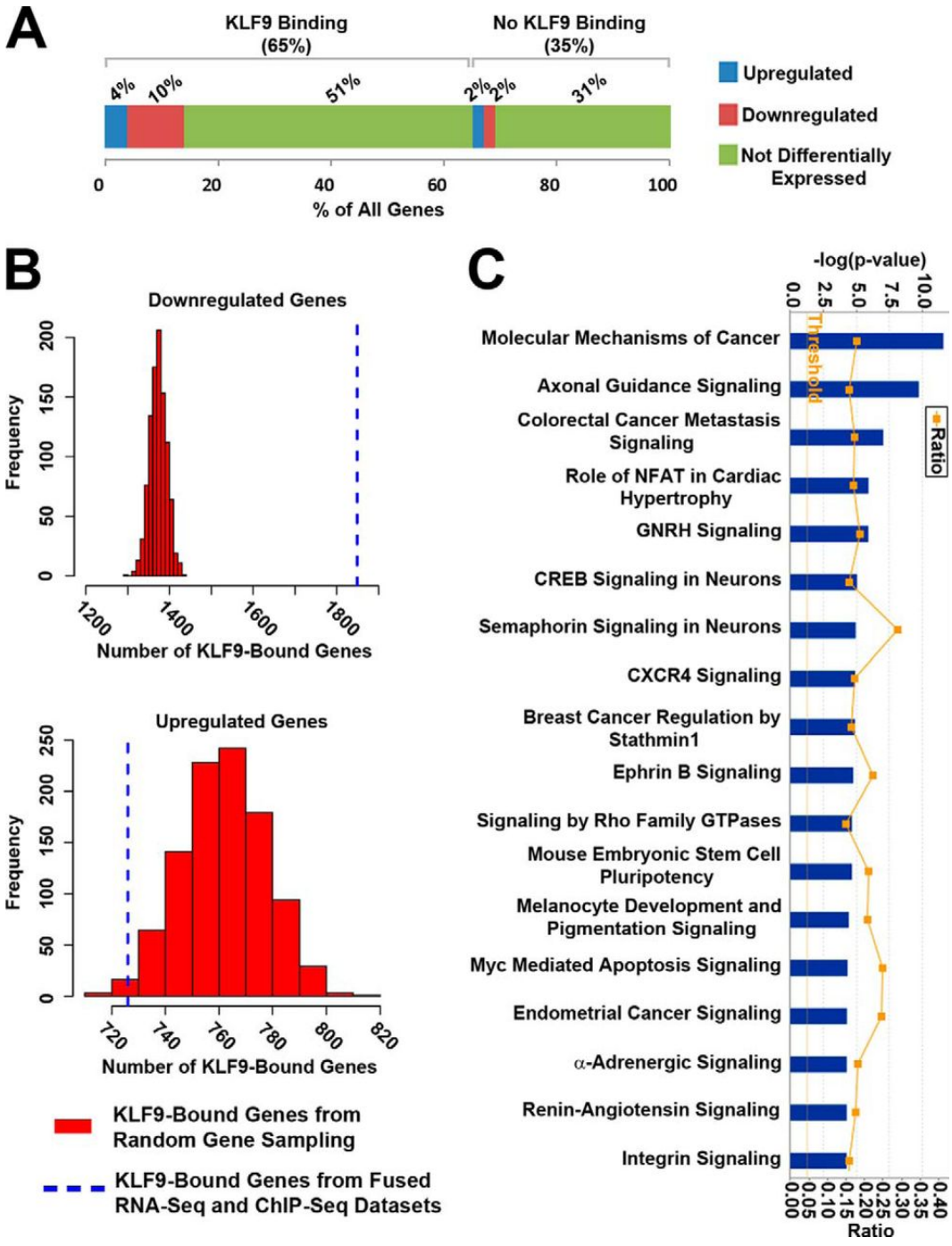
A
KLF9 Binding
(65%)
No KLF9 Binding
(35%)
4%
10%
51%
2%
2%
31%
0
20
40
60
80
100
% of All Genes
Upregulated
Downregulated
Not Differentially
Expressed
B
Downregulated Genes
Frequency
0
50
100
150
200
1200
1400
1600
1800
Number of KLF9-Bound Genes
Upregulated Genes
Frequency
0
50
100
150
200
250
720
740
760
780
800
820
Number of KLF9-Bound Genes
KLF9-Bound Genes from
Random Gene Sampling
KLF9-Bound Genes from Fused
RNA-Seq and ChIP-Seq Datasets
C
-log(p-value)
0.0
2.5
5.0
7.5
10.0
Threshold
Molecular Mechanisms of Cancer
Axonal Guidance Signaling
Colorectal Cancer Metastasis
Signaling
Role of NFAT in Cardiac
Hypertrophy
GNRH Signaling
CREB Signaling in Neurons
Semaphorin Signaling in Neurons
CXCR4 Signaling
Breast Cancer Regulation by
Stathmin1
Ephrin B Signaling
Signaling by Rho Family GTPases
Mouse Embryonic Stem Cell
Pluripotency
Melanocyte Development and
Pigmentation Signaling
Myc Mediated Apoptosis Signaling
Endometrial Cancer Signaling
α-Adrenergic Signaling
Renin-Angiotensin Signaling
Integrin Signaling
Ratio
0.00
0.05
0.10
0.15
0.20
0.25
0.30
0.35
0.40
Ratio

A subset of the KLF9 downregulated genes selected from pathways highly ranked by IPA (e.g. molecular mechanisms of cancer, CXCR4 signaling, Integrin signaling, Notch signaling) was further validated by qPCR in KLF9-GBM1b neurospheres and low-passage primary GBM neurospheres (GBM 551) (Figure 3.5A). The validated genes included Notch pathway members *NOTCH1*, *PSEN2* and *NUMBL; CXCR4*—a gene encoding a chemokine receptor that contributes to cytoskeletal organization and mediates metastasis in various cancers and *CAMK2G*—a gene encoding a serine/threonine protein kinase that has been associated with the proliferation, resistance and survival of cancer cells. Integrin signaling, which modulates multiple cellular processes including cell adhesion and migration, tumor cell invasion and cell stemness (Lathia et al., 2010; Takada, Ye, & Simon, 2007), was one of the top ranked and validated pathways enriched with KLF9 suppressed gene targets. *ITGA6*, encoding integrin α6 receptor subunit, was downregulated by up to 89% following KLF9 induction. Other downstream components of the integrin signaling pathway, such as *ARPC1B, CAPN5, GIT1* and *MYLK,* were also validated to be downregulated following KLF9 induction by up to 88%, 74%, 72% and 71%, respectively (Figure 3.5A). The presence of KLF9 binding peaks near the TSS of 12 KLF9 repressed genes was validated further by ChIP-PCR (Figure 3.5B & C). Quantitative ChIP-PCR was also employed to compare the enrichment of ChIP-Seq identified KLF9-binding peaks of 7 targets to the enrichment of genomic regions located either 10 or 20kb upstream. (Figure 3.5D). The ChIP-Seq identified peaks showed higher enrichment. These validation results render credibility to the predictive value of our genome-wide data.

Figure 3.5. Validation of KLF9 Gene Expression Regulation and Gene Binding. (A) 3xFLAG-KLF9 expression was induced in KLF9-GBM1b cells and low-passage primary GBM derived neurospheres (551) by Dox and lentivirus, respectively, for 48hours. Expression inhibition of a subset of the KLF9 target genes identified to be downregulated by ChIP-Seq and RNA-Seq analyses was validated by quantitative RT-PCR. **(B-D)** KLF9-GBM1b cells were treated + Dox and subjected to ChIP-PCR using anti-FLAG antibody and primer pairs designed to amplify promoter regions of KLF9 target genes containing at least one KLF9 binding motif (See Materials and Methods for details). **(B)** Representative tracks show the locations of KLF9 ChIP-Seq peaks proximal to the transcription start site (TSS)s of KLF9 gene targets identified by ChIP-seq and RNA-seq analyses. Red boxes indicate peaks validated by ChIP qPCR. **(C)** Quantitative ChIP-PCR analysis showing enrichment of the KLF9-binding motifs described in (B). **(D** Quantitative ChIP-PCR showing selective enrichment of KLF9-binding motifs in downregulated KLF9 target genes. Enrichment of ChIP-Seq identified binding peaks located in 7 downregulated KLF9 targets and DNA regions -10kb or -20kb upstream of these peaks is shown. Results show that KLF9-binding motifs are selectively enriched by anti-FLAG ChIP in Dox-treated KLF9-GBM1b cells. Data represents mean ± SEM; *, $p < .05$. See Materias and Methods for details.

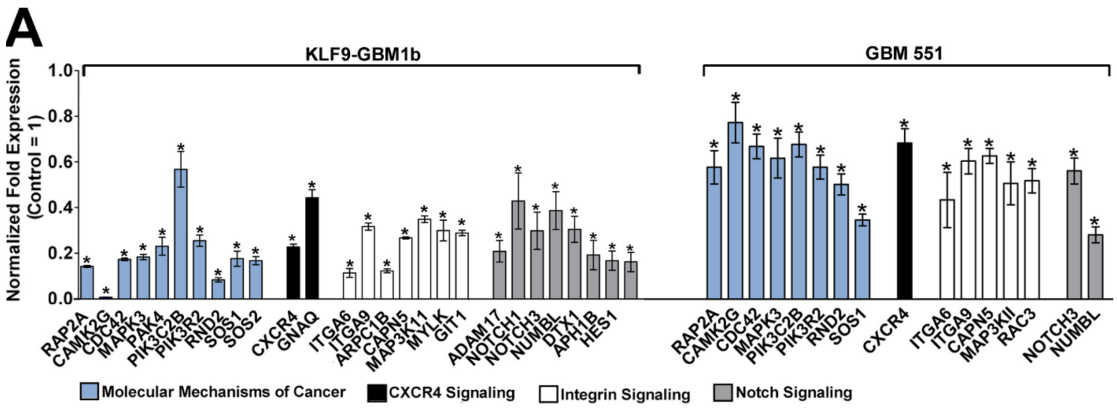
A
KLF9-GBM1b
GBM 551
Normalized Fold Expression (Control = 1)
1.0
0.8
0.6
0.4
0.2
0.0
RAP2A
CAMK2G
CDC42
MAPK3
PAK4
PIK3C2B
PIK3R2
RND2
SOS1
SOS2
CXCR4
GNAQ
ITGA6
ITGA9
ARPC1B
CAPN5
MAP3K11
MYLK
GIT1
ADAM17
NOTCH1
NOTCH3
NUMBL
DTX1
APH1B
HES1
RAP2A
CAMK2G
CDC42
MAPK3
PIK3C2B
PIK3R2
RND2
SOS1
CXCR4
ITGA6
ITGA9
CAPN5
MAP3KII
RAC3
NOTCH3
NUMBL
Molecular Mechanisms of Cancer
CXCR4 Signaling
Integrin Signaling
Notch Signaling

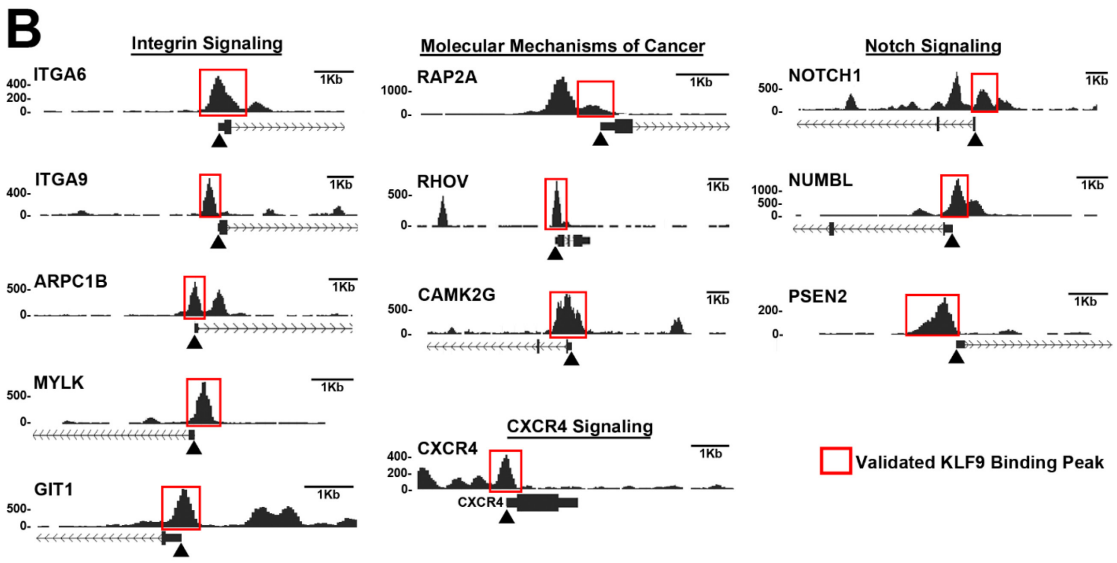
B
Integrin Signaling
Molecular Mechanisms of Cancer
Notch Signaling
ITGA6
RAP2A
NOTCH1
ITGA9
RHOV
NUMBL
ARPC1B
CAMK2G
PSEN2
MYLK
GIT1
CXCR4 Signaling
CXCR4
1Kb
Validated KLF9 Binding Peak

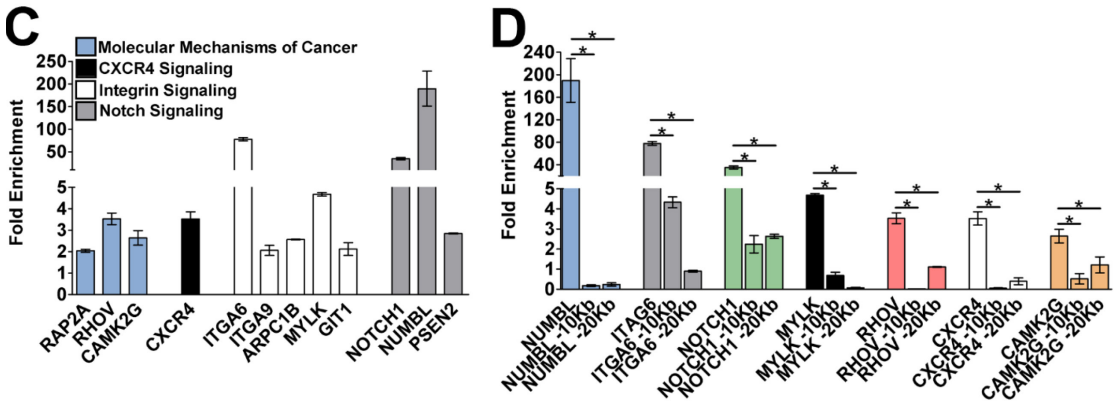
C
Molecular Mechanisms of Cancer
CXCR4 Signaling
Integrin Signaling
Notch Signaling
Fold Enrichment
RAP2A
RHOV
CAMK2G
CXCR4
ITGA6
ITGA9
ARPC1B
MYLK
GIT1
NOTCH1
NUMBL
PSEN2
D
Fold Enrichment
NUMBL -10Kb
NUMBL -20Kb
ITAG6 -10Kb
ITGA6 -20Kb
NOTCH1 -10Kb
NOTCH1 -20Kb
MYLK -10Kb
MYLK -20Kb
RHOV -10Kb
RHOV -20Kb
CXCR4 -10Kb
CXCR4 -20Kb
CAMK2G -10Kb
CAMK2G -20Kb

Chapter 4

KLF9 negatively regulates GSCs, in part, by suppressing integrin α6 gene expression and downstream functions

Integrin α6 is the most upstream component of the integrin signaling pathway that was identified to be regulated by KLF9 (Figure 4.1). Also, among the integrin pathway genes, *ITGA6* was found to be one of the most downregulated by KLF9 and its promoter had one of the most highly enriched KLF9-bound chromatin peaks. A detailed analysis of the integrin signaling pathway revealed that KLF9 inhibits GSC self-renewal and differentiates GBM stem cells, in part, by suppressing integrin-α6 gene expression and downstream functions.

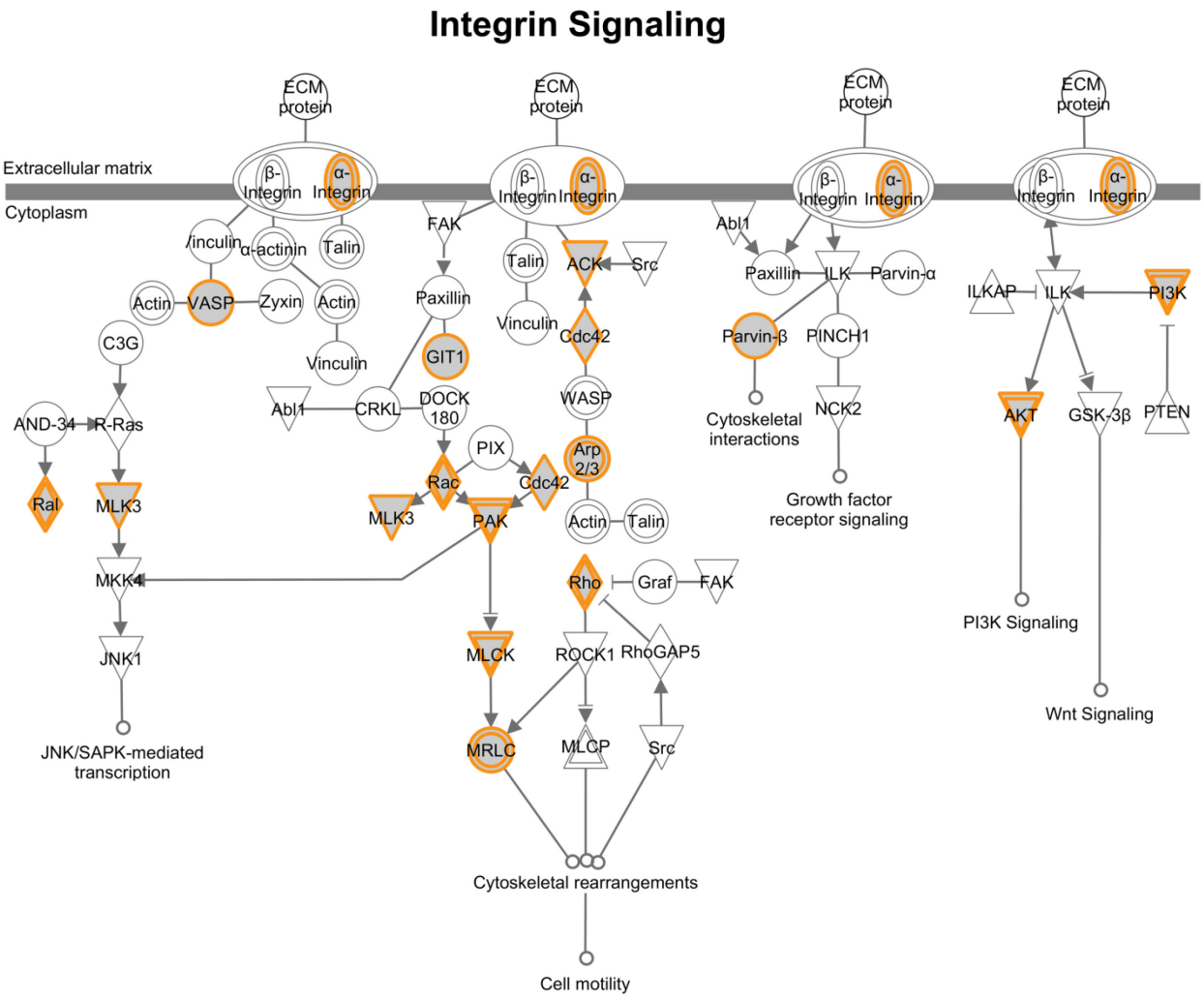

Figure 4.1. Integrin signaling pathway enriched with KLF9 downregulated targets. Ingenuity pathway analysis (IPA) representation of the integrin signaling pathway. Proteins shown in orange indicate proteins whose genes are bound and downregulated by KLF9.

4.1 KLF9 directly binds ITGA6 promoter

One KLF9 binding motif was identified in the human ITGA6 promoter at -396 bps relative to the TSS (referred to as basic transcription element, BTE, site) (Figure 4.2A). This site was also found to be conserved in the mouse ITGA6 promoter (data not shown). KLF9 binding to this ITGA6 promoter region was confirmed in KLF9-GBM1b neurospheres by ChIP-PCR. FLAG-KLF9 co-precipitated with ITGA6 promoter regions containing the BTE site (segment A and B) but not with control regions lacking a BTE site (segment C and D) (Figure 4.2A and B). BTE-containing segments A and B were enriched compared with control segments C and D (Fig. 3.2B, 16.4 and 67.8 fold enrichment for segments A and B vs. 4.3 and 0.9 fold enrichment for segments C and D, respectively).

4.2 KLF9 down-regulates integrin 6 expression

The effects of KLF9 induction on the level of integrin α6 mRNA and protein were quantified in two GBM neurosphere lines and two low passage primary GBM neurosphere isolates. KLF9 induction inhibited *ITGA6* mRNA levels in all cell cultures (Figure 4.3A) and also inhibited integrin α6 protein expression (Figure 4.3B). We further examined the dynamics of *ITGA6* expression in response to ectopic KLF9 expression controlled by Dox. ITGA6 expression levels changed inversely with KLF9 levels; *ITGA6* expression decreased along with *KLF9* induction and rapidly returned to baseline levels after Dox withdrawal (Figure 4.3C). The effect of KLF9 expression on the number of

integrin α6-positive cells within neurospheres mirrored its effects on bulk-culture integrin α6 levels. KLF9 induction reduced integrin α6-positive neurosphere cells within neurospheres from 14.4% to 7.0% (Figure 4.3D).

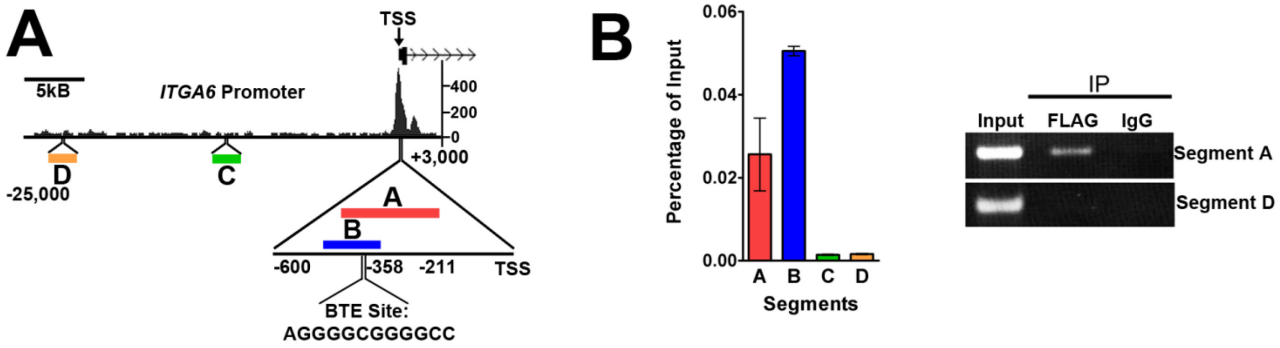

Figure 4.2. KLF9 directly binds to the ITGA6 promoter. (A) Schematic of the human ITGA6 promoter with a KLF9 binding peak identified by ChIP-Seq (-25,000 to +3,000bp relative to TSS). Primers were designed for segments A-D. **(B & C)** Dox-treated KLF9-GBM1b cells were subjected to ChIP using FLAG antibody and mouse IgG. Selective enrichment in qPCR **(B)** and conventional PCR **(C)** was detected for BTE-containing segments A and B but not for control segments C and D.

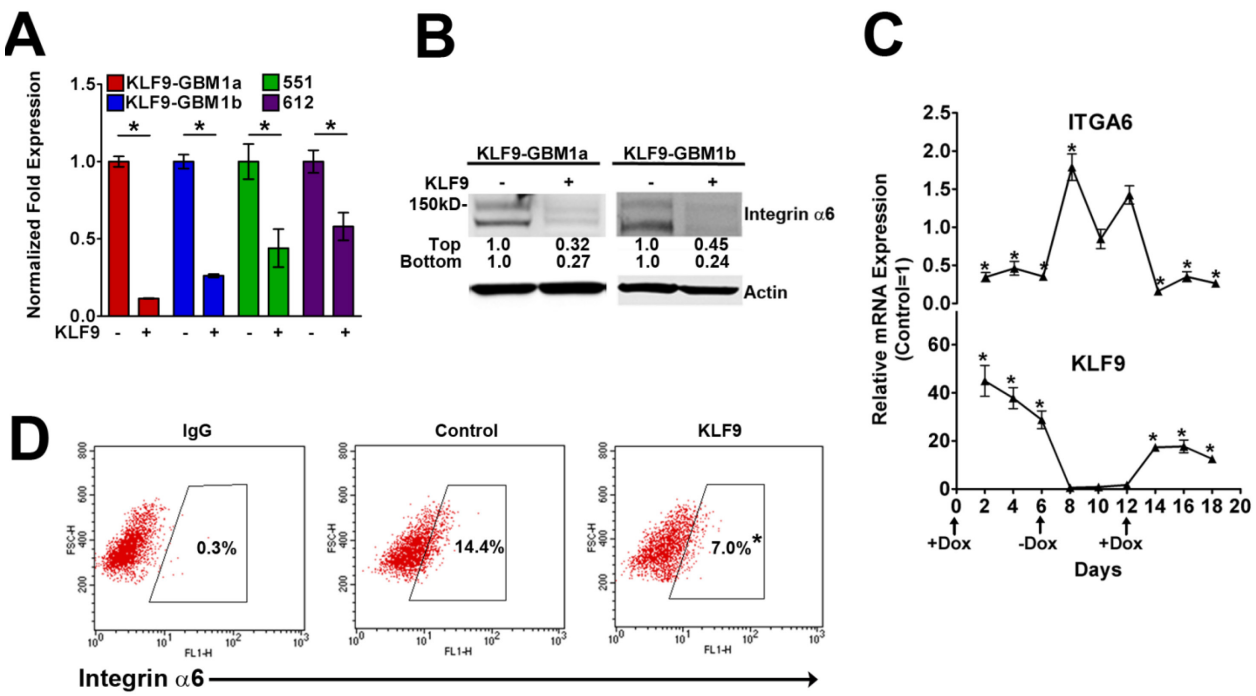

Figure 4.3. KLF9 regulates integrin α6 expression. (A) *ITGA6* expression was measured by qPCR in GBM neurosphere lines and primary GBM neurospheres after KLF9 induction for 48h. **(B)** KLF9 was induced by Dox for 96h in GBM1a and GBM1b cells. Membrane protein extraction was subjected to immunoblotting against integrin α6. **(C)** KLF9-GBM1b cells were treated with Dox for 6 days, passaged to Dox-free medium for 6 days, and then passage again to Dox-containing medium for 6 days. Cells were collected on the days indicated and subjected to qPCR for *ITGA6* and *KLF9*. *ITGA6* expression levels changed inversely with Dox-induced KLF9 expression. **(D)** KLF9-GBM1b cells were treated ± Dox for 96h and subjected to flow cytometry using anti-Integrin-α6-FITC antibody or isotype IgG control. Representative dot plots and the percentages of Integrin α6-positive cells are shown. Data represents mean ± SEM; *: $p<0.01$, t test.

4.3 ITGA6 repression by KLF9 regulates GBM neurosphere cell adhesion and migration and stem cell marker expression

We asked if KLF9 modulates GBM cell behavior and stemness by regulating integrin α6 expression. To this end, we examined how KLF9 induction modulates GSC adhesion and migration on laminin, an integrin α6 ligand and essential component of the perivascular niche that supports neoplastic stem-like cells (Lathia et al., 2012; Q. Shen et al., 2008). KLF9 was induced in GBM neurospheres for 4 days and cells were then transferred to laminin-coated tissue culture substrata. Control cells rapidly attached and spread within 2-6 hours. KLF9 induction inhibited cell spreading (Figure 4.4A, left panel) and decreased cell adhesion by 25-71% (Figure 4.4A, right panel). We asked if enforced integrin α6 expression could rescue the cell adhesion defects induced by KLF9. Lentivirus vectors were used to express KLF9, integrin α6, or both in GBM neurospheres for 48-96 hours prior to assessing cell adhesion and spreading on laminin. Enforced integrin α6 expression partially rescued the effect on cell spreading (Figure 4.4A, left panel) and abrogated KLF9's ability to inhibit cell adhesion by approximately 71%, 48%, 64% in the three GBM neurosphere cultures (Figure 4.4A, right panel). Migration through laminin-coated transwell membranes was reduced in response to KLF9 induction by 62-86% (Figure 4.4B). Enforced expression of integrin α6 also rescued cells from KLF9-induced cell migration inhibition (Figure 4.4B).

Integrin α6 is highly expressed in various stem cells (Lathia et al., 2010; Shinohara, Avarbock, & Brinster, 1999) and cell surface expression was found to be enriched in

GSCs and to maintain GSC self-renewal and tumorigenicity (Lathia et al., 2010). We hypothesized that KLF9 regulates glioma cell stemness in part by regulating integrin α6 expression. KLF9 downregulated the expression of multiple inducers and markers of the stem-like phenotype GBM neurospheres (Figure 6C). Enforced integrin α6 expression reversed KLF9-induced suppression of CD133, Nestin, Sox2, BMI1 and Olig2 expression (Figure 4.4C). These results support the conclusion that KLF9 regulates molecular markers and drivers of GSC stemness, in part, by repressing *ITGA6*.

4.4 Integrin 6 expression rescues KLF9-induced growth inhibition of glioma xenografts

We found previously that KLF9 induction reduces the growth of intracranial tumor xenografts established from GBM neurospheres and extends the survival of mice bearing xenograft tumors (Ying et al., 2011). We hypothesized that KLF9 reduces xenograft tumor growth in part by repressing integrin α6 expression. We investigated the effects of expressing KLF9, integrin α6, or both on the growth of intracranial (i.c.) xenografts established from GBM-derived neurospheres. KLF9, integrin α6, or both were expressed in GBM neurosphere cells by lentivirus infection (Figure 4.5A) and cells were implanted to the brains of immunocompromised mice 48h after virus infection. Mice (n=4 for each group) were sacrificed 60 days post transplantation and coronal histological brain sections were examined for tumor size. Enforced KLF9 expression significantly inhibited tumor xenograft growth compared to control xenografts (tumor volume ± SEM (mm^3):

9.0 ± 2.9 vs 34.4 ± 6.1, $p<0.01$). Integrin α6 expression rescued tumor growth inhibition induced by KLF9 (Figure 4.5B-C).

Figure 4.4. ITGA6 repression by KLF9 regulates GBM neurosphere cell adhesion, migration and stem cell marker expression. KLF9, ITGA6, or both were expressed in GBM neurosphere lines and primary GBM neurospheres. **(A)** KLF9-GBM1b cells were passaged onto laminin-coated culture substrata for 2-6h. Cell adhesion was evaluated by phase contrast microscopy (Left Panel) and quantitatively by spectrophotometric analysis of crystal violet-stained cells (Right Panel). KLF9 expression inhibited cell adhesion. Co-expressing Integrin α6 partially rescued cell adhesion inhibition by KLF9. **(B)** Cells were passaged to laminin-coated transwell membranes. Cell migration was evaluated 24 hours later by analyzing DAPI-stained cells. KLF9 expression inhibited transmembrane migration, which was rescued by Integrin α6. **(C)** Transfected KLF9-GBM cells were maintained in neurosphere growth medium for 96 hrs. Whole cell lysates were subjected to immunoblotting to assess the expression of FLAG-KLF9, Integrin α6, and the stem cell markers CD133, Nestin, SOX2, BMI1, and Olig2. Relative expression of each protein (normalized to Actin) is shown below each band. KLF9 inhibited the expression of stem cell markers and this response was partially rescued by enforced Integrin α6 expression.

Bar: 50 μm. Data represents mean ± SEM; *: $p<0.05$, **: $p<0.01$, ***: $p<0.001$, One-way ANOVA followed by Tukey test.

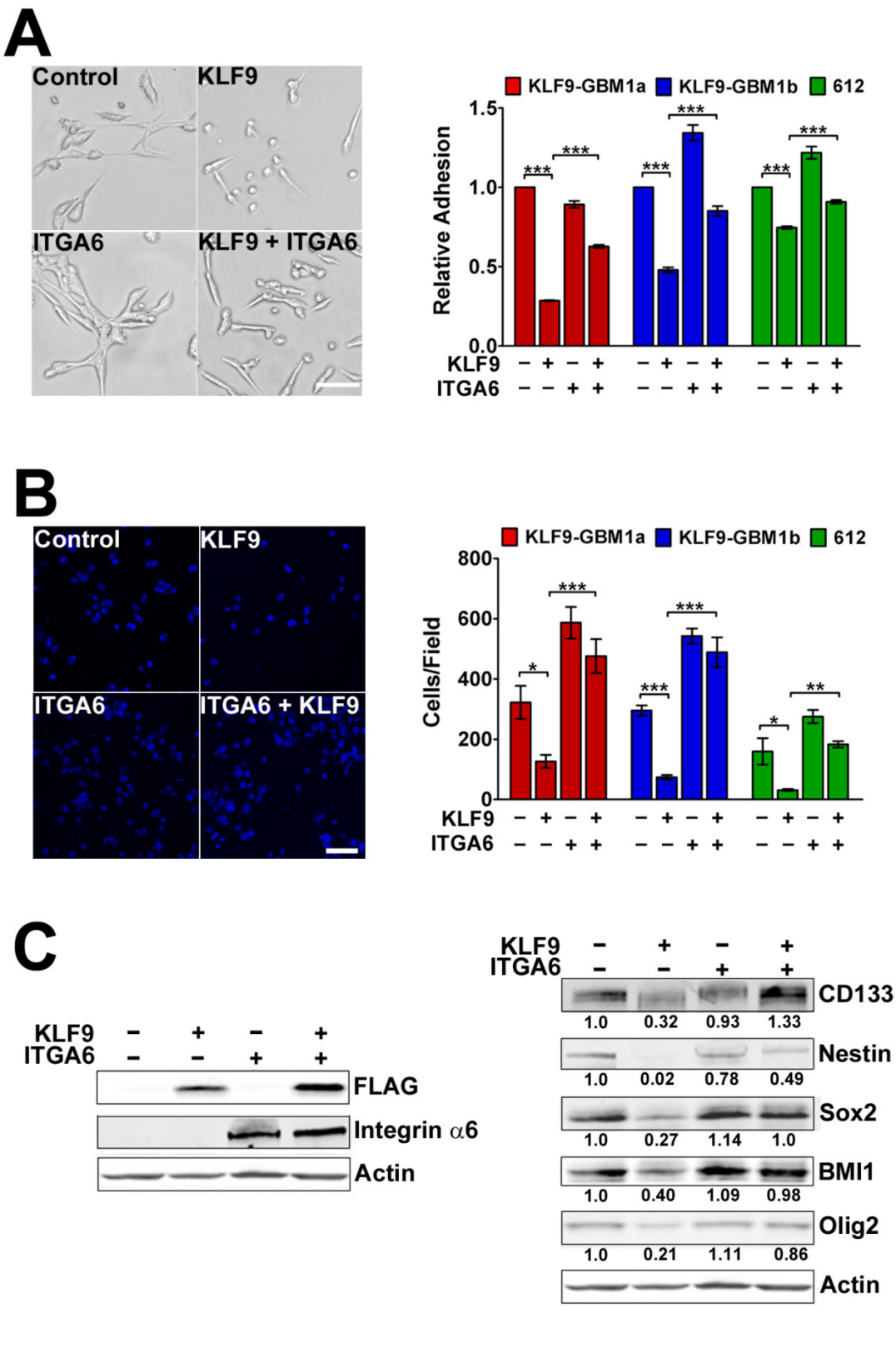
A
Control
KLF9
ITGA6
KLF9 + ITGA6
KLF9-GBM1a
KLF9-GBM1b
612
Relative Adhesion
1.5
1.0
0.5
0.0
***
KLF9 – + – + – + – + – + – +
ITGA6 – – + + – – + + – – + +
B
Control
KLF9
ITGA6
ITGA6 + KLF9
KLF9-GBM1a
KLF9-GBM1b
612
Cells/Field
800
600
400
200
0
*
**
***
KLF9 – + – + – + – + – + – +
ITGA6 – – + + – – + + – – + +
C
KLF9 – + – +
ITGA6 – – + +
FLAG
Integrin α6
Actin
KLF9 – + – +
ITGA6 – – + +
CD133
1.0 0.32 0.93 1.33
Nestin
1.0 0.02 0.78 0.49
Sox2
1.0 0.27 1.14 1.0
BMI1
1.0 0.40 1.09 0.98
Olig2
1.0 0.21 1.11 0.86
Actin

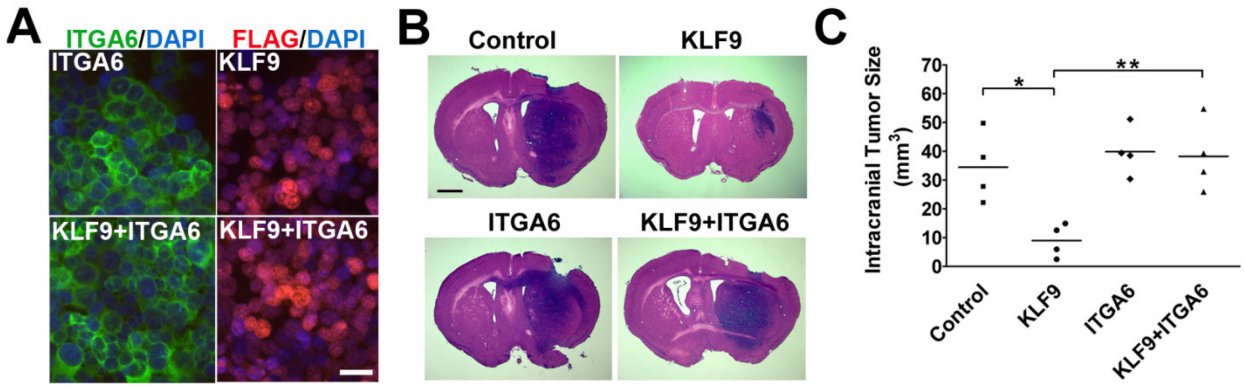

Figure 4.5. Integrin α6 expression rescues KLF9-Induced growth inhibition of glioma xenografts. GBM1b neurospheres were infected with lentivirus to express FLAG-KLF9, Integrin α6 or both. **(A)** Immunoflourescence of neurosphere cells shows the expression of ectopic FLAG-KLF9 and Integrin α6 (bar: 50 µm). **(B)** Equal numbers of viable cells were transplanted into the brains of SCID mice (n=4). H&E-stained coronal brain sections obtained from post implantation day 60 animals are shown (bar = 1 mm). **(C)** Quantification of tumor xenograft volumes shows that KLF9 induction inhibited xenograft growth and that integrin α6 expression rescued KLF9-induced anti-tumor response.

Data represents mean ± SEM; *: $p<0.01$, **: $p<0.001$, One-way ANOVA followed by Tukey test.

Chapter 5

CD151 regulates glioblastoma stem cell stemness and tumorigenity, in part, through interactions with laminin-binding integrins

5.1 KLF9 dynamically regulates CD151 expression

The effects of KLF9 induction on the level of CD151 mRNA and protein were quantified in two GBM neurosphere lines. KLF9 induction inhibited CD151 mRNA levels in all cell cultures (Figure 5.1A). We further examined the dynamics of CD151 expression in response to ectopic KLF9 expression controlled by Dox. CD151 expression levels changed inversely with KLF9 levels; CD151 expression decreased along with KLF9 induction and rapidly returned to baseline levels after Dox withdrawal (Figure 5.1B).

5.2 CD151 is highly expressed in glioma subtypes and GSCs

To examine the expression profile of CD151 in normal brain and glioma tissues, samples from the Repository for Molecular Brain Neoplasia Data (REMBRANDT) database (National Cancer Institute, https://caintegrator.nci.nih.gov/rembrandt/), which includes 28 non-tumor tissue and 443 glioma tissue samples, were analyzed. Analysis of CD151 mRNA expression revealed that CD151 expression is 4.9-, 2.1- and 2.1- fold

higher in GBM, oligodendroglioma, and astrocytoma, compared to non-tumor brain samples, and 2.3- and 2.4- fold higher in GBM samples compared to oligodendroglioma, and astrocytoma samples, respectively (Figure 5.2A).

To investigate potential correlations between CD151 expression and clinical outcome, we analyzed the prognostic significance of CD151 in the REMBRANDT samples using Kaplan-Meir survival curve analysis with a log-rank comparison. As shown in Figure 5.2B, survival for patients expressing upregulated CD151 was significantly shorter compared to those with intermediate expression in all glioma and specific glioma subtypes ($p < 0.001$, $p = 0.008$, $p = 0.027$ and $p = 0.012$ in all glioma, GBM, oligodendroglioma and astrocytoma samples, respectively, log-rank test).

We examined CD151 expression in GBM-derived neurosphere lines (GBM1A and GBM1B) and low passage GBM-derived primary neurospheres (612) enriched in GSCs. Immunostaining detected CD151 expression in permeabilized neurosphere cells (Figure 5.2C). CD151 was found to be expressed in membrane but not cytoplasmic fractions of multiple GSC lines using immunoblot analysis of membrane and cytoplasmic protein (Figure 5.2D). CD151 expression was further examined by qPCR analysis of CD133+ neurosphere cell subpopulations, which are widely considered to represent GBM-propagating SCs (Singh et al., 2004). CD151 expression was elevated in CD133+ cells relative to CD133- cells (Figure 5.2E).

To further study the association of CD151 with cell stemness and stemness-driving transcription factors, CD151 expression was analyzed using qPCR in GBM-derived neurospheres engineered to overexpress Oct4 and Sox2 (GBM1A Oct4/Sox2). Co-expressing transgenic Oct4 and Sox2, previously shown by us to induce tumor-

propagating GSCs (Lopez-Bertoni et al., 2014), increased CD151 expression 3- fold (Figure 5.2F). These results show that CD151 is upregulated in the most aggressive gliomas and CD151 upregulation is associated with poor prognosis independent of glioma grade. CD151 expression is also highly upregulated in glioma-propagating stem cells (SCs).

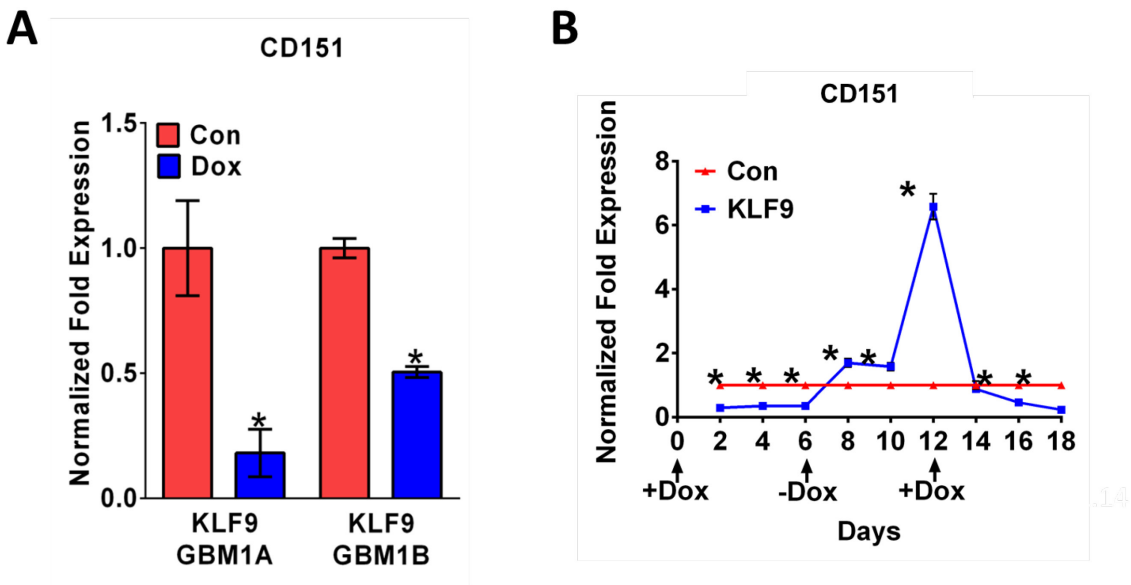

Figure 5.1 KLF9 regulates CD151 expression. (A) CD151 expression was measured by qPCR in GBM neurosphere lines after KLF9 induction for 48h. **(B)** KLF9-GBM1b cells were treated with Dox for 6 days, passaged to Dox-free medium for 6 days, and then passage again to Dox-containing medium for 6 days. Cells were collected on the days indicated and subjected to qPCR for CD151. CD151 expression levels changed inversely with Dox-induced KLF9 expression. Data represents mean ± SEM; *: $p<0.01$, t test.

Figure 5.2. CD151 expression in glioma and glioma stem cells (GSCs). (A) CD151 mean gene expression intensity from REMBRANDT database (*, #: $p<0.0001$ compared with non-neoplastic brain or GBM, respectively). CD151 expression is significantly up-regulated in glioblastoma multiforme (GBM) samples when compared with non-neoplastic brain, oligodendroglioma or astrocytoma samples. **(B)** Kaplan-Meier Survival Plots for glioma patients based on differential gene expression of CD151 (from REMBRANT database). The probability of survival is significantly lower in samples with high CD151 gene expression compared to samples with intermediate expression in all glioma, GBM, astrocytoma and oligodendroglioma samples ($P < 0.001$; $P < 0.01$; $P = 0.01$; $P < 0.05$). Inclusion of patients with low CD151 expression was not possible due to insufficient sample size. **(C)** Fluorescent photomicrography of GBM1B neurospheres permeabilized with triton X-100 and immunostained using anti-CD151 antibody (green fluorescence). Blue fluorescence indicates DAPI nuclear stain (bar = 10 μm). **(D)** Membrane and cytoplasmic protein fractions isolated from GBM neurosphere lines (GBM1A, GBM1B) and primary GBM neurosphere (612) were subjected to immunoblot analysis with anti-CD151 antibody. CD151 localizes to membrane, but not the cytoplasm of examined glioma stem cells. **(E)** GBM1A neurosphere cells expressing undetectable and high levels of CD133 (CD133-, CD133+, respectively) were separated by flow cytometry. Quantitative real-time polymerase chain reaction (qRT-PCR) analysis shows that CD151 mRNA expression is significantly higher in CD133+ cells (*, $P < 0.01$ compared to CD133- cells). **(F)** CD151 expression was analyzed by qPCR in GBM1A and GBM1A cells overexpressing stemness-associated transcription factors Oct4 and

Sox2 (GBM1A Oct4/Sox2). CD151 mRNA expression is higher in GBM1A Oct4/Sox2 cells compared to GBM1A cells. Data, mean ± SEM; *, $P < 0.05$ when compared to controls.

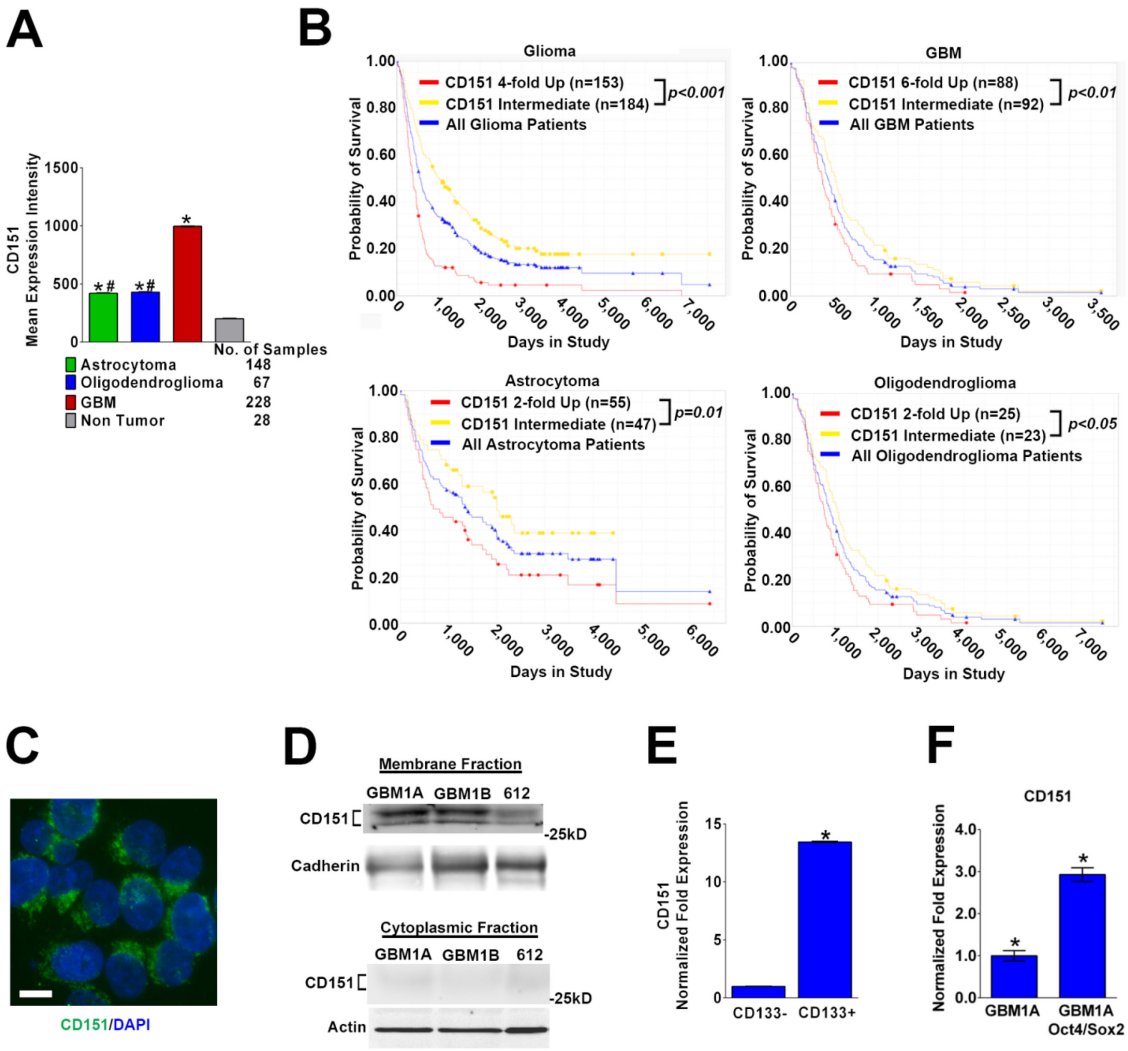
A
CD151
Mean Expression Intensity
1500
1000
500
0
*#
*#
*
No. of Samples
Astrocytoma 148
Oligodendroglioma 67
GBM 228
Non Tumor 28
B
Glioma
CD151 4-fold Up (n=153)
CD151 Intermediate (n=184)
All Glioma Patients
p<0.001
GBM
CD151 6-fold Up (n=88)
CD151 Intermediate (n=92)
All GBM Patients
p<0.01
Astrocytoma
CD151 2-fold Up (n=55)
CD151 Intermediate (n=47)
All Astrocytoma Patients
p=0.01
Oligodendroglioma
CD151 2-fold Up (n=25)
CD151 Intermediate (n=23)
All Oligodendroglioma Patients
p<0.05
Probability of Survival
Days in Study
C
CD151/DAPI
D
Membrane Fraction
GBM1A GBM1B 612
CD151
-25kD
Cadherin
Cytoplasmic Fraction
GBM1A GBM1B 612
CD151
-25kD
Actin
E
CD151
Normalized Fold Expression
CD133- CD133+
F
CD151
Normalized Fold Expression
GBM1A
GBM1A
Oct4/Sox2

5.3 CD151 expression regulates GSC self-renewal and CD151 knockdown impairs GSC proliferation

To determine if CD151 is essential to GSC stemness, GBM-derived neurospheres were transduced with lentiviral CD151 shRNAs (CD151 shRNA 1 and CD151 shRNA 2). CD151 protein and mRNA expression were significantly inhibited by each CD151 shRNA (Figure 5.3A and B) that decreased the number of CD151+ cells up to 99% (Figure 5.3C). We also engineered three independent neurosphere lines to express a Dox-inducible N-terminal 3xFLAG-tagged CD151 transgene (3F-CD151; designated as GBM1A 3F-CD151, GBM1B 3F-CD151 and 612 3F-CD151). Dox treatment for 48 hours induced expression of CD151 mRNA and membrane-associated CD151 protein (Figure 5.3D and E).

The effects of CD151 silencing on GSC self-renewal and cell proliferation were examined. Self-renewal as neurospheres, was markedly inhibited by CD151 knockdown from 61% to 96% in multiple neurosphere lines and primary isolates, including neurospheres derived from mesenchymal (M1123) and proneural (P146) glioblastoma subtypes (Figure 5.4A and B). Conversely, forced CD151 expression significantly increased neurosphere formation (Figure 5.4C). CD151 silencing impaired cell proliferation, somewhat more modestly, from 34% to 63% (Figure 5.4D). However, CD151 knockdown did not induce significant cell death in vitro (Figure 5.4E).

Figure 5.3. CD151 knockdown and Dox-inducible CD151 forced expression in glioma neurospheres. (A-C) GBM neurospheres (GBM1A and GBM1B) were transduced with lentivirus coding for control shRNA, CD151 shRNA 1 or CD151 shRNA 2. CD151 expression was quantified by **(A)** immunoblot analysis of membrane protein collected 72 hours later using anti-CD151 antibody and **(B)** quantitative real-time polymerase chain reaction (qPCR) analysis of mRNA. **(C)** Neurosphere cells were analyzed by flow cytometry 6 days after transduction with lenti-CD151 shRNA using CD151 antibodies and isotype IgG control. CD151 knockdown significantly reduced the number of CD151+ cells. Representative histograms and the percentage of CD151+ cells are shown. **(D & E)** GBM-derived neurosphere cells expressing a Dox-inducible 3FLAG-tagged CD151 (GBM1A 3F-CD151 and GBM1B 3F-CD151) were treated ± Dox. CD151 expression was analyzed by **(D)** immunoblot of cell membrane fractions using antibodies against CD151 and Flag and by **(E)** quantitative real time polymerase chain reaction 48 hours later for CD151 expression. Data, mean ± SEM; *, $P < 0.001$ when compared to controls.

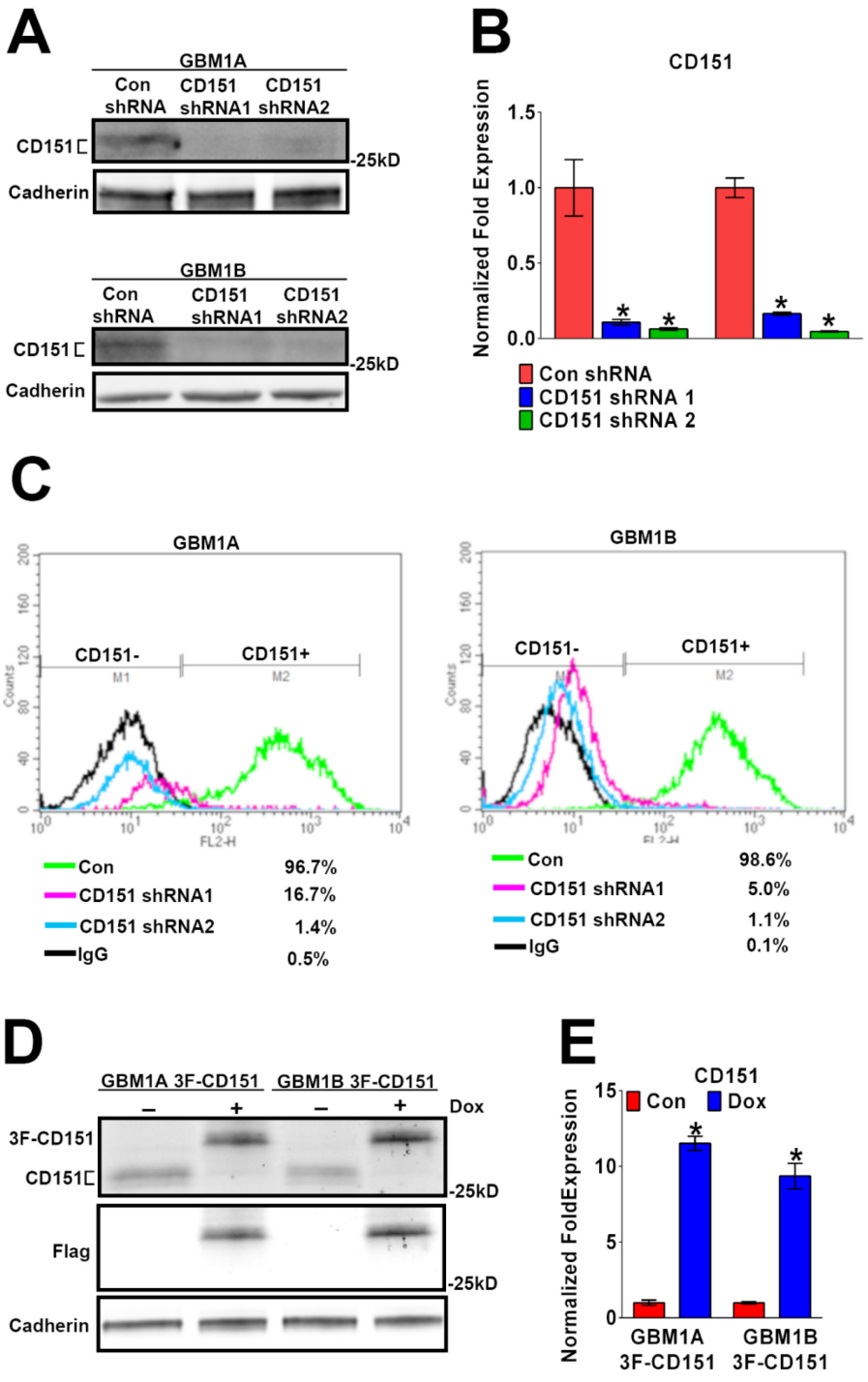
A
GBM1A
Con shRNA
CD151 shRNA1
CD151 shRNA2
CD151
-25kD
Cadherin
GBM1B
Con shRNA
CD151 shRNA1
CD151 shRNA2
CD151
-25kD
Cadherin
B
CD151
Normalized Fold Expression
1.5
1.0
0.5
0.0
*
*
*
*
Con shRNA
CD151 shRNA 1
CD151 shRNA 2
C
GBM1A
CD151-
CD151+
M1
M2
Counts
FL2-H
Con 96.7%
CD151 shRNA1 16.7%
CD151 shRNA2 1.4%
IgG 0.5%
GBM1B
CD151-
CD151+
Con 98.6%
CD151 shRNA1 5.0%
CD151 shRNA2 1.1%
IgG 0.1%
D
GBM1A 3F-CD151
GBM1B 3F-CD151
–
+
–
+
Dox
3F-CD151
CD151
-25kD
Flag
-25kD
Cadherin
E
CD151
Con
Dox
Normalized FoldExpression
15
10
5
0
*
*
GBM1A 3F-CD151
GBM1B 3F-CD151

Figure 5.4. Effects of CD151 on neurosphere formation and neurosphere self-renewal and viability. (A & B) GBM neurosphere lines (GBM1A, GBM1B, M1123, P146) and primary GBM neurospheres (612) were transduced with lentivirus coding for control shRNA, CD151 shRNA 1 or CD151 shRNA 2. **(A)** Equal numbers of viable cells were cultured for 14 days post transduction to form neurospheres. (Bar = 100 μm) Representative microscopic images of GBM1B neurospheres with control or CD151 shRNA are shown. **(B)** Neurospheres (>100 μm diameter) were counted. CD151 silencing inhibited neurosphere formation in all neurosphere isolates examined. **(C)** GBM1A 3F-CD151 and GBM1B 3F-CD151 neurospheres were treated ± Dox. Viable cells were cultured for 7 days ± Dox to form neurospheres. Neurospheres (>100 μm diameter) were quantified. CD151 overexpression increased neurosphere formation. **(D & E)** GBM1A, GBM1B, M1123 and 612 neurospheres were infected with lentivirus coding for control shRNA, CD151 shRNA 1 or CD151 shRNA 2. Cells were stained with Trypan blue. Viable (unlabeled) cells and labeled cells were counted on the days indicated post transduction. CD151 knockdown **(D)** inhibited cell growth, but **(E)** did not alter cell viability. Data, mean ± SEM; *, $P < 0.05$ when compared to controls.

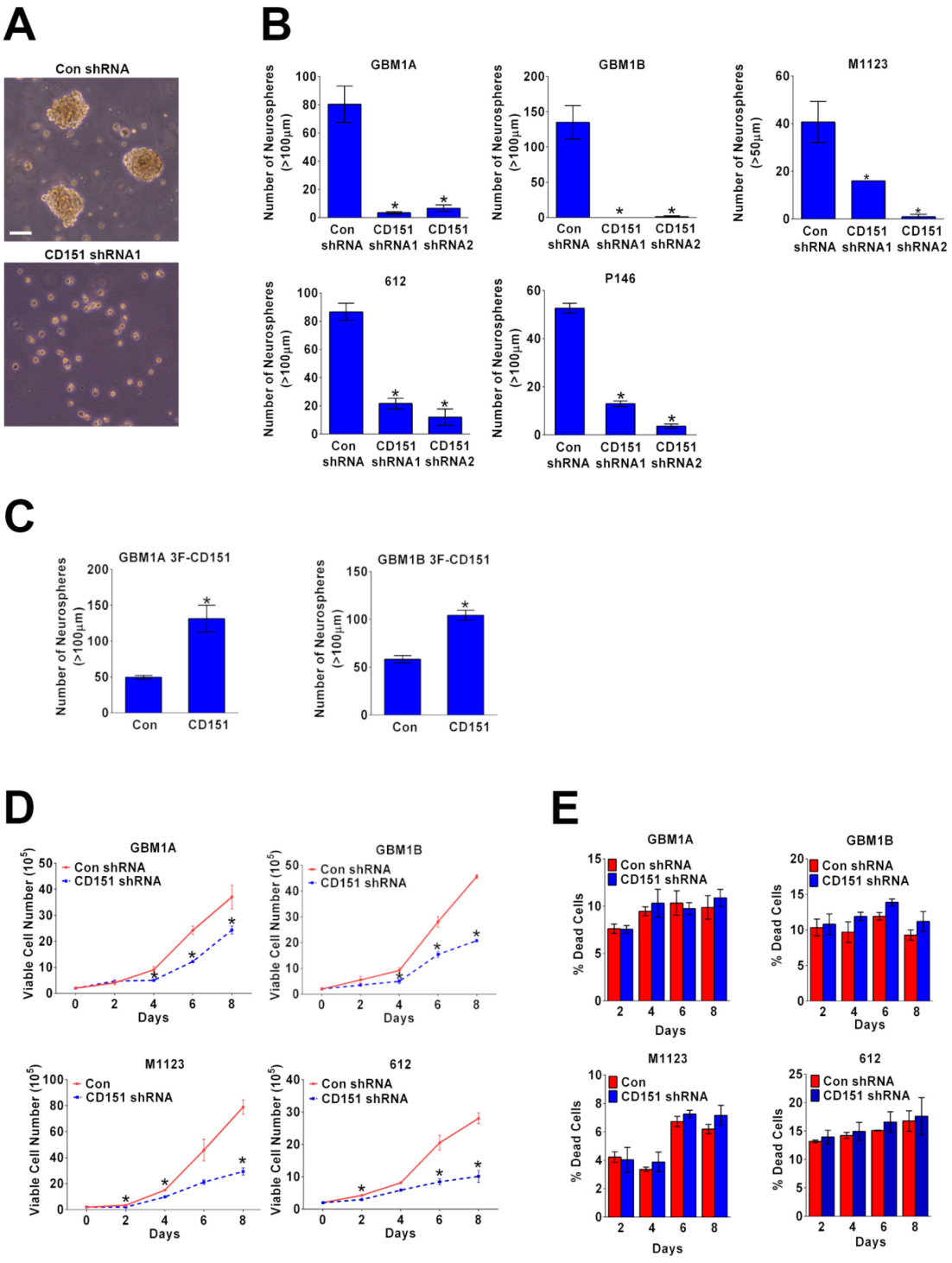
A
Con shRNA
CD151 shRNA1
B
GBM1A
GBM1B
M1123
612
P146
Number of Neurospheres (>100μm)
Number of Neurospheres (>50μm)
Con shRNA
CD151 shRNA1
CD151 shRNA2
C
GBM1A 3F-CD151
GBM1B 3F-CD151
Number of Neurospheres (>100μm)
Con
CD151
D
GBM1A
GBM1B
M1123
612
Viable Cell Number (10^5)
Con shRNA
CD151 shRNA
Con
Days
E
GBM1A
GBM1B
M1123
612
% Dead Cells
Con shRNA
CD151 shRNA
Con
Days

5.4 CD151 expression regulates expression of stemness associated markers and regulators

We investigated the effect of CD151 silencing on the expression of markers and regulators of GBM cell stemness. CD151 knockdown in neurospheres reduced the number of CD133+ cells by 32%-52% (Figure 5.5A and B). GSCs are regulated by several stemness-associated transcription factors, including Olig2 and Sox2 (Gangemi et al., 2009; Y. Li et al., 2011; Lopez-Bertoni et al., 2014). CD151 silencing decreased expression of Sox2 and Olig2 on a protein level and Sox2, Olig2 and BMI1 on an mRNA level (Figure 5.5C and D). Conversely, forced CD151 expression increased expression of stemness associated factors Oct4, Sox2, Olig2 and BMI1 (Figure 5.5E and F). Taken together, these results indicate that CD151 expression supports GSC stemness.

Figure 5.5. CD151 regulates GBM cell stemness. (A-D) GBM1A and GBM1B neurospheres were transduced with lentivirus coding for control shRNA, CD151 shRNA 1 or CD151 shRNA 2. **(A & B)** GBM1A and GBM1B cells were analyzed by flow cytometry 6 days post transduction using anti- CD133 and isotope IgG control. **(A)** A representative histogram and the percentages of CD133+ cells are shown. **(B)** CD151 silencing decreases the number of CD133+ cells. **(C)** Total cell lysates were extracted and analyzed by immunoblot for Sox2, Olig2 and β-Actin. CD151 inhibition decreases expression of Sox2 and Olig2. **(D)** CD151 silencing inhibits Sox2, Olig2 and BMI1 mRNA expression, as shown by quantitative real time polymerase chain reaction (qPCR) analysis. **(E & F)** GBM1A 3F-CD151 and GBM1B 3F-CD151 neurospheres were treated ± Dox. Whole cell extracts were analyzed by immunoblot for Olig2 and Sox2. **(E)** CD151 overexpression promotes expression of Olig2 in both cells and Sox2 in GBM1B 3F-CD151 GSCs. **(F)** Analysis of Oct4, Sox2, Olig2 and BMI1 expression by qPCR analysis shows that CD151 promotes mRNA expression of the stemness-associated factors.

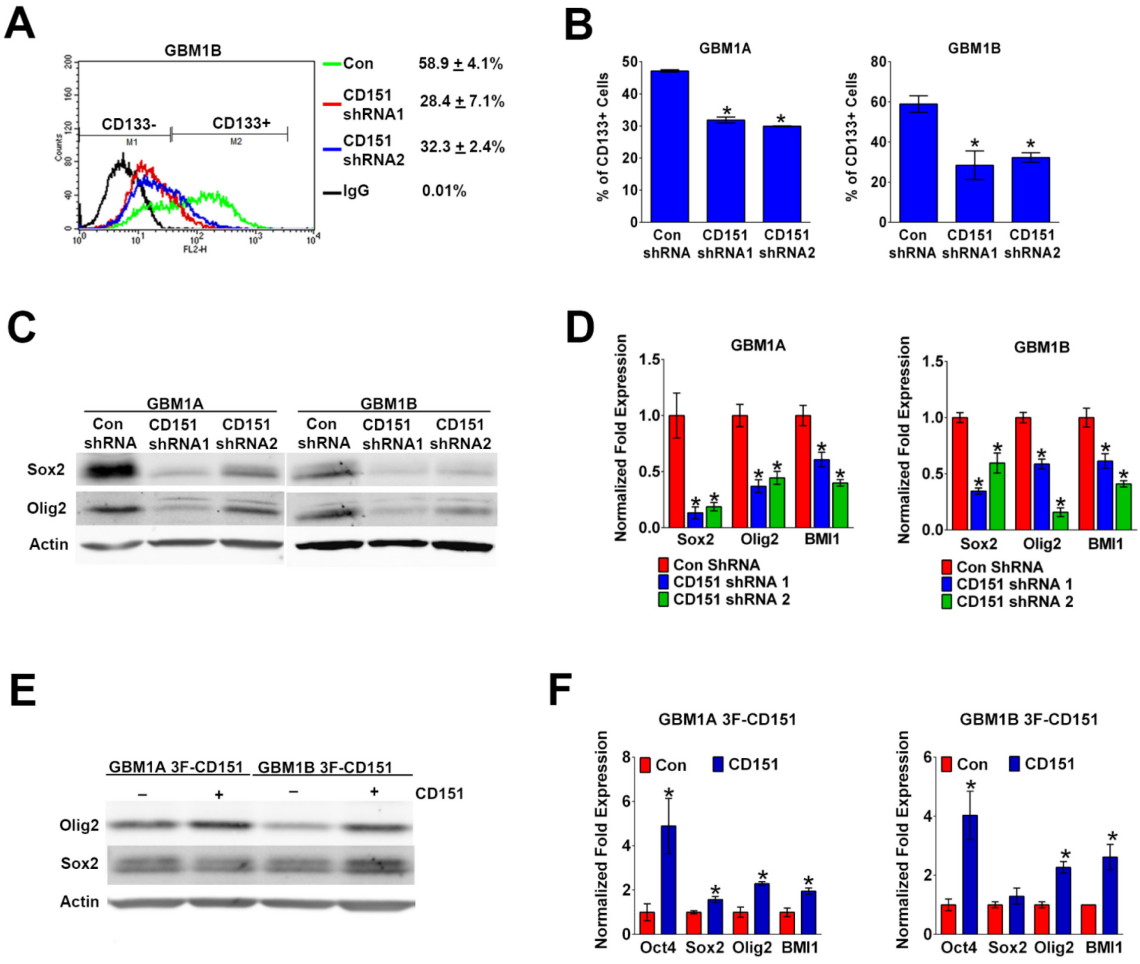
A
GBM1B
CD133-
CD133+
M1
M2
Counts
FL2-H
Con 58.9 ± 4.1%
CD151 shRNA1 28.4 ± 7.1%
CD151 shRNA2 32.3 ± 2.4%
IgG 0.01%
B
GBM1A
GBM1B
% of CD133+ Cells
Con shRNA
CD151 shRNA1
CD151 shRNA2
C
GBM1A
GBM1B
Sox2
Olig2
Actin
D
GBM1A
GBM1B
Normalized Fold Expression
Sox2
Olig2
BMI1
Con ShRNA
CD151 shRNA 1
CD151 shRNA 2
E
GBM1A 3F-CD151
GBM1B 3F-CD151
CD151
Olig2
Sox2
Actin
F
GBM1A 3F-CD151
GBM1B 3F-CD151
Con
CD151
Normalized Fold Expression
Oct4
Sox2
Olig2
BMI1

5.5 Targeting CD151 inhibits GSC migration and adhesion on laminin

GBM-derived neurosphere cells transduced with control lentivirus or with lentiviral vectors engineered to express either CD151 shRNA were seeded on laminin-coated transwell membranes to evaluate migration capacity. CD151 silencing reduced migration 47%- 87% (Fig 5.6A and B).In contrast, forced CD151 expression enhanced cell migration on laminin-coated transwells by 42% to 109% in GBM1A 3F-CD151, GBM1B 3F-CD151 and 612 3F-CD151 cells (Figure 5.6C).

The glioma microenvironment constitutes a physically and chemically diverse terrain that influences cell migration. For example, glioma cells preferentially migrate along structured pathways such as myelinated neuronal tracts and blood vessels (Bellail, Hunter, Brat, Tan, & Van Meir, 2004). To further study the effect of CD151 on GSC migration and how this effect is influenced by an ECM mimicked environment, 612 cells transfected with control or CD151 shRNA lentivirus were seeded on a laminin-coated substrate consisting of nanoscale grooves. Migration along the nanoscale ridges enables a more precise assessment of migration parameters such as cell speed and distance travelled over several hours. CD151 silencing significantly reduced average cell migration speed by 41% to 57% (Figure 5.6D and E). Control shRNA transfected cells also traveled at higher maximum speeds than CD151 shRNA transfected cells (Figure 5.6F). CD151 knockdown also reduced the average distance migrated over 10 hours (Fig 5.6G and H).

Cell adhesion events impact cell migration capacity. To determine if CD151 modulates neurosphere cell adhesion, GBM-derived neurosphere cells transduced with

control lentivirus or lentivirus coding for CD151 shRNA were seeded on a laminin coated substrata. CD151 silencing resulted in a delayed rate of adhesion and cell spreading (Figure 5.6I and J). Forced CD151 expression had no effect on cell adhesion 2 hours after seeding on a laminin-coated surface, but significantly increased adhesion after 6 hours (Figure 5.6K). Collectively, the data indicates that CD151 regulates neurosphere cell adhesive and migratory interactions with laminin-containing matrices.

Figure 5.6. CD151 regulates GBM neurosphere cell adhesion and migration. (A-C) GBM neurospheres (GBM1A, GBM1B, P146, M1123, 612) were transduced with lentivirus coding for control shRNA, CD151 shRNA 1 or CD151 shRNA 2 cDNA or GBM1A 3F-CD151, GBM1B 3F-CD151 and 612 3F-CD151 neurospheres were treated ± Dox for 24 hours. Cells were plated on laminin-coated transwell membranes and migration was evaluated 8 hours later by counting DAPI-stained cells. **(A)** Representative microscopic fields of GBM1B neurosphere cells transduced with control or CD151 shRNA lentivirus are shown (Bar = 50 μm). Cells per field were counted. **(B)** CD151 silencing inhibited migration on laminin while **(C)** CD151 overexpression promoted migration on laminin. **(D-J)** GBM neurospheres (GBM1A, GBM1B, M1123, 612) were transduced with lentivirus coding for control shRNA, CD151 shRNA 1 or CD151 shRNA 2 cDNA., Cells were plated on a laminin-coated multi-well nanopatterned device used to track brain tumor-propagating cell migration. Cell migration was recorded for 10 hours and individual cells were tracked using a custom MATLAB program. **(D)** The average cell speed travelled per 10 minute interval and **(E)** the overall average speed were calculated. **(F)** A histogram of average speed for individual cells is shown. Control cells migrate faster than CD151 shRNA transduced cells. **(G)** Average distance migrated was calculated. CD151 knockdown reduced cell distances travelled. **(H)** Representative trajectories of control shRNA and CD151 shRNA cells are shown (Bar = 100 μm). The start location (red dots) and final locations at 10 hours (blue dots) of individual cells are shown. The green line indicates the path traveled by individual cells. **(I & J)** Cells were plated on a laminin-coated tissue culture substrata for 2 and 6 hours. Cell adhesion and morphology were evaluated by phase-contrast microscopy (Bar = 100 μm) and

quantitatively by spectrophotometric analysis of crystal violet-stained cells. CD151 silencing **(I)** inhibited cell spreading and **(J)** delayed cell adhesion. **(K)** GBM1A 3F-CD151, GBM1B 3F-CD151 and 612 3F-CD151 neurospheres were treated ± Dox for 24 hours. Adhesion was evaluated by spectrophotometric analysis of crystal violet-stained cells 2 and 6 hours after cells were plated on a laminin-coated surface. CD151 expression promoted adhesion 6 hours after seeding. Data, mean ± SEM; *, $P < 0.05$ when compared to controls.

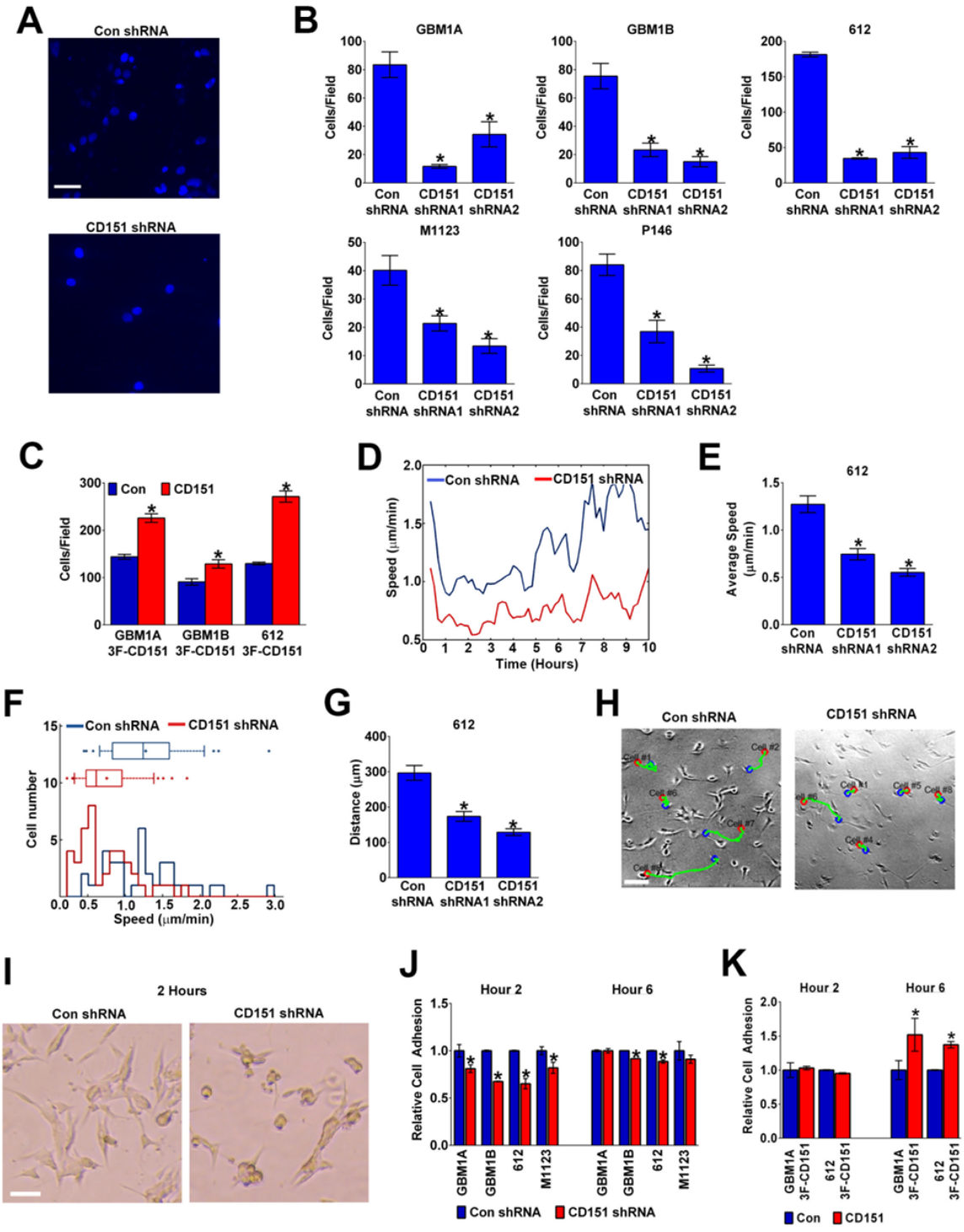
A
Con shRNA
CD151 shRNA
B
GBM1A
GBM1B
612
M1123
P146
Cells/Field
Con shRNA
CD151 shRNA1
CD151 shRNA2
C
Con
CD151
GBM1A 3F-CD151
GBM1B 3F-CD151
612 3F-CD151
D
Con shRNA
CD151 shRNA
Speed (μm/min)
Time (Hours)
E
612
Average Speed (μm/min)
F
Con shRNA
CD151 shRNA
Cell number
Speed (μm/min)
G
612
Distance (μm)
H
Con shRNA
CD151 shRNA
I
2 Hours
Con shRNA
CD151 shRNA
J
Hour 2
Hour 6
Relative Cell Adhesion
GBM1A
GBM1B
612
M1123
Con shRNA
CD151 shRNA
K
Hour 2
Hour 6
Relative Cell Adhesion
GBM1A 3F-CD151
612 3F-CD151
Con
CD151

5.6 CD151 silencing impairs growth of GSC-derived tumor xenografts and pathological angiogenesis

A most crucial characteristic of GSCs is the ability to propagate tumors *in vivo*. Hence, we examined the effects of CD151 silencing on the growth of subcutaneous (s.c) and intracranial (i.c.) xenografts established from GBM-derived neurospheres. Subcutaneous xenografts were established in mice with M1123 neurosphere cells engineered to express a Dox-inducible CD151 shRNA (M1123 CD151 shRNA). A randomly selected subset of mice was transitioned to Dox feed when tumors reached 50mm^3. Tumors were measured from post implantation day (PID) 8 through PID 15 to monitor the effects of CD151 silencing. Average tumor size increased from 74 mm^3 to 1,853 mm^3 in control mice and from 85 mm^3 to 540 mm^3 in Dox treated mice. By PID 15, CD151 shRNA had inhibited tumor growth by 71% (Figure 5.7A). CD151 knockdown *in vivo* was confirmed by immunoblot of whole tumor protein extracts using CD151 antibody (Figure 5.7B).

To examine the effect of CD151 silencing on i.c. tumor formation, GBM1A cells were infected with lentiviral control or CD151 shRNA. Viable cells were implanted 24 hours later into the brains of severe combined immunodeficiency (SCID) mice. Mice were sacrificed 52 days later and coronal brain sections were examined for tumor size. Tumor formation was significantly reduced in mice implanted with CD151 shRNA treated cells (19.1 ± 3.9 mm^3 max tumor volume) compared to control shRNA tumors (54.3 ± 5.0 mm^3 max tumor volume) (Figure 5.7C and D).

We also examined tumor cell apoptosis by immunohistochemistry (IHC) staining for the apoptosis marker, cleaved caspase-3. We found that silencing CD151 in pre-established M1123 s.c. xenografts increased the percentage of cells expressing active cleaved caspase-3 by 3.7- fold (Figure 5.7E and F). To investigate the role of CD151 on GBM tumor xenograft vascularization, vessels were visualized in s.c. tumor sections by IHC staining with antibody against laminin. Vascular index decreased by 43% in response to CD151 shRNA (Figure 5.7G and H). Taken together, the data supports that targeting CD151 inhibits the growth of neurosphere-derived GBM xenografts by targeting cell survival and angiogenic mechanisms.

Figure 5.7. CD151 knockdown inhibits the growth of neurosphere-derived tumor xenografts. (A and B) Mice were implanted subcutaneously with Dox-inducible M1123 CD151 shRNA cells. Mice were started on Dox in rodent diet when tumors reached 50mm3. Tumor sizes were measured as described in "Materials and Methods". **(A)** CD151 knockdown inhibited xenograft growth. **(B)** Protein extractions from subcutaneous xenografts obtained at day 15 were analyzed by immunoblot for CD151, confirming Dox-induced knockdown of CD151. **(C and D)** GBM1A cells were transduced with lentivirus coding for control shRNA or CD151 shRNA cDNA. After 24 hours, 5,000 cells were transplanted into the brains of severe combined immunodeficiency (SCID) mice. **(C)** Hematoxylin and eosin-stained coronal brain sections (20 μm) obtained from animals on PID 52 are shown (Bar = 1 mm). **(D)** Quantification of xenograft tumor volume shows that silencing CD151 repressed xenograft growth (H; $P < 0.001$ when compared with control shRNA). **(E-H)** Subcutaneous xenografts from mice implanted with Dox-inducible M1123 CD151 shRNA cells were examined for cell apoptosis by **(E)** immunohistochemistry (IHC) using anti-cleaved caspase-3 antibody (Bar = 10 μm). Labeled cells were quantified by computer-assisted image analysis. **(F)** CD151 silencing increased cell apoptosis ($p<0.001$ compared to controls). **(G)** S.c. xenografts were examined by anti-laminin IHC (Bar = 10μm). **(H)** Computer-assisted quantification shows that CD151 knockdown decreased tumor vascularization (H; $p<0.01$ compared to controls).

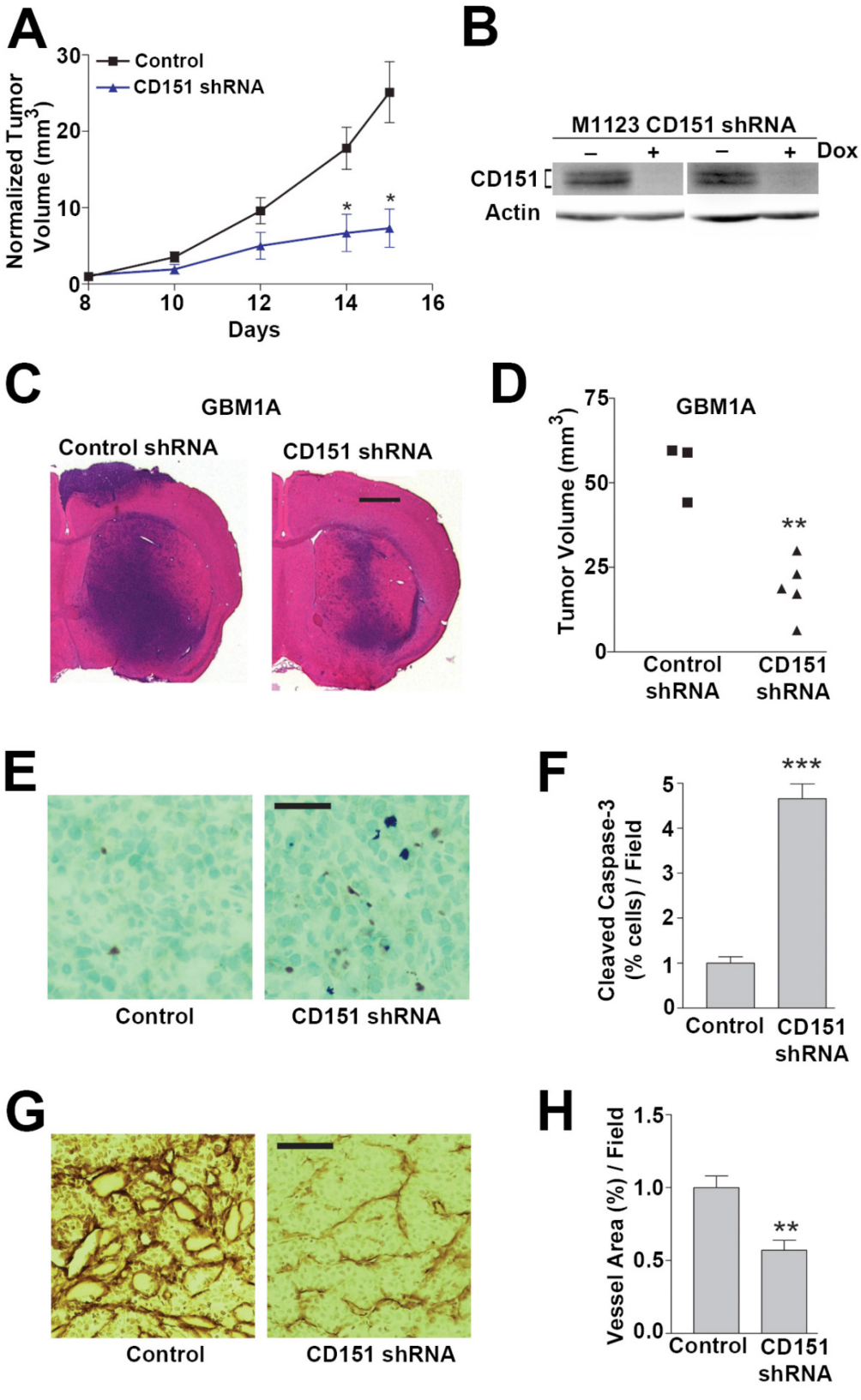
A
Control
CD151 shRNA
Normalized Tumor Volume (mm3)
30
20
10
0
8
10
12
14
16
Days
*
*
B
M1123 CD151 shRNA
– + – + Dox
CD151
Actin
C
GBM1A
Control shRNA
CD151 shRNA
D
GBM1A
Tumor Volume (mm3)
75
50
25
0
**
Control shRNA
CD151 shRNA
E
Control
CD151 shRNA
F
***
Cleaved Caspase-3 (% cells) / Field
5
4
3
2
1
0
Control
CD151 shRNA
G
Control
CD151 shRNA
H
Vessel Area (%) / Field
1.5
1.0
0.5
0.0
**
Control
CD151 shRNA

5.7 CD151 modulates integrin-dependent signaling and cell behavior in GSCs

CD151 complexes with laminin-binding integrins and influences integrin driven biological processes in several cell types (Sterk et al., 2002; Winterwood, Varzavand, Meland, Ashman, & Stipp, 2006). Integrins are also highly expressed in stem cells, including GSCs, and thought to contribute to stemness by anchoring stem cells to certain micoenvironmental niches (S. Chen, Lewallen, & Xie, 2013; Lathia et al., 2010). Immunofluorescent staining showed that CD151 colocalizes with integrins α3, α6 and β1 in the plasma membrane of GBM neurosphere cells (Figure 5.8A). To further investigate CD151's association with integrins, GBM1A 3F-CD151 neurosphere cells were treated ± Dox for 48 hours to induce CD151 expression. Immunoprecipitation using anti-FLAG revealed associations between CD151 and integrins α3, α6 and β1 (Figure 5.8B).

We then investigated the effect of CD151 expression on activation of the integrin signaling pathway in GBM neurosphere cells. We found that CD151 knockdown reduced phosphorylation of Akt, a downstream effector of integrin signaling that promotes various biological processes including survival and cell motility (Cox, Natarajan, Stettner, & Gladson, 2006), while forced CD151 expression enhanced Akt phosphorylation (Figure 5.8C and D).

To determine if interactions between CD151 and integrins are required for CD151 modulated GSC behavior, we treated cells with the anti-CD151 antibody TS151r previously shown to block the interaction between CD151 and integrins α3 and α6 (Kazarov et al., 2002; Serru et al., 1999; Sterk et al., 2002; Yauch, Kazarov, Desai, Lee,

& Hemler, 2000). Incubation with the TS151r mimicked CD151 expression knockdown by multiple criteria. TS151r reduced neurosphere formation by 77%-95% (Figure 5.8E), reduced cell migration on laminin by 70%-75% (Figure 5.8F), and inhibited Akt phosphorylation (Figure 5.8G). Taken together, the results strongly support a mechanism by which CD151-laminin interactions support GSC self-renewal and migration in part by altering integrin function and downstream signaling.

To verify CD151's association with integrins α3, α6 and β1 and to determine what other proteins CD151 may interact with in GSCs to influence GSC behavior, GBM1A 3F-CD151 neurosphere cells were treated ± Dox for 48 hours to induce CD151 expression. Proteins immunoprecipitated with anti-Flag were analyzed by tandem mass spectrometry. The analysis revealed 305 proteins isoforms that were enriched during forced expression of CD151 compared to controls, including integrins α3, α6 and β1 and known CD151 binding partners CD9 and CD81 (Data not shown). Among the most enriched proteins were integrin α7, another laminin-binding integrin previously shown to associate with CD151 (Sterk, 2002 43), Nestin, a neuroprogenitor marker {Gilyarov, 2008), and Isocitrate dehydrogenase 1, a protein that is typically mutated in low grade gliomas and glioblastoma with oligodendroglial component (Ha, 2013; Cohen, 2013). This suggests that CD151 may interact with other proteins in order to modulate GSC behavior.

Figure 5.8. CD151 regulates neurosphere cell self-renewal, migration and Akt activation by complexing with integrins. (A) GBM1A neurosphere cells collected by cytospin were co-immunostained with antibodies against CD151 and either integrin α3, integrin α6 or integrin β1 (bar = 10μm). CD151 distribution overlaps with the integrins. **(B)** GBM1A 3F-CD151 cells were treated ± Dox for 48 hours. Brij-O1 collected protein lysates subjected to immunoprecipitation with anti-FLAG or control IgG antibodies specifically precipitated 3F-CD151, Integrin α3, Integrin α6 and integrin β1 proteins. **(C)** GBM neurosphere lines GBM1A and GBM1B were transduced with lentivirus coding for control shRNA, CD151 shRNA 1 or CD151 shRNA 2. Total cell lysates were extracted and analyzed by immunoblot using antibodies against phosphorylated Akt (pAkt) and total Akt (tAKT). CD151 inhibition decreases expression of phosphorylated Akt. **(D)** GBM1A 3F-CD151 and GBM1B 3F-CD151 neurospheres were treated ± Dox. Whole cell extracts were analyzed by immunoblot for phosphorylated Akt and total Akt. CD151 overexpression promotes phosphorylation of Akt. **(E-G)** GBM1A and GBM1B cells were treated with anti-CD151 antibody TS151r, which blocks integrin α3 binding. Isotype IgG was used as control. **(E)** Equal numbers of viable cells were cultured in 48-well plates with antibody for 14 days to form neurospheres. Neurospheres (>50 μm diameter) were counted. Neurosphere formation was inhibited by TS151r. **(F)** Cells were plated on laminin-coated transwell membranes. Migration was evaluated 8 hours later by counting DAPI-stained cells. Cells per field were counted. TS151r inhibited migration on laminin. **(G)** Whole cell lysates were collected and subjected to immunoblot analysis for phosphorylated Akt and total Akt. CD151 knockdown inhibits Akt phosphorylation. Data, mean ± SEM; *, $P < 0.01$ when compared to controls.

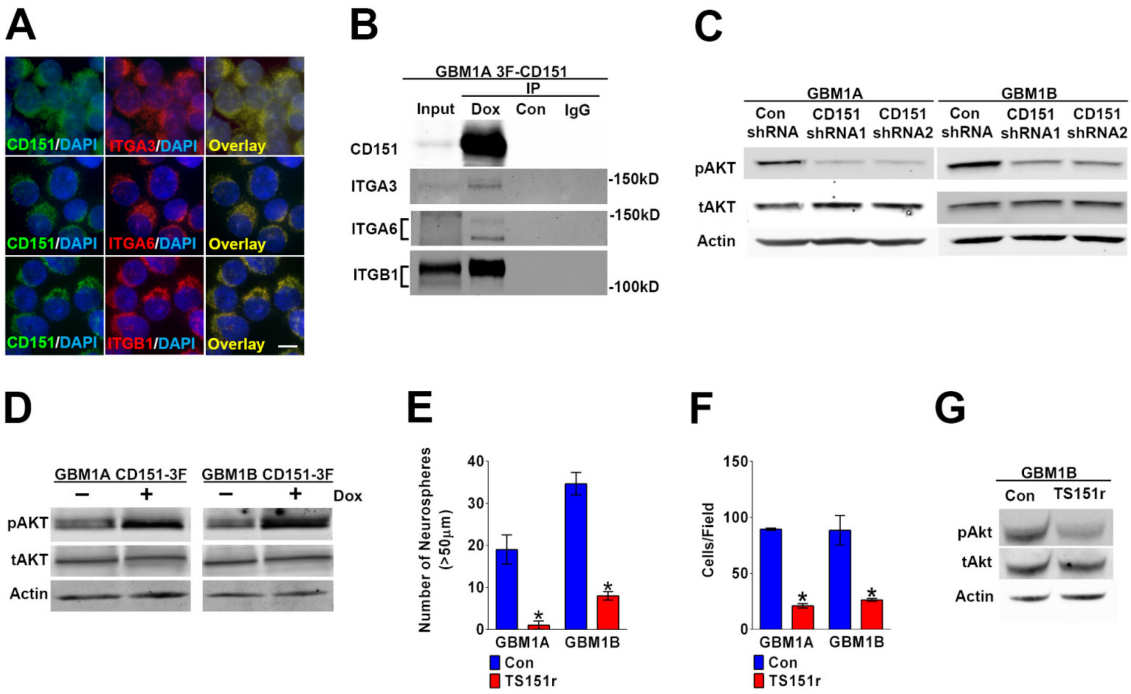
A
CD151/DAPI
ITGA3/DAPI
Overlay
CD151/DAPI
ITGA6/DAPI
Overlay
CD151/DAPI
ITGB1/DAPI
Overlay
B
GBM1A 3F-CD151
IP
Input
Dox
Con
IgG
CD151
ITGA3
-150kD
ITGA6
-150kD
ITGB1
-100kD
C
GBM1A
GBM1B
Con shRNA
CD151 shRNA1
CD151 shRNA2
Con shRNA
CD151 shRNA1
CD151 shRNA2
pAKT
tAKT
Actin
D
GBM1A CD151-3F
GBM1B CD151-3F
−
+
−
+
Dox
pAKT
tAKT
Actin
E
Number of Neurospheres (>50μm)
40
30
20
10
0
GBM1A
GBM1B
Con
TS151r
F
Cells/Field
150
100
50
0
GBM1A
GBM1B
Con
TS151r
G
GBM1B
Con
TS151r
pAkt
tAkt
Actin

Chapter 6

Discussion

Cancer cells are highly plastic in their ability to shift between more differentiated and more stem-like states. This phenotypic plasticity is dynamically controlled by transcription factor networks that regulate cell multipotency, differentiation, and tumor propagating capacity (Y. Li & Laterra, 2012). Identification of these regulatory networks is paramount to understanding cancer cell hierarchy, malignant progression and mechanisms of therapeutic resistance.

We previously reported that the KLF9 transcription factor inhibits glioma cell stemness (Ying et al., 2011). Induction of KLF9 was found to promote glioma cell differentiation and inhibit the expression of cell markers and drivers of stemness and the aggressiveness of orthotopic tumor xenografts based on multiple endpoints. These include inhibition of sphere-forming capacity, reduced expression of cell surface CD133, BMI1, Nestin, Sox2 and Olig2, increased expression of neural and astroglial differentiation markers, and decreased tumor xenograft growth and invasiveness . The inhibitory effect of KLF9 on stemness diverges from the stemness-supporting effects of other KLFs, such as KLF2, 4 and 5 (Boyer et al., 2005; Jiang et al., 2008; J. Wang et al., 2006). The molecular mechanism underlying KLF9's function in GSCs has not been extensively examined.

This current study establishes for the first time a genome-wide map of KLF9-regulated targets in a human cancer stem cell model. 31,261 genome-wide KLF9 binding peaks were identified in GBM neurosphere cells under biological conditions of KLF9-induced stemness inhibition. Amongst these peaks, 1,849 gene targets were found to be directly downregulated by KLF9. The predictive value of these datasets is supported by our validation of KLF9-regulated gene expression and KLF9 binding sites in gene subsets by qPCR and ChIP-PCR, respectively.

The majority of KLF9 binding sites were found to be located in intergenic regions and introns, and KLF9 binding peaks were found to be most enriched proximal to the TSS, patterns that support the gene expression regulatory function for KLF9. Statistical analyses of the differentially expressed genes bound by KLF9 proximal to TSS showed that KLF9 functions primarily as a transcriptional repressor in the context of glioma neurospheres. This does not absolutely rule out the possibility that KLF9 has some transactivating activity under other biological contexts, particularly given the strong influence of biological context and genetic background on the gene regulatory activities including those of KLF family members (McConnell & Yang, 2010; Tetreault, Yang, & Katz, 2013). One particularly relevant example is the findings of Mitchell and DiMario (2010) who found in human myoblasts that KLF9 transactivated an *FGFR1* promoter-reporter construct driven by a 3,284 bp DNA sequence upstream from the *FGFR1* TSS and that the same reporter was repressed in differentiated myotubes; however the capacity for these reporters to accurately mirror the regulation of endogenous *FGFR1* expression in these same models was not addressed.

This is the first application of genome-wide de novo motif discovery to define the KLF9 binding DNA consensus sequence, 5' G/A G/T GGG C/T G G/T GGCN 3'. This result is consistent with a previous report showing that KLF9 (also known as BTEB1) binds to a GC-rich DNA sequence (Imataka et al., 1992). We also confirmed the similarity of this KLF9 binding motif to the motifs of SP/KLF family members such as Sp1 and KLF4. KLF2, KLF4 and KLF5, KLFs that maintain the self-renewal of ES cells, extensively colocalized to specific genomic regions (Jiang et al., 2008). These and other SP/KLF family members share DNA binding motifs by virtue of highly conserved zinc-finger DNA-binding domains located in the carboxy terminal (Pearson et al., 2008). The activating or repressing transcriptional effects of KLF family members can be attributed at least in part to their divergent amino terminal domains that determine

complex formation with other transcriptional co-regulators (Pearson et al., 2008). Within this context, it is particularly interesting that KLF4 promotes epithelial cell stemness and transformation via a mechanism involving direct *Notch1* transactivation (Z. Liu et al., 2009) in contrast to the stemness-inhibiting and direct *Notch1* repressing effects of KLF9 in glioblastoma (Ying et al., 2011). Considerably more information regarding SP/KLF family member-specific transcriptional co-regulators and their context-dependent activities is needed to fully understand mechanisms behind the collaborative or competitive interplay among SP/KLF family members and the effects of this transcriptional network on cell stemness and malignancy.

Gene function annotation and pathway analyses revealed that signaling pathways relevant to cancer signaling, stem cell regulation and neural cell function are enriched in KLF9 downregulated gene targets. Signaling pathways CXCR4 and Notch, which regulate malignancy and stem cell biology, were among those significantly downregulated by KLF9. CXCR4 is a chemokine receptor with multiple functions including the regulation of stem cell and neuronal cell homing and cancer cell migration (Liekens, Schols, & Hatse, 2010; R. J. Miller, Banisadr, & Bhattacharyya, 2008). CXCR4 signaling is active in over 20 human tumors, including gliomas and contributes to tumor promotion in multiple ways (Ehtesham et al., 2013; Liekens et al., 2010). CXCR4 is highly expressed in GSCs (Ping et al., 2011) and was recently reported to facilitate the recruitment of GSC-derived pericytes to CXCL12-positive endothelial cells to support the tumor vasculature and tumor growth (Cheng et al., 2013). In addition to our novel findings with KLF9, several other KLFs have been reported to regulate CXCR4 expression in cancer cells. KLF2 downregulates CXCR4 in oral cancer cells (D. Uchida et al., 2009), while KLF5 has been shown to upregulate CXCR4 in prostate cancer (Frigo et al., 2009). Notch signaling has a prominent role in maintaining stem cell phenotypes within a variety of developmental and neoplastic contexts (e.g. neural stem cells, mammary stem cells, leukemia,

glioblastoma and mammary carcinoma) by promoting self-renewal and inhibiting differentiating programs (Farnie & Clarke, 2007; Kanamori et al., 2007; Weng et al., 2004). Our current finding that KLF9 represses multiple Notch pathway components further supports our earlier discovery that KLF9 inhibits GBM cell stemness , in part, by directly repressing Notch1 expression and downstream signaling (Ying et al., 2011). We now broaden these earlier findings by showing that KLF9 also downregulates NUMBL, a component of the Notch signaling pathway (L. Liu, Lanner, Lendahl, & Das, 2011). Evidence supports a regulatory role for NUMBL in cell stemness. For example, NUMBL increases expression of ES pluripotency markers by synergizing with Shh signaling (L. Liu et al., 2011).

Integrin pathway members including *ITGA6, ITGA9, ARPC1B, CAPN5, GIT1* and *MYLK* were also found to be enriched for KLF9-regulated gene targets. Integrin signaling modulates various cellular processes, such as proliferation, migration and differentiation, through cell-cell and cell-matrix interactions (Barczyk, Carracedo, & Gullberg, 2010). Integrins, a family of cell adhesion receptors, are upregulated in stem cells and believed to support cell stemness by mediating adhesive interactions with stem cell niches (S. Chen et al., 2013). Integrin α6, a subunit for two laminin receptors, is also highly expressed in several types of stem cells, including subventricular neural stem cells (NSCs) (Qian, Tryggvason, Jacobsen, & Ekblom, 2006; Staquicini et al., 2009) and facilitates NSC adherence to endothelial cells in the perivascular niche (Staquicini et al., 2009). Integrin α6 has also been identified as a marker for cancer stem cells including GSCs (Lathia et al., 2010; Shinohara et al., 1999). It has been proposed that integrin α6 is essential for the maintenance of GSC self-renewal and tumor-initiating cell phenotype providing a potential target for anti-GBM therapies (Lathia et al., 2010). Despite the involvement of integrin α6 in stem cell maintenance, little was known about the mechanisms that regulate its expression in cancer cells or how it regulates stem cell phenotypes.

We present the novel findings that KLF9 represses integrin α6 expression, a transcriptional response that in turn inhibits GBM cell stemness. Multiple complementary criteria were used to show that KLF9 induction inhibits integrin α6 expression by directly repressing *ITGA6* promoter activity. These include reductions in integrin α6 mRNA and protein, and KLF9 binding to the *ITGA6* promoter. The biological relevance of integrin α6 repression by KLF9 is supported by the concurrent inhibition of laminin-dependent GBM neurosphere cell adhesion, cell migration, and cell stemness in response to KLF9 induction and their normalization by enforced integrin α6 expression. The capacity for forced integrin α6 expression to reverse the inhibition of stem cell marker expression by KLF9 shows that KLF9 also regulates stemness in part by downregulating integrin α6 expression. GBM is a very hypervascular neoplasm and integrin α6-expressing GSCs preferentially localize to the perivascular niche that serves as a source of trophic signals and adhesive matrix proteins, including laminin, to promote tumor cell stemness (Filatova, Acker, & Garvalov, 2013). Lathia et al. (2010) found that silencing integrin α6 reduces the self-renewal and tumor-propagating capacity of GSCs consistent with this trophic interaction. Further investigation into KLF9's effects on the interaction between GSCs and perivascular niche could provide further insight into the mechanisms behind KLF9's inhibitory role in GSC stemness and tumor suppression.

A limitation of this study is that pathway analysis was only conducted with downregulated targets. Although statistical analyses suggest that KLF9 functions primarily as a transcriptional repressor, this does not rule out the possibility that some of the upregulated genes directly bound by KLF9 are true KLF9 targets. Future studies validating KLF9's regulation of upregulated gene targets and identifying pathways upregulated during its overexpression in GBM neurospheres may provide a more accurate map of the transcriptional network regulated by KLF9 in GSCs. Another potential limitation is that we only examined the influence of forced integrin

α6 expression on GSC behavior. Because forced expression could potentially create a physiologically irrelevant environment that could induce activation of unrelated signaling pathways and cell activities, the addition of studies examining the inhibition of integrin α6 expression on GSC behavior may provide a more comprehensive view of the influence of integrin α6 expression on GSC behavior.

Expression of the gene encoding CD151, an integrin α6 binding partner and facilitator of integrin signaling, is also directly downregulated by KLF9. In the present study, we present the novel findings that KLF9 represses *CD151* expression and identifies CD151 and its direct interactions with integrins as novel regulators of GSC stemness and tumorigenicity. Our multiple approaches revealed that CD151 associates with and actively regulates GBM cell stemness. Glioma neurosphere cells expressing the stemness marker CD133 were found to express high levels of CD151 compared to CD133-negative cells and silencing CD151 blocked glioma cell capacity to self-renew as spheres, impaired proliferation and inhibited expression of markers and drivers of cell stemness including CD133, Sox2 and Olig2. Alternatively, forcing the expression of the Oct4 and Sox2 transcription factors under conditions that induce glioma-propagating cells and CD133-positive cells (Lopez-Bertoni et al., 2014) increased expression of CD151; conversely forcing the expression of CD151 enhanced glioma cell self-renewal and increased expression of stemness-associated factors. These findings demonstrate a strong mechanistic link between CD151 expression and GSC stemness and provide a novel functional context to our recent report showing that *CD151* resides within a transcriptional network that is repressed by KLF9, a transcription factor that induces GSC differentiation and inhibits GSC tumor-propagating potential. Our data is supported by previous studies from other investigators in different organ systems showing the association of CD151 expression with the capacity of prostate cancer cells to

self-renew as spheres (Rajasekhar et al., 2011) and the CD151-dependent regulation of progenitor cell pools during mammary development (Yin et al., 2014).

Our results point to a role for integrins in the mechanism by which CD151 regulates GSCs. Laminin-binding integrin receptor subunits (integrin α3, α6, β1, β4) in particular have been shown to support GSC stemness. Integrin α3 is upregulated in GSCs and contributes to GSC migration and invasion (Nakada et al., 2013). Integrin α6 has been found to mark GSCs and regulate GSC self-renewal and tumor-initiating capacity (Lathia et al., 2010).We now show that CD151 directly complexes with integrin receptor subunits α3, α6 and β1 in GBM neurosphere cells and that cell responses activated by forced CD151 expression (i.e. self-renewal as spheres and Akt activation) are inhibited by blocking the CD151-integrin interaction. These findings complement previous studies in other cell models showing that CD151 forms tight complexes with laminin-binding integrins and influences activation of downstream integrin signaling (Hong et al., 2012; Kazarov et al., 2002; Sincock et al., 1999a; Sterk et al., 2002; Yauch et al., 2000). For example, CD151's interaction with integrins α3 and α6 are maintained under stringent lysis conditions (Triton X-100 or NP-40) in melanoma, hepatocellular carcinoma and endothelial cells (Fei et al., 2012; Hong et al., 2012; W. F. Liu et al., 2011). W. F. Liu et al. (2011) also showed that overexpression of CD151 activates several downstream proteins in the integrin signaling pathway including FAK, PI3K, Akt, ERK1/2, cdc42 and Rac1 in endothelial cells. Because *CD151* and *ITGA6* are both downregulated by KLF9, both genes reside within a transcriptional network that regulates GSC stemness and glioma propagation.

A limitation of this study is that it does not extensively explore the involvement of other CD151 interactions in GSC regulation. Because CD151 participates in several interactions at the cell surface in tetraspanin-enriched microdomains, it is possible that CD151 influences several signaling pathways in order to regulate GBM cell stemness. Our preliminary proteomics analysis

identified 305 other proteins that CD151 may interact with in GSCs. Future studies examining the influence of the interaction between CD151 and these proteins on GSC behavior would help tease out the mechanism by which CD151 regulates these cells.

A prominent feature of clinical gliomas and GSCs is their capacity to invade surrounding brain (Sever & Brugge, 2015), and CD151 has been shown to promote the adhesion and migratory capacity of several cancer cell types (Devbhandari et al., 2011; Fei et al., 2012; Klosek et al., 2005; Winterwood et al., 2006; X. H. Yang et al., 2008). We now show that CD151 stimulates GBM neurosphere cell migration and the rate of neurosphere cell adhesion to integrin-binding substrata. Our data showing that blocking CD151 binding to integrins α3 and α6 inhibits neurosphere cell migration on laminin complements the findings of Fei et al. (2012) who found that transfecting hepatocellular carcinoma cells with pAAV-CD151-AAA, which codes for a mutant CD151 deficient in integrin-binding capacity, inhibits invasion. Similarly, pAAV-CD151-AAA has been shown to inhibit CD151 promoted cell migration in prostate cancer cells (W. Yang et al., 2012).

Our finding that CD151 expression knock-down inhibits the growth of neurosphere-derived GBM xenografts supports the translational potential of targeting CD151 and/or CD151-integrin interactions in malignant glioma. CD151 silencing also increased tumor cell apoptosis, identifying CD151 as a GBM cell survival factor in vivo. It is possible that this apoptosis response reflects the effect of CD151 inhibition on AKT activation, a known driver of cancer cell survival (Sever & Brugge, 2015). Interestingly, we found that GBM neurosphere cell viability is not significantly affected by CD151 knockdown in vitro, suggesting that interactions between CD151 and elements specific to the in vivo tumor microenvironment support GSC-derived tumor cell survival. The tumor vasculature may represent one such element since CD151 silencing also reduced tumor vascular density, a response that may deprive tumors of their perivascular stem

cell niche and thereby reduce GBM cell viability and inhibit tumor formation. This antiangiogenic response mirrors previous studies showing that Lewis lung carcinoma xenografts display reduced angiogenic potential when established in CD151-null mice (Y. Takeda et al., 2007).

In conclusion, we have identified gene targets directly regulated by KLF9 on a genome-wide scale in GBM-derived neurosphere cultures. In this GBM-derived CSC model, we show that KLF9 inhibits GBM cell stemness and functions predominantly as a transcriptional repressor within this context. KLF9 is shown to regulate multiple signaling pathways including those involved in oncogenesis, stem cell regulation, neuronal cell signaling, and integrin signaling. KLF9 is shown to inhibit GBM cell stemness and tumorigenicity, in part, by directly repressing integrin α6 expression and potentially through downregulation of its binding partner CD151. CD151 supports GBM cell stemness and self- renewal, and inhibiting CD151 expression in vivo induces GBM cell apoptosis, inhibits GBM angiogenesis and inhibits GBM xenograft growth. CD151 binding to integrins α3 and α6 and CD151-integrin complex-dependent Akt activation are implicated in CD151's oncogenic activities. Our findings contribute to the understanding of the transcriptional networks underlying cancer stem cell maintenance and differentiation, and provide new regulatory mechanisms applicable to cancer therapeutics.

References

Abbadi, S., Rodarte, J. J., Abutaleb, A., Lavell, E., Smith, C. L., Ruff, W., . . . Quinones-Hinojosa, A. (2014). Glucose-6-phosphatase is a key metabolic regulator of glioblastoma invasion. *Mol Cancer Res, 12*(11), 1547-1559. doi: 10.1158/1541-7786.MCR-14-0106-T

Abounader, R., Lal, B., Luddy, C., Koe, G., Davidson, B., Rosen, E. M., & Laterra, J. (2002). In vivo targeting of SF/HGF and c-met expression via U1snRNA/ribozymes inhibits glioma growth and angiogenesis and promotes apoptosis. *FASEB J, 16*(1), 108-110. doi: 10.1096/fj.01-0421fje

Ahmed, R., Oborski, M. J., Hwang, M., Lieberman, F. S., & Mountz, J. M. (2014). Malignant gliomas: current perspectives in diagnosis, treatment, and early response assessment using advanced quantitative imaging methods. *Cancer Manag Res, 6*, 149-170. doi: 10.2147/CMAR.S54726

Ailane, N., Greco, C., Zhu, Y., Sala-Valdes, M., Billard, M., Casal, I., . . . Boucheix, C. (2014). Effect of an anti-human Co-029/tspan8 mouse monoclonal antibody on tumor growth in a nude mouse model. *Front Physiol, 5*, 364. doi: 10.3389/fphys.2014.00364

Ajani, J. A., Song, S., Hochster, H. S., & Steinberg, I. B. (2015). Cancer stem cells: the promise and the potential. *Semin Oncol, 42 Suppl 1*, S3-17. doi: 10.1053/j.seminoncol.2015.01.001

Al-Hajj, M., Wicha, M. S., Benito-Hernandez, A., Morrison, S. J., & Clarke, M. F. (2003). Prospective identification of tumorigenic breast cancer cells. *Proc Natl Acad Sci U S A, 100*(7), 3983-3988. doi: 10.1073/pnas.0530291100

Al-Nbaheen, M., Vishnubalaji, R., Ali, D., Bouslimi, A., Al-Jassir, F., Megges, M., . . . Aldahmash, A. (2013). Human stromal (mesenchymal) stem cells from bone marrow,

adipose tissue and skin exhibit differences in molecular phenotype and differentiation potential. *Stem Cell Rev, 9*(1), 32-43. doi: 10.1007/s12015-012-9365-8

Alentorn, A., Marie, Y., Carpentier, C., Boisselier, B., Giry, M., Labussiere, M., . . . Idbaih, A. (2012). Prevalence, clinico-pathological value, and co-occurrence of PDGFRA abnormalities in diffuse gliomas. *Neuro Oncol, 14*(11), 1393-1403. doi: 10.1093/neuonc/nos217

Alifieris, C., & Trafalis, D. T. (2015). Glioblastoma multiforme: Pathogenesis and treatment. *Pharmacol Ther*. doi: 10.1016/j.pharmthera.2015.05.005

Anami, K., Oue, N., Noguchi, T., Sakamoto, N., Sentani, K., Hayashi, T., . . . Yasui, W. (2015). TSPAN8, identified by Escherichia coli ampicillin secretion trap, is associated with cell growth and invasion in gastric cancer. *Gastric Cancer*. doi: 10.1007/s10120-015-0478-z

Aumailley, M., Timpl, R., & Sonnenberg, A. (1990). Antibody to integrin alpha 6 subunit specifically inhibits cell-binding to laminin fragment 8. *Exp Cell Res, 188*(1), 55-60.

Bababeygy, S. R., Cheshier, S. H., Hou, L. C., Higgins, D. M., Weissman, I. L., & Tse, V. C. (2008). Hematopoietic stem cell-derived pericytic cells in brain tumor angio-architecture. *Stem Cells Dev, 17*(1), 11-18. doi: 10.1089/scd.2007.0117

Bachoo, R. M., Maher, E. A., Ligon, K. L., Sharpless, N. E., Chan, S. S., You, M. J., . . . DePinho, R. A. (2002). Epidermal growth factor receptor and Ink4a/Arf: convergent mechanisms governing terminal differentiation and transformation along the neural stem cell to astrocyte axis. *Cancer Cell, 1*(3), 269-277.

Bao, S., Wu, Q., McLendon, R. E., Hao, Y., Shi, Q., Hjelmeland, A. B., . . . Rich, J. N. (2006). Glioma stem cells promote radioresistance by preferential activation of the DNA damage response. *Nature, 444*(7120), 756-760. doi: 10.1038/nature05236

Barczyk, M., Carracedo, S., & Gullberg, D. (2010). Integrins. *Cell Tissue Res, 339*(1), 269-280. doi: 10.1007/s00441-009-0834-6

Becher, O. J., Hambardzumyan, D., Fomchenko, E. I., Momota, H., Mainwaring, L., Bleau, A. M., . . . Holland, E. C. (2008). Gli activity correlates with tumor grade in platelet-derived growth factor-induced gliomas. *Cancer Res, 68*(7), 2241-2249. doi: 10.1158/0008-5472.CAN-07-6350

Becher, O. J., & Holland, E. C. (2014). Sox2, a marker for stem-like tumor cells in skin squamous cell carcinoma and hedgehog subgroup medulloblastoma. *EMBO J, 33*(18), 1984-1986. doi: 10.15252/embj.201489479

Begum, N. A., Mori, M., Matsumata, T., Takenaka, K., Sugimachi, K., & Barnard, G. F. (1995). Differential display and integrin alpha 6 messenger RNA overexpression in hepatocellular carcinoma. *Hepatology, 22*(5), 1447-1455.

Bellail, A. C., Hunter, S. B., Brat, D. J., Tan, C., & Van Meir, E. G. (2004). Microregional extracellular matrix heterogeneity in brain modulates glioma cell invasion. *Int J Biochem Cell Biol, 36*(6), 1046-1069. doi: 10.1016/j.biocel.2004.01.013

Ben-Porath, I., Thomson, M. W., Carey, V. J., Ge, R., Bell, G. W., Regev, A., & Weinberg, R. A. (2008). An embryonic stem cell-like gene expression signature in poorly differentiated aggressive human tumors. *Nat Genet, 40*(5), 499-507. doi: 10.1038/ng.127

Benjamini, Y., Drai, D., Elmer, G., Kafkafi, N., & Golani, I. (2001). Controlling the false discovery rate in behavior genetics research. *Behav Brain Res, 125*(1-2), 279-284.

Berthier-Vergnes, O., Kharbili, M. E., de la Fouchardiere, A., Pointecouteau, T., Verrando, P., Wierinckx, A., . . . Lamartine, J. (2011). Gene expression profiles of human melanoma cells with different invasive potential reveal TSPAN8 as a novel mediator of invasion. *Br J Cancer, 104*(1), 155-165. doi: 10.1038/sj.bjc.6605994

Blumenthal, A., Giebel, J., Ummanni, R., Schluter, R., Endlich, K., & Endlich, N. (2012). Morphology and migration of podocytes are affected by CD151 levels. *Am J Physiol Renal Physiol, 302*(10), F1265-1277. doi: 10.1152/ajprenal.00468.2011

Bonardi, F., Fusetti, F., Deelen, P., van Gosliga, D., Vellenga, E., & Schuringa, J. J. (2013). A proteomics and transcriptomics approach to identify leukemic stem cell (LSC) markers. *Mol Cell Proteomics, 12*(3), 626-637. doi: 10.1074/mcp.M112.021931

Bonnet, D., & Dick, J. E. (1997). Human acute myeloid leukemia is organized as a hierarchy that originates from a primitive hematopoietic cell. *Nat Med, 3*(7), 730-737.

Bourguignon, L. Y., Earle, C., Wong, G., Spevak, C. C., & Krueger, K. (2012). Stem cell marker (Nanog) and Stat-3 signaling promote MicroRNA-21 expression and chemoresistance in hyaluronan/CD44-activated head and neck squamous cell carcinoma cells. *Oncogene, 31*(2), 149-160. doi: 10.1038/onc.2011.222

Boyer, L. A., Lee, T. I., Cole, M. F., Johnstone, S. E., Levine, S. S., Zucker, J. P., . . . Young, R. A. (2005). Core transcriptional regulatory circuitry in human embryonic stem cells. *Cell, 122*(6), 947-956. doi: 10.1016/j.cell.2005.08.020

Bragado, P., Estrada, Y., Sosa, M. S., Avivar-Valderas, A., Cannan, D., Genden, E., . . . Aguirre-Ghiso, J. A. (2012). Analysis of marker-defined HNSCC subpopulations reveals a dynamic regulation of tumor initiating properties. *PLoS One, 7*(1), e29974. doi: 10.1371/journal.pone.0029974

Bredel, M., Bredel, C., Juric, D., Harsh, G. R., Vogel, H., Recht, L. D., & Sikic, B. I. (2005). Functional network analysis reveals extended gliomagenesis pathway maps and three novel MYC-interacting genes in human gliomas. *Cancer Res, 65*(19), 8679-8689. doi: 10.1158/0008-5472.CAN-05-1204

Brooks, P. C., Clark, R. A., & Cheresh, D. A. (1994). Requirement of vascular integrin alpha v beta 3 for angiogenesis. *Science, 264*(5158), 569-571.

Bruce, W. R., & Van Der Gaag, H. (1963). A Quantitative Assay for the Number of Murine Lymphoma Cells Capable of Proliferation in Vivo. *Nature, 199*, 79-80.

Bryne, J. C., Valen, E., Tang, M. H., Marstrand, T., Winther, O., da Piedade, I., . . . Sandelin, A. (2008). JASPAR, the open access database of transcription factor-binding profiles: new content and tools in the 2008 update. *Nucleic Acids Res, 36*(Database issue), D102-106. doi: 10.1093/nar/gkm955

Cajot, J. F., Sordat, I., Silvestre, T., & Sordat, B. (1997). Differential display cloning identifies motility-related protein (MRP1/CD9) as highly expressed in primary compared to metastatic human colon carcinoma cells. *Cancer Res, 57*(13), 2593-2597.

Campbell, I. D., & Humphries, M. J. (2011). Integrin structure, activation, and interactions. *Cold Spring Harb Perspect Biol, 3*(3). doi: 10.1101/cshperspect.a004994

Campos, B., Wan, F., Farhadi, M., Ernst, A., Zeppernick, F., Tagscherer, K. E., . . . Herold-Mende, C. (2010). Differentiation therapy exerts antitumor effects on stem-like glioma cells. *Clin Cancer Res, 16*(10), 2715-2728. doi: 10.1158/1078-0432.CCR-09-1800

Campos, L. S., Decker, L., Taylor, V., & Skarnes, W. (2006). Notch, epidermal growth factor receptor, and beta1-integrin pathways are coordinated in neural stem cells. *J Biol Chem, 281*(8), 5300-5309. doi: 10.1074/jbc.M511886200

Cancer Genome Atlas Research, N. (2008). Comprehensive genomic characterization defines human glioblastoma genes and core pathways. *Nature, 455*(7216), 1061-1068. doi: 10.1038/nature07385

Cariati, M., Naderi, A., Brown, J. P., Smalley, M. J., Pinder, S. E., Caldas, C., & Purushotham, A. D. (2008). Alpha-6 integrin is necessary for the tumourigenicity of a stem cell-like subpopulation within the MCF7 breast cancer cell line. *Int J Cancer, 122*(2), 298-304. doi: 10.1002/ijc.23103

Carlson, C. M., Endrizzi, B. T., Wu, J., Ding, X., Weinreich, M. A., Walsh, E. R., . . . Jameson, S. C. (2006). Kruppel-like factor 2 regulates thymocyte and T-cell migration. *Nature, 442*(7100), 299-302. doi: 10.1038/nature04882

Carlson, M., Pages, H., Aboyoun, P., Falcon, S., Morgan, M., Sarkar, D., & Lawrence, M. GenomicFeatures: Tools for making and manipulating transcript centric annotations.

Charles, N., & Holland, E. C. (2010). The perivascular niche microenvironment in brain tumor progression. *Cell Cycle, 9*(15), 3012-3021. doi: 10.4161/cc.9.15.12710

Charrin, S., le Naour, F., Silvie, O., Milhiet, P. E., Boucheix, C., & Rubinstein, E. (2009). Lateral organization of membrane proteins: tetraspanins spin their web. *Biochem J, 420*(2), 133-154. doi: 10.1042/BJ20082422

Chen, S., Lewallen, M., & Xie, T. (2013). Adhesion in the stem cell niche: biological roles and regulation. *Development, 140*(2), 255-265. doi: 10.1242/dev.083139

Chen, Z., Mustafa, T., Trojanowicz, B., Brauckhoff, M., Gimm, O., Schmutzler, C., . . . Hoang-Vu, C. (2004). CD82, and CD63 in thyroid cancer. *Int J Mol Med, 14*(4), 517-527.

Cheng, L., Huang, Z., Zhou, W., Wu, Q., Donnola, S., Liu, J. K., . . . Bao, S. (2013). Glioblastoma stem cells generate vascular pericytes to support vessel function and tumor growth. *Cell, 153*(1), 139-152. doi: 10.1016/j.cell.2013.02.021

Chiou, S. H., Yu, C. C., Huang, C. Y., Lin, S. C., Liu, C. J., Tsai, T. H., . . . Lo, J. F. (2008). Positive correlations of Oct-4 and Nanog in oral cancer stem-like cells and high-grade oral squamous cell carcinoma. *Clin Cancer Res, 14*(13), 4085-4095. doi: 10.1158/1078-0432.CCR-07-4404

Chung, J., Bachelder, R. E., Lipscomb, E. A., Shaw, L. M., & Mercurio, A. M. (2002). Integrin (alpha 6 beta 4) regulation of eIF-4E activity and VEGF translation: a survival mechanism for carcinoma cells. *J Cell Biol, 158*(1), 165-174. doi: 10.1083/jcb.200112015

Claas, C., Seiter, S., Claas, A., Savelyeva, L., Schwab, M., & Zoller, M. (1998). Association between the rat homologue of CO-029, a metastasis-associated tetraspanin molecule and consumption coagulopathy. *J Cell Biol, 141*(1), 267-280.

Clement, V., Sanchez, P., de Tribolet, N., Radovanovic, I., & Ruiz i Altaba, A. (2007). HEDGEHOG-GLI1 signaling regulates human glioma growth, cancer stem cell self-renewal, and tumorigenicity. *Curr Biol, 17*(2), 165-172. doi: 10.1016/j.cub.2006.11.033

Clevers, H., Loh, K. M., & Nusse, R. (2014). Stem cell signaling. An integral program for tissue renewal and regeneration: Wnt signaling and stem cell control. *Science, 346*(6205), 1248012. doi: 10.1126/science.1248012

Colombel, M., Eaton, C. L., Hamdy, F., Ricci, E., van der Pluijm, G., Cecchini, M., . . . Thalmann, G. (2012). Increased expression of putative cancer stem cell markers in primary prostate cancer is associated with progression of bone metastases. *Prostate, 72*(7), 713-720. doi: 10.1002/pros.21473

Covello, K. L., Kehler, J., Yu, H., Gordan, J. D., Arsham, A. M., Hu, C. J., . . . Keith, B. (2006). HIF-2alpha regulates Oct-4: effects of hypoxia on stem cell function, embryonic development, and tumor growth. *Genes Dev, 20*(5), 557-570. doi: 10.1101/gad.1399906

Cowin, A. J., Adams, D., Geary, S. M., Wright, M. D., Jones, J. C., & Ashman, L. K. (2006). Wound healing is defective in mice lacking tetraspanin CD151. *J Invest Dermatol, 126*(3), 680-689. doi: 10.1038/sj.jid.5700142

Cox, B. D., Natarajan, M., Stettner, M. R., & Gladson, C. L. (2006). New concepts regarding focal adhesion kinase promotion of cell migration and proliferation. *J Cell Biochem, 99*(1), 35-52. doi: 10.1002/jcb.20956

Crespo, I., Vital, A. L., Gonzalez-Tablas, M., Patino, M. D., Otero, A., Lopes, M. C., . . . Tabernero, M. D. (2015). Molecular and Genomic Alterations in Glioblastoma Multiforme. *Am J Pathol*. doi: 10.1016/j.ajpath.2015.02.023

Cui, L., Johkura, K., Yue, F., Ogiwara, N., Okouchi, Y., Asanuma, K., & Sasaki, K. (2004). Spatial distribution and initial changes of SSEA-1 and other cell adhesion-related

molecules on mouse embryonic stem cells before and during differentiation. *J Histochem Cytochem, 52*(11), 1447-1457. doi: 10.1369/jhc.3A6241.2004

Cuiffo, B. G., & Karnoub, A. E. (2012). Mesenchymal stem cells in tumor development: emerging roles and concepts. *Cell Adh Migr, 6*(3), 220-230. doi: 10.4161/cam.20875

D'Ippolito, G., Diabira, S., Howard, G. A., Menei, P., Roos, B. A., & Schiller, P. C. (2004). Marrow-isolated adult multilineage inducible (MIAMI) cells, a unique population of postnatal young and old human cells with extensive expansion and differentiation potential. *J Cell Sci, 117*(Pt 14), 2971-2981. doi: 10.1242/jcs.01103

Dasari, V. R., Kaur, K., Velpula, K. K., Gujrati, M., Fassett, D., Klopfenstein, J. D., . . . Rao, J. S. (2010). Upregulation of PTEN in glioma cells by cord blood mesenchymal stem cells inhibits migration via downregulation of the PI3K/Akt pathway. *PLoS One, 5*(4), e10350. doi: 10.1371/journal.pone.0010350

DeMali, K. A., Sun, X., & Bui, G. A. (2014). Force transmission at cell-cell and cell-matrix adhesions. *Biochemistry, 53*(49), 7706-7717. doi: 10.1021/bi501181p

Deng, X., Li, Q., Hoff, J., Novak, M., Yang, H., Jin, H., . . . Yang, X. H. (2012). Integrin-associated CD151 drives ErbB2-evoked mammary tumor onset and metastasis. *Neoplasia, 14*(8), 678-689.

Desgrosellier, J. S., & Cheresh, D. A. (2010). Integrins in cancer: biological implications and therapeutic opportunities. *Nat Rev Cancer, 10*(1), 9-22. doi: 10.1038/nrc2748

Detchokul, S., Newell, B., Williams, E. D., & Frauman, A. G. (2014). CD151 is associated with prostate cancer cell invasion and lymphangiogenesis in vivo. *Oncol Rep, 31*(1), 241-247. doi: 10.3892/or.2013.2823

Devbhandari, R. P., Shi, G. M., Ke, A. W., Wu, F. Z., Huang, X. Y., Wang, X. Y., . . . Zhou, J. (2011). Profiling of the tetraspanin CD151 web and conspiracy of CD151/integrin beta1

complex in the progression of hepatocellular carcinoma. *PLoS One, 6*(9), e24901. doi: 10.1371/journal.pone.0024901

Diaz-Romero, J., Nesic, D., Grogan, S. P., Heini, P., & Mainil-Varlet, P. (2008). Immunophenotypic changes of human articular chondrocytes during monolayer culture reflect bona fide dedifferentiation rather than amplification of progenitor cells. *J Cell Physiol, 214*(1), 75-83. doi: 10.1002/jcp.21161

Dolecek, T. A., Propp, J. M., Stroup, N. E., & Kruchko, C. (2012). CBTRUS statistical report: primary brain and central nervous system tumors diagnosed in the United States in 2005-2009. *Neuro Oncol, 14 Suppl 5*, v1-49. doi: 10.1093/neuonc/nos218

Dong, J. T., Lamb, P. W., Rinker-Schaeffer, C. W., Vukanovic, J., Ichikawa, T., Isaacs, J. T., & Barrett, J. C. (1995). KAI1, a metastasis suppressor gene for prostate cancer on human chromosome 11p11.2. *Science, 268*(5212), 884-886.

Dong, Z., Yang, L., & Lai, D. (2013). KLF5 strengthens drug resistance of ovarian cancer stem-like cells by regulating survivin expression. *Cell Prolif, 46*(4), 425-435. doi: 10.1111/cpr.12043

Drissen, R., von Lindern, M., Kolbus, A., Driegen, S., Steinlein, P., Beug, H., . . . Philipsen, S. (2005). The erythroid phenotype of EKLF-null mice: defects in hemoglobin metabolism and membrane stability. *Mol Cell Biol, 25*(12), 5205-5214. doi: 10.1128/MCB.25.12.5205-5214.2005

Ehtesham, M., Min, E., Issar, N. M., Kasl, R. A., Khan, I. S., & Thompson, R. C. (2013). The role of the CXCR4 cell surface chemokine receptor in glioma biology. *J Neurooncol, 113*(2), 153-162. doi: 10.1007/s11060-013-1108-4

Emdad, L., Sarkar, D., Lee, S. G., Su, Z. Z., Yoo, B. K., Dash, R., . . . Fisher, P. B. (2010). Astrocyte elevated gene-1: a novel target for human glioma therapy. *Mol Cancer Ther, 9*(1), 79-88. doi: 10.1158/1535-7163.MCT-09-0752

Erovic, B. M., Pammer, J., Hollemann, D., Woegerbauer, M., Geleff, S., Fischer, M. B., . . . Neuchrist, C. (2003). Motility-related protein-1/CD9 expression in head and neck squamous cell carcinoma. *Head Neck, 25*(10), 848-857. doi: 10.1002/hed.10306

Fan, X., Aalto, Y., Sanko, S. G., Knuutila, S., Klatzmann, D., & Castresana, J. S. (2002). Genetic profile, PTEN mutation and therapeutic role of PTEN in glioblastomas. *Int J Oncol, 21*(5), 1141-1150.

Farnie, G., & Clarke, R. B. (2007). Mammary stem cells and breast cancer--role of Notch signalling. *Stem Cell Rev, 3*(2), 169-175.

Fei, Y., Wang, J., Liu, W., Zuo, H., Qin, J., Wang, D., . . . Liu, Z. (2012). CD151 promotes cancer cell metastasis via integrins alpha3beta1 and alpha6beta1 in vitro. *Mol Med Rep, 6*(6), 1226-1230. doi: 10.3892/mmr.2012.1095

Filatova, A., Acker, T., & Garvalov, B. K. (2013). The cancer stem cell niche(s): the crosstalk between glioma stem cells and their microenvironment. *Biochim Biophys Acta, 1830*(2), 2496-2508. doi: 10.1016/j.bbagen.2012.10.008

Fitter, S., Tetaz, T. J., Berndt, M. C., & Ashman, L. K. (1995). Molecular cloning of cDNA encoding a novel platelet-endothelial cell tetra-span antigen, PETA-3. *Blood, 86*(4), 1348-1355.

Friedlander, M., Brooks, P. C., Shaffer, R. W., Kincaid, C. M., Varner, J. A., & Cheresh, D. A. (1995). Definition of two angiogenic pathways by distinct alpha v integrins. *Science, 270*(5241), 1500-1502.

Frigo, D. E., Sherk, A. B., Wittmann, B. M., Norris, J. D., Wang, Q., Joseph, J. D., . . . McDonnell, D. P. (2009). Induction of Kruppel-like factor 5 expression by androgens results in increased CXCR4-dependent migration of prostate cancer cells in vitro. *Mol Endocrinol, 23*(9), 1385-1396. doi: 10.1210/me.2009-0010

Fu, D. Z., Cheng, Y., He, H., Liu, H. Y., & Liu, Y. F. (2014). The fate of Kruppel-like factor 9-positive hepatic carcinoma cells may be determined by the programmed cell death protein 5. *Int J Oncol, 44*(1), 153-160. doi: 10.3892/ijo.2013.2147

Fukamachi, H., Seol, H. S., Shimada, S., Funasaka, C., Baba, K., Kim, J. H., . . . Yuasa, Y. (2013). CD49f(high) cells retain sphere-forming and tumor-initiating activities in human gastric tumors. *PLoS One, 8*(8), e72438. doi: 10.1371/journal.pone.0072438

Galli, R., Binda, E., Orfanelli, U., Cipelletti, B., Gritti, A., De Vitis, S., . . . Vescovi, A. (2004). Isolation and characterization of tumorigenic, stem-like neural precursors from human glioblastoma. *Cancer Res, 64*(19), 7011-7021. doi: 10.1158/0008-5472.CAN-04-1364

Gammon, L., Biddle, A., Heywood, H. K., Johannessen, A. C., & Mackenzie, I. C. (2013). Sub-sets of cancer stem cells differ intrinsically in their patterns of oxygen metabolism. *PLoS One, 8*(4), e62493. doi: 10.1371/journal.pone.0062493

Gangemi, R. M., Griffero, F., Marubbi, D., Perera, M., Capra, M. C., Malatesta, P., . . . Corte, G. (2009). SOX2 silencing in glioblastoma tumor-initiating cells causes stop of proliferation and loss of tumorigenicity. *Stem Cells, 27*(1), 40-48. doi: 10.1634/stemcells.2008-0493

Garcia-Lopez, M. A., Barreiro, O., Garcia-Diez, A., Sanchez-Madrid, F., & Penas, P. F. (2005). Role of tetraspanins CD9 and CD151 in primary melanocyte motility. *J Invest Dermatol, 125*(5), 1001-1009. doi: 10.1111/j.0022-202X.2005.23882.x

Garmy-Susini, B., Jin, H., Zhu, Y., Sung, R. J., Hwang, R., & Varner, J. (2005). Integrin alpha4beta1-VCAM-1-mediated adhesion between endothelial and mural cells is required for blood vessel maturation. *J Clin Invest, 115*(6), 1542-1551. doi: 10.1172/JCI23445

Garzon-Muvdi, T., Schiapparelli, P., ap Rhys, C., Guerrero-Cazares, H., Smith, C., Kim, D. H., . . . Quinones-Hinojosa, A. (2012). Regulation of brain tumor dispersal by NKCC1 through a novel role in focal adhesion regulation. *PLoS Biol, 10*(5), e1001320. doi: 10.1371/journal.pbio.1001320

Geary, S. M., Cowin, A. J., Copeland, B., Baleato, R. M., Miyazaki, K., & Ashman, L. K. (2008). The role of the tetraspanin CD151 in primary keratinocyte and fibroblast functions: implications for wound healing. *Exp Cell Res, 314*(11-12), 2165-2175. doi: 10.1016/j.yexcr.2008.04.011

Gemei, M., Di Noto, R., Mirabelli, P., & Del Vecchio, L. (2013). Cytometric profiling of CD133+ cells in human colon carcinoma cell lines identifies a common core phenotype and cell type-specific mosaics. *Int J Biol Markers, 28*(3), 267-273. doi: 10.5301/JBM.5000020

Gesierich, S., Paret, C., Hildebrand, D., Weitz, J., Zgraggen, K., Schmitz-Winnenthal, F. H., . . . Zoller, M. (2005). Colocalization of the tetraspanins, CO-029 and CD151, with integrins in human pancreatic adenocarcinoma: impact on cell motility. *Clin Cancer Res, 11*(8), 2840-2852. doi: 10.1158/1078-0432.CCR-04-1935

Ghani, F. I., Yamazaki, H., Iwata, S., Okamoto, T., Aoe, K., Okabe, K., . . . Morimoto, C. (2011). Identification of cancer stem cell markers in human malignant mesothelioma cells. *Biochem Biophys Res Commun, 404*(2), 735-742. doi: 10.1016/j.bbrc.2010.12.054

Goffart, N., Kroonen, J., & Rogister, B. (2013). Glioblastoma-initiating cells: relationship with neural stem cells and the micro-environment. *Cancers (Basel), 5*(3), 1049-1071. doi: 10.3390/cancers5031049

Greco, C., Bralet, M. P., Ailane, N., Dubart-Kupperschmitt, A., Rubinstein, E., Le Naour, F., & Boucheix, C. (2010). E-cadherin/p120-catenin and tetraspanin Co-029 cooperate for cell motility control in human colon carcinoma. *Cancer Res, 70*(19), 7674-7683. doi: 10.1158/0008-5472.CAN-09-4482

Grosse-Gehling, P., Fargeas, C. A., Dittfeld, C., Garbe, Y., Alison, M. R., Corbeil, D., & Kunz-Schughart, L. A. (2013). CD133 as a biomarker for putative cancer stem cells in solid

tumours: limitations, problems and challenges. *J Pathol, 229*(3), 355-378. doi: 10.1002/path.4086

Guo, P., Hu, B., Gu, W., Xu, L., Wang, D., Huang, H. J., . . . Cheng, S. Y. (2003). Platelet-derived growth factor-B enhances glioma angiogenesis by stimulating vascular endothelial growth factor expression in tumor endothelia and by promoting pericyte recruitment. *Am J Pathol, 162*(4), 1083-1093. doi: 10.1016/S0002-9440(10)63905-3

Ha, S. Y., Kang, S. Y., Do, I. G., & Suh, Y. L. (2013). Glioblastoma with oligodendroglial component represents a subgroup of glioblastoma with high prevalence of IDH1 mutation and association with younger age. *J Neurooncol, 112*(3), 439-448. doi: 10.1007/s11060-013-1073-y

Hambardzumyan, D., Becher, O. J., Rosenblum, M. K., Pandolfi, P. P., Manova-Todorova, K., & Holland, E. C. (2008). PI3K pathway regulates survival of cancer stem cells residing in the perivascular niche following radiation in medulloblastoma in vivo. *Genes Dev, 22*(4), 436-448. doi: 10.1101/gad.1627008

Hamburger, A. W., & Salmon, S. E. (1977). Primary bioassay of human tumor stem cells. *Science, 197*(4302), 461-463.

Haraguchi, N., Ishii, H., Mimori, K., Ohta, K., Uemura, M., Nishimura, J., . . . Mori, M. (2013). CD49f-positive cell population efficiently enriches colon cancer-initiating cells. *Int J Oncol, 43*(2), 425-430. doi: 10.3892/ijo.2013.1955

Harkness, L., Christiansen, H., Nehlin, J., Barington, T., Andersen, J. S., & Kassem, M. (2008). Identification of a membrane proteomic signature for human embryonic stem cells independent of culture conditions. *Stem Cell Res, 1*(3), 219-227. doi: 10.1016/j.scr.2008.06.001

Hasegawa, H., Utsunomiya, Y., Kishimoto, K., Yanagisawa, K., & Fujita, S. (1996). SFA-1, a novel cellular gene induced by human T-cell leukemia virus type 1, is a member of the transmembrane 4 superfamily. *J Virol, 70*(5), 3258-3263.

Heddleston, J. M., Li, Z., McLendon, R. E., Hjelmeland, A. B., & Rich, J. N. (2009). The hypoxic microenvironment maintains glioblastoma stem cells and promotes reprogramming towards a cancer stem cell phenotype. *Cell Cycle, 8*(20), 3274-3284.

Hemler, M. E. (2014). Tetraspanin proteins promote multiple cancer stages. *Nat Rev Cancer, 14*(1), 49-60.

Hemler, M. E., Crouse, C., Takada, Y., & Sonnenberg, A. (1988). Multiple very late antigen (VLA) heterodimers on platelets. Evidence for distinct VLA-2, VLA-5 (fibronectin receptor), and VLA-6 structures. *J Biol Chem, 263*(16), 7660-7665.

Hemler, M. E., Jacobson, J. G., & Strominger, J. L. (1985). Biochemical characterization of VLA-1 and VLA-2. Cell surface heterodimers on activated T cells. *J Biol Chem, 260*(28), 15246-15252.

Higashiyama, M., Taki, T., Ieki, Y., Adachi, M., Huang, C. L., Koh, T., . . . Miyake, M. (1995). Reduced motility related protein-1 (MRP-1/CD9) gene expression as a factor of poor prognosis in non-small cell lung cancer. *Cancer Res, 55*(24), 6040-6044.

Holland, E. C., Celestino, J., Dai, C., Schaefer, L., Sawaya, R. E., & Fuller, G. N. (2000). Combined activation of Ras and Akt in neural progenitors induces glioblastoma formation in mice. *Nat Genet, 25*(1), 55-57. doi: 10.1038/75596

Hong, I. K., Jeoung, D. I., Ha, K. S., Kim, Y. M., & Lee, H. (2012). Tetraspanin CD151 stimulates adhesion-dependent activation of Ras, Rac, and Cdc42 by facilitating molecular association between beta1 integrins and small GTPases. *J Biol Chem, 287*(38), 32027-32039. doi: 10.1074/jbc.M111.314443

Hoopfer, E. D., Huang, L., & Denver, R. J. (2002). Basic transcription element binding protein is a thyroid hormone-regulated transcription factor expressed during metamorphosis in Xenopus laevis. *Dev Growth Differ, 44*(5), 365-381.

Horwitz, A., Duggan, K., Greggs, R., Decker, C., & Buck, C. (1985). The cell substrate attachment (CSAT) antigen has properties of a receptor for laminin and fibronectin. *J Cell Biol, 101*(6), 2134-2144.

Houle, C. D., Ding, X. Y., Foley, J. F., Afshari, C. A., Barrett, J. C., & Davis, B. J. (2002). Loss of expression and altered localization of KAI1 and CD9 protein are associated with epithelial ovarian cancer progression. *Gynecol Oncol, 86*(1), 69-78.

Hu, L., McArthur, C., & Jaffe, R. B. (2010). Ovarian cancer stem-like side-population cells are tumourigenic and chemoresistant. *Br J Cancer, 102*(8), 1276-1283. doi: 10.1038/sj.bjc.6605626

Hu, P., & Luo, B. H. (2013). Integrin bi-directional signaling across the plasma membrane. *J Cell Physiol, 228*(2), 306-312. doi: 10.1002/jcp.24154

Huang, F. T., Zhuan-Sun, Y. X., Zhuang, Y. Y., Wei, S. L., Tang, J., Chen, W. B., & Zhang, S. N. (2012). Inhibition of hedgehog signaling depresses self-renewal of pancreatic cancer stem cells and reverses chemoresistance. *Int J Oncol, 41*(5), 1707-1714. doi: 10.3892/ijo.2012.1597

Huang, P. H., Xu, A. M., & White, F. M. (2009). Oncogenic EGFR signaling networks in glioma. *Sci Signal, 2*(87), re6. doi: 10.1126/scisignal.287re6

Huang, S., Wang, C., Yi, Y., Sun, X., Luo, M., Zhou, Z., . . . Ke, Y. (2015). Kruppel-like factor 9 inhibits glioma cell proliferation and tumorigenicity via downregulation of miR-21. *Cancer Lett, 356*(2 Pt B), 547-555. doi: 10.1016/j.canlet.2014.10.007

Hynes, R. O. (2004). The emergence of integrins: a personal and historical perspective. *Matrix Biol, 23*(6), 333-340. doi: 10.1016/j.matbio.2004.08.001

Ibrahim, E. E., Babaei-Jadidi, R., Saadeddin, A., Spencer-Dene, B., Hossaini, S., Abuzinadah, M., . . . Nateri, A. S. (2012). Embryonic NANOG activity defines colorectal cancer stem cells and modulates through AP1- and TCF-dependent mechanisms. *Stem Cells, 30*(10), 2076-2087. doi: 10.1002/stem.1182

Ignatova, T. N., Kukekov, V. G., Laywell, E. D., Suslov, O. N., Vrionis, F. D., & Steindler, D. A. (2002). Human cortical glial tumors contain neural stem-like cells expressing astroglial and neuronal markers in vitro. *Glia, 39*(3), 193-206. doi: 10.1002/glia.10094

Imataka, H., Sogawa, K., Yasumoto, K., Kikuchi, Y., Sasano, K., Kobayashi, A., . . . Fujii-Kuriyama, Y. (1992). Two regulatory proteins that bind to the basic transcription element (BTE), a GC box sequence in the promoter region of the rat P-4501A1 gene. *EMBO J, 11*(10), 3663-3671.

Jeter, C. R., Liu, B., Liu, X., Chen, X., Liu, C., Calhoun-Davis, T., . . . Tang, D. G. (2011). NANOG promotes cancer stem cell characteristics and prostate cancer resistance to androgen deprivation. *Oncogene, 30*(36), 3833-3845. doi: 10.1038/onc.2011.114

Ji, H., Jiang, H., Ma, W., Johnson, D. S., Myers, R. M., & Wong, W. H. (2008). An integrated software system for analyzing ChIP-chip and ChIP-seq data. *Nat Biotechnol, 26*(11), 1293-1300. doi: 10.1038/nbt.1505

Ji, H., Vokes, S. A., & Wong, W. H. (2006). A comparative analysis of genome-wide chromatin immunoprecipitation data for mammalian transcription factors. *Nucleic Acids Res, 34*(21), e146. doi: 10.1093/nar/gkl803

Jiang, J., Chan, Y. S., Loh, Y. H., Cai, J., Tong, G. Q., Lim, C. A., . . . Ng, H. H. (2008). A core Klf circuitry regulates self-renewal of embryonic stem cells. *Nat Cell Biol, 10*(3), 353-360. doi: 10.1038/ncb1698

Johnson, M. S., Lu, N., Denessiouk, K., Heino, J., & Gullberg, D. (2009). Integrins during evolution: evolutionary trees and model organisms. *Biochim Biophys Acta, 1788*(4), 779-789. doi: 10.1016/j.bbamem.2008.12.013

Jones, J. C., Kurpakus, M. A., Cooper, H. M., & Quaranta, V. (1991). A function for the integrin alpha 6 beta 4 in the hemidesmosome. *Cell Regul, 2*(6), 427-438.

Kanamori, M., Kawaguchi, T., Nigro, J. M., Feuerstein, B. G., Berger, M. S., Miele, L., & Pieper, R. O. (2007). Contribution of Notch signaling activation to human glioblastoma multiforme. *J Neurosurg, 106*(3), 417-427. doi: 10.3171/jns.2007.106.3.417

Kanetaka, K., Sakamoto, M., Yamamoto, Y., Yamasaki, S., Lanza, F., Kanematsu, T., & Hirohashi, S. (2001). Overexpression of tetraspanin CO-029 in hepatocellular carcinoma. *J Hepatol, 35*(5), 637-642.

Kang, L., Lu, B., Xu, J., Hu, H., & Lai, M. (2008). Downregulation of Kruppel-like factor 9 in human colorectal cancer. *Pathol Int, 58*(6), 334-338. doi: 10.1111/j.1440-1827.2008.02233.x

Kazarov, A. R., Yang, X., Stipp, C. S., Sehgal, B., & Hemler, M. E. (2002). An extracellular site on tetraspanin CD151 determines alpha 3 and alpha 6 integrin-dependent cellular morphology. *J Cell Biol, 158*(7), 1299-1309.

Kim, D. H., Han, K., Gupta, K., Kwon, K. W., Suh, K. Y., & Levchenko, A. (2009). Mechanosensitivity of fibroblast cell shape and movement to anisotropic substratum topography gradients. *Biomaterials, 30*(29), 5433-5444. doi: 10.1016/j.biomaterials.2009.06.042

Kim, D. H., Seo, C. H., Han, K., Kwon, K. W., Levchenko, A., & Suh, K. Y. (2009). Guided Cell Migration on Microtextured Substrates with Variable Local Density and Anisotropy. *Adv Funct Mater, 19*(10), 1579-1586. doi: 10.1002/adfm.200990041

Kim, J. W., Tchernyshyov, I., Semenza, G. L., & Dang, C. V. (2006). HIF-1-mediated expression of pyruvate dehydrogenase kinase: a metabolic switch required for cellular adaptation to hypoxia. *Cell Metab, 3*(3), 177-185. doi: 10.1016/j.cmet.2006.02.002

Kim, R. J., & Nam, J. S. (2011). OCT4 Expression Enhances Features of Cancer Stem Cells in a Mouse Model of Breast Cancer. *Lab Anim Res, 27*(2), 147-152. doi: 10.5625/lar.2011.27.2.147

Kimura, H., & Fujimori, K. (2014). Activation of early phase of adipogenesis through Kruppel-like factor KLF9-mediated, enhanced expression of CCAAT/enhancer-binding protein beta in 3T3-L1 cells. *Gene, 534*(2), 169-176. doi: 10.1016/j.gene.2013.10.065

Klosek, S. K., Nakashiro, K., Hara, S., Shintani, S., Hasegawa, H., & Hamakawa, H. (2005). CD151 forms a functional complex with c-Met in human salivary gland cancer cells. *Biochem Biophys Res Commun, 336*(2), 408-416. doi: 10.1016/j.bbrc.2005.08.106

Knudsen, K. A., Horwitz, A. F., & Buck, C. A. (1985). A monoclonal antibody identifies a glycoprotein complex involved in cell-substratum adhesion. *Exp Cell Res, 157*(1), 218-226.

Kondapalli, K. C., Llongueras, J. P., Capilla-Gonzalez, V., Prasad, H., Hack, A., Smith, C., . . . Rao, R. (2015). A leak pathway for luminal protons in endosomes drives oncogenic signalling in glioblastoma. *Nat Commun, 6*, 6289. doi: 10.1038/ncomms7289

Koul, D. (2008). PTEN signaling pathways in glioblastoma. *Cancer Biol Ther, 7*(9), 1321-1325.

Krishnamurthy, S., Dong, Z., Vodopyanov, D., Imai, A., Helman, J. I., Prince, M. E., . . . Nor, J. E. (2010). Endothelial cell-initiated signaling promotes the survival and self-renewal of cancer stem cells. *Cancer Res, 70*(23), 9969-9978. doi: 10.1158/0008-5472.CAN-10-1712

Kroon, P., Berry, P. A., Stower, M. J., Rodrigues, G., Mann, V. M., Simms, M., . . . Collins, A. T. (2013). JAK-STAT blockade inhibits tumor initiation and clonogenic recovery of

prostate cancer stem-like cells. *Cancer Res, 73*(16), 5288-5298. doi: 10.1158/0008-5472.CAN-13-0874

Kuo, C. T., Veselits, M. L., Barton, K. P., Lu, M. M., Clendenin, C., & Leiden, J. M. (1997). The LKLF transcription factor is required for normal tunica media formation and blood vessel stabilization during murine embryogenesis. *Genes Dev, 11*(22), 2996-3006.

Kusukawa, J., Ryu, F., Kameyama, T., & Mekada, E. (2001). Reduced expression of CD9 in oral squamous cell carcinoma: CD9 expression inversely related to high prevalence of lymph node metastasis. *J Oral Pathol Med, 30*(2), 73-79.

Kwon, J., Lee, T. S., Lee, H. W., Kang, M. C., Yoon, H. J., Kim, J. H., & Park, J. H. (2013). Integrin alpha 6: a novel therapeutic target in esophageal squamous cell carcinoma. *Int J Oncol, 43*(5), 1523-1530. doi: 10.3892/ijo.2013.2097

Lagadec, C., Vlashi, E., Alhiyari, Y., Phillips, T. M., Bochkur Dratver, M., & Pajonk, F. (2013). Radiation-induced Notch signaling in breast cancer stem cells. *Int J Radiat Oncol Biol Phys, 87*(3), 609-618. doi: 10.1016/j.ijrobp.2013.06.2064

Lal, B., Xia, S., Abounader, R., & Laterra, J. (2005). Targeting the c-Met pathway potentiates glioblastoma responses to gamma-radiation. *Clin Cancer Res, 11*(12), 4479-4486. doi: 10.1158/1078-0432.CCR-05-0166

Langmead, B., Trapnell, C., Pop, M., & Salzberg, S. L. (2009). Ultrafast and memory-efficient alignment of short DNA sequences to the human genome. *Genome Biol, 10*(3). doi: Artn R25

Doi 10.1186/Gb-2009-10-3-R25

Lathia, J. D., Gallagher, J., Heddleston, J. M., Wang, J., Eyler, C. E., Macswords, J., . . . Rich, J. N. (2010). Integrin alpha 6 regulates glioblastoma stem cells. *Cell Stem Cell, 6*(5), 421-432. doi: 10.1016/j.stem.2010.02.018

Lathia, J. D., Li, M., Hall, P. E., Gallagher, J., Hale, J. S., Wu, Q., . . . Rich, J. N. (2012). Laminin alpha 2 enables glioblastoma stem cell growth. *Ann Neurol, 72*(5), 766-778. doi: 10.1002/ana.23674

Lawson, D. A., Xin, L., Lukacs, R. U., Cheng, D., & Witte, O. N. (2007). Isolation and functional characterization of murine prostate stem cells. *Proc Natl Acad Sci U S A, 104*(1), 181-186. doi: 10.1073/pnas.0609684104

Lee, D., Suh, Y. L., Park, T. I., Do, I. G., Seol, H. J., Nam, D. H., & Kim, S. T. (2013). Prognostic significance of tetraspanin CD151 in newly diagnosed glioblastomas. *J Surg Oncol, 107*(6), 646-652. doi: 10.1002/jso.23249

Lee da, Y., Gianino, S. M., & Gutmann, D. H. (2012). Innate neural stem cell heterogeneity determines the patterning of glioma formation in children. *Cancer Cell, 22*(1), 131-138. doi: 10.1016/j.ccr.2012.05.036

Lee, E. C., Lotz, M. M., Steele, G. D., Jr., & Mercurio, A. M. (1992). The integrin alpha 6 beta 4 is a laminin receptor. *J Cell Biol, 117*(3), 671-678.

Lee, H. J., Choi, B. H., Min, B. H., & Park, S. R. (2009). Changes in surface markers of human mesenchymal stem cells during the chondrogenic differentiation and dedifferentiation processes in vitro. *Arthritis Rheum, 60*(8), 2325-2332. doi: 10.1002/art.24786

Lee, S. H., Oh, S. Y., Do, S. I., Lee, H. J., Kang, H. J., Rho, Y. S., . . . Lim, Y. C. (2014). SOX2 regulates self-renewal and tumorigenicity of stem-like cells of head and neck squamous cell carcinoma. *Br J Cancer, 111*(11), 2122-2130. doi: 10.1038/bjc.2014.528

Leng, Z., Tao, K., Xia, Q., Tan, J., Yue, Z., Chen, J., . . . Zheng, H. (2013). Kruppel-like factor 4 acts as an oncogene in colon cancer stem cell-enriched spheroid cells. *PLoS One, 8*(2), e56082. doi: 10.1371/journal.pone.0056082

Lewis, C. E., & Pollard, J. W. (2006). Distinct role of macrophages in different tumor microenvironments. *Cancer Res, 66*(2), 605-612. doi: 10.1158/0008-5472.CAN-05-4005

Li, Q., Wijesekera, O., Salas, S. J., Wang, J. Y., Zhu, M., Aprhys, C., . . . Quinones-Hinojosa, A. (2014). Mesenchymal stem cells from human fat engineered to secrete BMP4 are nononcogenic, suppress brain cancer, and prolong survival. *Clin Cancer Res, 20*(9), 2375-2387. doi: 10.1158/1078-0432.CCR-13-1415

Li, Y., & Laterra, J. (2012). Cancer stem cells: distinct entities or dynamically regulated phenotypes? *Cancer Res, 72*(3), 576-580. doi: 10.1158/0008-5472.CAN-11-3070

Li, Y., Li, A., Glas, M., Lal, B., Ying, M., Sang, Y., . . . Laterra, J. (2011). c-Met signaling induces a reprogramming network and supports the glioblastoma stem-like phenotype. *Proc Natl Acad Sci U S A, 108*(24), 9951-9956. doi: 10.1073/pnas.1016912108

Li, Z., Bao, S., Wu, Q., Wang, H., Eyler, C., Sathornsumetee, S., . . . Rich, J. N. (2009). Hypoxia-inducible factors regulate tumorigenic capacity of glioma stem cells. *Cancer Cell, 15*(6), 501-513. doi: 10.1016/j.ccr.2009.03.018

Liekens, S., Schols, D., & Hatse, S. (2010). CXCL12-CXCR4 axis in angiogenesis, metastasis and stem cell mobilization. *Curr Pharm Des, 16*(35), 3903-3920.

Lin, H. T., Chiou, S. H., Kao, C. L., Shyr, Y. M., Hsu, C. J., Tarng, Y. W., . . . Ku, H. H. (2006). Characterization of pancreatic stem cells derived from adult human pancreas ducts by fluorescence activated cell sorting. *World J Gastroenterol, 12*(28), 4529-4535.

Lin, K. K., Rossi, L., Boles, N. C., Hall, B. E., George, T. C., & Goodell, M. A. (2011). CD81 is essential for the re-entry of hematopoietic stem cells to quiescence following stress-induced proliferation via deactivation of the Akt pathway. *PLoS Biol, 9*(9), e1001148. doi: 10.1371/journal.pbio.1001148

Lin, L., Liu, A., Peng, Z., Lin, H. J., Li, P. K., Li, C., & Lin, J. (2011). STAT3 is necessary for proliferation and survival in colon cancer-initiating cells. *Cancer Res, 71*(23), 7226-7237. doi: 10.1158/0008-5472.CAN-10-4660

Lindberg, N., Kastemar, M., Olofsson, T., Smits, A., & Uhrbom, L. (2009). Oligodendrocyte progenitor cells can act as cell of origin for experimental glioma. *Oncogene, 28*(23), 2266-2275. doi: 10.1038/onc.2009.76

Liu, A., Yu, X., & Liu, S. (2013). Pluripotency transcription factors and cancer stem cells: small genes make a big difference. *Chin J Cancer, 32*(9), 483-487. doi: 10.5732/cjc.012.10282

Liu, L., Lanner, F., Lendahl, U., & Das, D. (2011). Numblike and Numb differentially affect p53 and Sonic Hedgehog signaling. *Biochem Biophys Res Commun, 413*(3), 426-431. doi: 10.1016/j.bbrc.2011.08.108

Liu, W. F., Zuo, H. J., Chai, B. L., Peng, D., Fei, Y. J., Lin, J. Y., . . . Liu, Z. X. (2011). Role of tetraspanin CD151-alpha3/alpha6 integrin complex: Implication in angiogenesis CD151-integrin complex in angiogenesis. *Int J Biochem Cell Biol, 43*(4), 642-650. doi: 10.1016/j.biocel.2011.01.004

Liu, Z., Teng, L., Bailey, S. K., Frost, A. R., Bland, K. I., LoBuglio, A. F., . . . Lobo-Ruppert, S. M. (2009). Epithelial transformation by KLF4 requires Notch1 but not canonical Notch1 signaling. *Cancer Biol Ther, 8*(19), 1840-1851.

Ljubimova, J. Y., Fugita, M., Khazenzon, N. M., Das, A., Pikul, B. B., Newman, D., . . . Black, K. L. (2004). Association between laminin-8 and glial tumor grade, recurrence, and patient survival. *Cancer, 101*(3), 604-612. doi: 10.1002/cncr.20397

Lobo, N. A., Shimono, Y., Qian, D., & Clarke, M. F. (2007). The biology of cancer stem cells. *Annu Rev Cell Dev Biol, 23*, 675-699. doi: 10.1146/annurev.cellbio.22.010305.104154

Lopez-Bertoni, H., Lal, B., Li, A., Caplan, M., Guerrero-Cazares, H., Eberhart, C. G., . . . Li, Y. (2014). DNMT-dependent suppression of microRNA regulates the induction of GBM tumor-propagating phenotype by Oct4 and Sox2. *Oncogene*. doi: 10.1038/onc.2014.334

Lopez, J., Poitevin, A., Mendoza-Martinez, V., Perez-Plasencia, C., & Garcia-Carranca, A. (2012). Cancer-initiating cells derived from established cervical cell lines exhibit stem-

cell markers and increased radioresistance. *BMC Cancer, 12*, 48. doi: 10.1186/1471-2407-12-48

Lu, P., Weaver, V. M., & Werb, Z. (2012). The extracellular matrix: a dynamic niche in cancer progression. *J Cell Biol, 196*(4), 395-406. doi: 10.1083/jcb.201102147

Luo, M., Fan, H., Nagy, T., Wei, H., Wang, C., Liu, S., . . . Guan, J. L. (2009). Mammary epithelial-specific ablation of the focal adhesion kinase suppresses mammary tumorigenesis by affecting mammary cancer stem/progenitor cells. *Cancer Res, 69*(2), 466-474. doi: 10.1158/0008-5472.CAN-08-3078

Mabray, M. C., Barajas, R. F., Jr., & Cha, S. (2015). Modern brain tumor imaging. *Brain Tumor Res Treat, 3*(1), 8-23. doi: 10.14791/btrt.2015.3.1.8

Martin, T. A., & Jiang, W. G. (2014). Evaluation of the expression of stem cell markers in human breast cancer reveals a correlation with clinical progression and metastatic disease in ductal carcinoma. *Oncol Rep, 31*(1), 262-272. doi: 10.3892/or.2013.2813

McConnell, B. B., & Yang, V. W. (2010). Mammalian Kruppel-like factors in health and diseases. *Physiol Rev, 90*(4), 1337-1381. doi: 10.1152/physrev.00058.2009

McGirt, M. J., Than, K. D., Weingart, J. D., Chaichana, K. L., Attenello, F. J., Olivi, A., . . . Quinones-Hinojosa, A. (2009). Gliadel (BCNU) wafer plus concomitant temozolomide therapy after primary resection of glioblastoma multiforme. *J Neurosurg, 110*(3), 583-588. doi: 10.3171/2008.5.17557

Miller, I. J., & Bieker, J. J. (1993). A novel, erythroid cell-specific murine transcription factor that binds to the CACCC element and is related to the Kruppel family of nuclear proteins. *Mol Cell Biol, 13*(5), 2776-2786.

Miller, R. J., Banisadr, G., & Bhattacharyya, B. J. (2008). CXCR4 signaling in the regulation of stem cell migration and development. *J Neuroimmunol, 198*(1-2), 31-38. doi: 10.1016/j.jneuroim.2008.04.008

Mitchell, D. L., & DiMario, J. X. (2010). Bimodal, reciprocal regulation of fibroblast growth factor receptor 1 promoter activity by BTEB1/KLF9 during myogenesis. *Mol Biol Cell, 21*(15), 2780-2787. doi: 10.1091/mbc.E10-04-0290

Morita, M., Kobayashi, A., Yamashita, T., Shimanuki, T., Nakajima, O., Takahashi, S., . . . Fujii-Kuriyama, Y. (2003). Functional analysis of basic transcription element binding protein by gene targeting technology. *Mol Cell Biol, 23*(7), 2489-2500.

Morsczeck, C., Schmalz, G., Reichert, T. E., Vollner, F., Saugspier, M., Viale-Bouroncle, S., & Driemel, O. (2009). Gene expression profiles of dental follicle cells before and after osteogenic differentiation in vitro. *Clin Oral Investig, 13*(4), 383-391. doi: 10.1007/s00784-009-0260-x

Mulholland, D. J., Xin, L., Morim, A., Lawson, D., Witte, O., & Wu, H. (2009). Lin-Sca-1+CD49fhigh stem/progenitors are tumor-initiating cells in the Pten-null prostate cancer model. *Cancer Res, 69*(22), 8555-8562. doi: 10.1158/0008-5472.CAN-08-4673

Nagano, K., Taoka, M., Yamauchi, Y., Itagaki, C., Shinkawa, T., Nunomura, K., . . . Isobe, T. (2005). Large-scale identification of proteins expressed in mouse embryonic stem cells. *Proteomics, 5*(5), 1346-1361. doi: 10.1002/pmic.200400990

Nakada, M., Nambu, E., Furuyama, N., Yoshida, Y., Takino, T., Hayashi, Y., . . . Hamada, J. I. (2013). Integrin alpha3 is overexpressed in glioma stem-like cells and promotes invasion. *Br J Cancer, 108*(12), 2516-2524. doi: 10.1038/bjc.2013.218

Nakamura, K., Iinuma, H., Aoyagi, Y., Shibuya, H., & Watanabe, T. (2010). Predictive value of cancer stem-like cells and cancer-associated genetic markers for peritoneal recurrence of colorectal cancer in patients after curative surgery. *Oncology, 78*(5-6), 309-315. doi: 10.1159/000318862

Narla, G., Heath, K. E., Reeves, H. L., Li, D., Giono, L. E., Kimmelman, A. C., . . . Friedman, S. L. (2001). KLF6, a candidate tumor suppressor gene mutated in prostate cancer. *Science, 294*(5551), 2563-2566. doi: 10.1126/science.1066326

Nemer, M., & Horb, M. E. (2007). The KLF family of transcriptional regulators in cardiomyocyte proliferation and differentiation. *Cell Cycle, 6*(2), 117-121.

Nguyen, L. V., Vanner, R., Dirks, P., & Eaves, C. J. (2012). Cancer stem cells: an evolving concept. *Nat Rev Cancer, 12*(2), 133-143. doi: 10.1038/nrc3184

Nishioka, C., Ikezoe, T., Furihata, M., Yang, J., Serada, S., Naka, T., . . . Yokoyama, A. (2013). CD34(+)/CD38(-) acute myelogenous leukemia cells aberrantly express CD82 which regulates adhesion and survival of leukemia stem cells. *Int J Cancer, 132*(9), 2006-2019. doi: 10.1002/ijc.27904

Notta, F., Doulatov, S., Laurenti, E., Poeppl, A., Jurisica, I., & Dick, J. E. (2011). Isolation of single human hematopoietic stem cells capable of long-term multilineage engraftment. *Science, 333*(6039), 218-221. doi: 10.1126/science.1201219

Novitskaya, V., Romanska, H., Dawoud, M., Jones, J. L., & Berditchevski, F. (2010). Tetraspanin CD151 regulates growth of mammary epithelial cells in three-dimensional extracellular matrix: implication for mammary ductal carcinoma in situ. *Cancer Res, 70*(11), 4698-4708. doi: 10.1158/0008-5472.CAN-09-4330

O'Brien, C. A., Pollett, A., Gallinger, S., & Dick, J. E. (2007). A human colon cancer cell capable of initiating tumour growth in immunodeficient mice. *Nature, 445*(7123), 106-110. doi: 10.1038/nature05372

Ohe, N., Yamasaki, Y., Sogawa, K., Inazawa, J., Ariyama, T., Oshimura, M., & Fujii-Kuriyama, Y. (1993). Chromosomal localization and cDNA sequence of human BTEB, a GC box binding protein. *Somat Cell Mol Genet, 19*(5), 499-503.

Oka, M., Tagoku, K., Russell, T. L., Nakano, Y., Hamazaki, T., Meyer, E. M., . . . Terada, N. (2002). CD9 is associated with leukemia inhibitory factor-mediated maintenance of embryonic stem cells. *Molecular Biology of the Cell, 13*(4), 1274-1281. doi: 10.1091/mbc.02-01-0600

Pabona, J. M., Velarde, M. C., Zeng, Z., Simmen, F. A., & Simmen, R. C. (2009). Nuclear receptor co-regulator Kruppel-like factor 9 and prohibitin 2 expression in estrogen-induced epithelial cell proliferation in the mouse uterus. *J Endocrinol, 200*(1), 63-73. doi: 10.1677/JOE-08-0383

Page, D. C., Mosher, R., Simpson, E. M., Fisher, E. M., Mardon, G., Pollack, J., . . . Brown, L. G. (1987). The sex-determining region of the human Y chromosome encodes a finger protein. *Cell, 51*(6), 1091-1104.

Palmer, T. D., Martinez, C. H., Vasquez, C., Hebron, K. E., Jones-Paris, C., Arnold, S. A., . . . Zijlstra, A. (2014). Integrin-free tetraspanin CD151 can inhibit tumor cell motility upon clustering and is a clinical indicator of prostate cancer progression. *Cancer Res, 74*(1), 173-187. doi: 10.1158/0008-5472.CAN-13-0275

Park, K. R., Inoue, T., Ueda, M., Hirano, T., Higuchi, T., Konishi, I., . . . Fujii, S. (2000). Anti-CD9 monoclonal antibody-stimulated invasion of endometrial cancer cell lines in vitro: possible inhibitory effect of CD9 in endometrial cancer invasion. *Mol Hum Reprod, 6*(8), 719-725.

Patil, C. G., Nuno, M., Elramsisy, A., Mukherjee, D., Carico, C., Dantis, J., . . . Bannykh, S. I. (2013). High levels of phosphorylated MAP kinase are associated with poor survival among patients with glioblastoma during the temozolomide era. *Neuro Oncol, 15*(1), 104-111. doi: 10.1093/neuonc/nos272

Pearson, R., Fleetwood, J., Eaton, S., Crossley, M., & Bao, S. (2008). Kruppel-like transcription factors: a functional family. *Int J Biochem Cell Biol, 40*(10), 1996-2001. doi: 10.1016/j.biocel.2007.07.018

Peng, D., Zuo, H., Liu, Z., Qin, J., Zhou, Y., Li, P., . . . Zhang, X. A. (2013). The tetraspanin CD151-ARSA mutant inhibits angiogenesis via the YRSL sequence. *Mol Med Rep, 7*(3), 836-842. doi: 10.3892/mmr.2012.1250

Phillips, T. M., McBride, W. H., & Pajonk, F. (2006). The response of CD24(-/low)/CD44+ breast cancer-initiating cells to radiation. *J Natl Cancer Inst, 98*(24), 1777-1785. doi: 10.1093/jnci/djj495

Pierce, G. B., & Wallace, C. (1971). Differentiation of malignant to benign cells. *Cancer Res, 31*(2), 127-134.

Ping, Y. F., Yao, X. H., Jiang, J. Y., Zhao, L. T., Yu, S. C., Jiang, T., . . . Bian, X. W. (2011). The chemokine CXCL12 and its receptor CXCR4 promote glioma stem cell-mediated VEGF production and tumour angiogenesis via PI3K/AKT signalling. *J Pathol, 224*(3), 344-354. doi: 10.1002/path.2908

Pollard, S. M., Yoshikawa, K., Clarke, I. D., Danovi, D., Stricker, S., Russell, R., . . . Dirks, P. (2009). Glioma stem cell lines expanded in adherent culture have tumor-specific phenotypes and are suitable for chemical and genetic screens. *Cell Stem Cell, 4*(6), 568-580. doi: 10.1016/j.stem.2009.03.014

Price, R. L., Song, J., Bingmer, K., Kim, T. H., Yi, J. Y., Nowicki, M. O., . . . Kwon, C. H. (2013). Cytomegalovirus contributes to glioblastoma in the context of tumor suppressor mutations. *Cancer Res, 73*(11), 3441-3450. doi: 10.1158/0008-5472.CAN-12-3846

Prowse, A. B., Chong, F., Gray, P. P., & Munro, T. P. (2011). Stem cell integrins: implications for ex-vivo culture and cellular therapies. *Stem Cell Res, 6*(1), 1-12. doi: 10.1016/j.scr.2010.09.005

Qian, H., Tryggvason, K., Jacobsen, S. E., & Ekblom, M. (2006). Contribution of alpha6 integrins to hematopoietic stem and progenitor cell homing to bone marrow and collaboration with alpha4 integrins. *Blood, 107*(9), 3503-3510. doi: 10.1182/blood-2005-10-3932

Qiao, F., Yao, F., Chen, L., Lu, C., Ni, Y., Fang, W., & Jin, H. (2015). Kruppel-like factor 9 was down-regulated in esophageal squamous cell carcinoma and negatively regulated beta-catenin/TCF signaling. *Mol Carcinog*. doi: 10.1002/mc.22277

Rajasekhar, V. K., Studer, L., Gerald, W., Socci, N. D., & Scher, H. I. (2011). Tumour-initiating stem-like cells in human prostate cancer exhibit increased NF-kappaB signalling. *Nat Commun, 2*, 162. doi: 10.1038/ncomms1159

Rajasekhar, V. K., Viale, A., Socci, N. D., Wiedmann, M., Hu, X., & Holland, E. C. (2003). Oncogenic Ras and Akt signaling contribute to glioblastoma formation by differential recruitment of existing mRNAs to polysomes. *Mol Cell, 12*(4), 889-901.

Rao Malla, R., Gopinath, S., Alapati, K., Gorantla, B., Gondi, C. S., & Rao, J. S. (2013). Knockdown of cathepsin B and uPAR inhibits CD151 and alpha3beta1 integrin-mediated cell adhesion and invasion in glioma. *Mol Carcinog, 52*(10), 777-790. doi: 10.1002/mc.21915

Reynolds, B. A., & Weiss, S. (1992). Generation of neurons and astrocytes from isolated cells of the adult mammalian central nervous system. *Science, 255*(5052), 1707-1710.

Reya, T. Morrison S. J., Clarke, M. F., & Weissman, I.L. (2001). Stem cells, cancer and cancer stem cells. *Nature,* 414(6859), 105-11.

Robinson, M. D., McCarthy, D. J., & Smyth, G. K. (2010). edgeR: a Bioconductor package for differential expression analysis of digital gene expression data. *Bioinformatics, 26*(1), 139-140. doi: 10.1093/bioinformatics/btp616

Robinson, M. D., & Oshlack, A. (2010). A scaling normalization method for differential expression analysis of RNA-seq data. *Genome Biol, 11*(3). doi: Artn R25

Doi 10.1186/Gb-2010-11-3-R25

Romanska, H. M., Potemski, P., Collins, S. I., Williams, H., Parmar, S., & Berditchevski, F. (2013). Loss of CD151/Tspan24 from the complex with integrin alpha3beta1 in invasive front of the tumour is a negative predictor of disease-free survival in oral squamous cell carcinoma. *Oral Oncol, 49*(3), 224-229. doi: 10.1016/j.oraloncology.2012.09.013

Rowland, B. D., Bernards, R., & Peeper, D. S. (2005). The KLF4 tumour suppressor is a transcriptional repressor of p53 that acts as a context-dependent oncogene. *Nat Cell Biol, 7*(11), 1074-1082. doi: 10.1038/ncb1314

Samanna, V., Wei, H., Ego-Osuala, D., & Chellaiah, M. A. (2006). Alpha-V-dependent outside-in signaling is required for the regulation of CD44 surface expression, MMP-2 secretion, and cell migration by osteopontin in human melanoma cells. *Exp Cell Res, 312*(12), 2214-2230. doi: 10.1016/j.yexcr.2006.03.022

Santini, R., Pietrobono, S., Pandolfi, S., Montagnani, V., D'Amico, M., Penachioni, J. Y., . . . Stecca, B. (2014). SOX2 regulates self-renewal and tumorigenicity of human melanoma-initiating cells. *Oncogene, 33*(38), 4697-4708. doi: 10.1038/onc.2014.71

Sarvi, S., Mackinnon, A. C., Avlonitis, N., Bradley, M., Rintoul, R. C., Rassl, D. M., . . . Sethi, T. (2014). CD133+ cancer stem-like cells in small cell lung cancer are highly tumorigenic and chemoresistant but sensitive to a novel neuropeptide antagonist. *Cancer Res, 74*(5), 1554-1565. doi: 10.1158/0008-5472.CAN-13-1541

Savignac, M., Mellstrom, B., Bebin, A. G., Oliveros, J. C., Delpy, L., Pinaud, E., & Naranjo, J. R. (2010). Increased B cell proliferation and reduced Ig production in DREAM transgenic mice. *J Immunol, 185*(12), 7527-7536. doi: 10.4049/jimmunol.1000152

Schrader, J., Gordon-Walker, T. T., Aucott, R. L., van Deemter, M., Quaas, A., Walsh, S., . . . Iredale, J. P. (2011). Matrix stiffness modulates proliferation, chemotherapeutic response, and dormancy in hepatocellular carcinoma cells. *Hepatology, 53*(4), 1192-1205. doi: 10.1002/hep.24108

Scobie, K. N., Hall, B. J., Wilke, S. A., Klemenhagen, K. C., Fujii-Kuriyama, Y., Ghosh, A., . . . Sahay, A. (2009). Kruppel-like factor 9 is necessary for late-phase neuronal maturation in the developing dentate gyrus and during adult hippocampal neurogenesis. *J Neurosci, 29*(31), 9875-9887. doi: 10.1523/JNEUROSCI.2260-09.2009

Seguin, L., Desgrosellier, J. S., Weis, S. M., & Cheresh, D. A. (2015). Integrins and cancer: regulators of cancer stemness, metastasis, and drug resistance. *Trends Cell Biol, 25*(4), 234-240. doi: 10.1016/j.tcb.2014.12.006

Seidel, S., Garvalov, B. K., Wirta, V., von Stechow, L., Schanzer, A., Meletis, K., . . . Acker, T. (2010). A hypoxic niche regulates glioblastoma stem cells through hypoxia inducible factor 2 alpha. *Brain, 133*(Pt 4), 983-995. doi: 10.1093/brain/awq042

Serru, V., Le Naour, F., Billard, M., Azorsa, D. O., Lanza, F., Boucheix, C., & Rubinstein, E. (1999). Selective tetraspan-integrin complexes (CD81/alpha4beta1, CD151/alpha3beta1, CD151/alpha6beta1) under conditions disrupting tetraspan interactions. *Biochem J, 340 (Pt 1)*, 103-111.

Sever, R., & Brugge, J. S. (2015). Signal Transduction in Cancer. *Cold Spring Harb Perspect Med, 5*(4). doi: 10.1101/cshperspect.a006098

Shen, P., Sun, J., Xu, G., Zhang, L., Yang, Z., Xia, S., . . . Shi, G. (2014). KLF9, a transcription factor induced in flutamide-caused cell apoptosis, inhibits AKT activation and suppresses tumor growth of prostate cancer cells. *Prostate, 74*(9), 946-958. doi: 10.1002/pros.22812

Shen, Q., Wang, Y., Kokovay, E., Lin, G., Chuang, S. M., Goderie, S. K., . . . Temple, S. (2008). Adult SVZ stem cells lie in a vascular niche: a quantitative analysis of niche cell-cell interactions. *Cell Stem Cell, 3*(3), 289-300. doi: 10.1016/j.stem.2008.07.026

Shinohara, T., Avarbock, M. R., & Brinster, R. L. (1999). beta1- and alpha6-integrin are surface markers on mouse spermatogonial stem cells. *Proc Natl Acad Sci U S A, 96*(10), 5504-5509.

Simmen, F. A., Xiao, R., Velarde, M. C., Nicholson, R. D., Bowman, M. T., Fujii-Kuriyama, Y., . . . Simmen, R. C. (2007). Dysregulation of intestinal crypt cell proliferation and villus cell migration in mice lacking Kruppel-like factor 9. *Am J Physiol Gastrointest Liver Physiol, 292*(6), G1757-1769. doi: 10.1152/ajpgi.00013.2007

Sims-Mourtada, J., Izzo, J. G., Apisarnthanarax, S., Wu, T. T., Malhotra, U., Luthra, R., . . . Chao, K. S. (2006). Hedgehog: an attribute to tumor regrowth after chemoradiotherapy and a target to improve radiation response. *Clin Cancer Res, 12*(21), 6565-6572. doi: 10.1158/1078-0432.CCR-06-0176

Sincock, P. M., Fitter, S., Parton, R. G., Berndt, M. C., Gamble, J. R., & Ashman, L. K. (1999a). PETA-3/CD151, a member of the transmembrane 4 superfamily, is localised to the plasma membrane and endocytic system of endothelial cells, associates with multiple integrins and modulates cell function. *J Cell Sci, 112*(6), 833-844.

Sincock, P. M., Fitter, S., Parton, R. G., Berndt, M. C., Gamble, J. R., & Ashman, L. K. (1999b). PETA-3/CD151, a member of the transmembrane 4 superfamily, is localised to the plasma membrane and endocytic system of endothelial cells, associates with multiple integrins and modulates cell function. *J Cell Sci, 112 (Pt 6)*, 833-844.

Sincock, P. M., Mayrhofer, G., & Ashman, L. K. (1997). Localization of the transmembrane 4 superfamily (TM4SF) member PETA-3 (CD151) in normal human tissues: comparison with CD9, CD63, and alpha5beta1 integrin. *J Histochem Cytochem, 45*(4), 515-525.

Singh, S. K., Hawkins, C., Clarke, I. D., Squire, J. A., Bayani, J., Hide, T., . . . Dirks, P. B. (2004). Identification of human brain tumour initiating cells. *Nature, 432*(7015), 396-401. doi: 10.1038/nature03128

Smith, A. L., Robin, T. P., & Ford, H. L. (2012). Molecular pathways: targeting the TGF-beta pathway for cancer therapy. *Clin Cancer Res, 18*(17), 4514-4521. doi: 10.1158/1078-0432.CCR-11-3224

Soda, Y., Myskiw, C., Rommel, A., & Verma, I. M. (2013). Mechanisms of neovascularization and resistance to anti-angiogenic therapies in glioblastoma multiforme. *J Mol Med (Berl), 91*(4), 439-448. doi: 10.1007/s00109-013-1019-z

Solinas, G., Schiarea, S., Liguori, M., Fabbri, M., Pesce, S., Zammataro, L., . . . Allavena, P. (2010). Tumor-conditioned macrophages secrete migration-stimulating factor: a new marker for M2-polarization, influencing tumor cell motility. *J Immunol, 185*(1), 642-652. doi: 10.4049/jimmunol.1000413

Sporl, F., Korge, S., Jurchott, K., Wunderskirchner, M., Schellenberg, K., Heins, S., . . . Kramer, A. (2012). Kruppel-like factor 9 is a circadian transcription factor in human epidermis that controls proliferation of keratinocytes. *Proc Natl Acad Sci U S A, 109*(27), 10903-10908. doi: 10.1073/pnas.1118641109

Springer, T. A., & Dustin, M. L. (2012). Integrin inside-out signaling and the immunological synapse. *Curr Opin Cell Biol, 24*(1), 107-115. doi: 10.1016/j.ceb.2011.10.004

Staquicini, F. I., Dias-Neto, E., Li, J., Snyder, E. Y., Sidman, R. L., Pasqualini, R., & Arap, W. (2009). Discovery of a functional protein complex of netrin-4, laminin gamma1 chain, and integrin alpha6beta1 in mouse neural stem cells. *Proc Natl Acad Sci U S A, 106*(8), 2903-2908. doi: 10.1073/pnas.0813286106

Sterk, L. M., Geuijen, C. A., Oomen, L. C., Calafat, J., Janssen, H., & Sonnenberg, A. (2000). The tetraspan molecule CD151, a novel constituent of hemidesmosomes, associates with

the integrin alpha6beta4 and may regulate the spatial organization of hemidesmosomes. *J Cell Biol, 149*(4), 969-982.

Sterk, L. M., Geuijen, C. A., van den Berg, J. G., Claessen, N., Weening, J. J., & Sonnenberg, A. (2002). Association of the tetraspanin CD151 with the laminin-binding integrins alpha3beta1, alpha6beta1, alpha6beta4 and alpha7beta1 in cells in culture and in vivo. *J Cell Sci, 115*(Pt 6), 1161-1173.

Suman, S., Das, T. P., & Damodaran, C. (2013). Silencing NOTCH signaling causes growth arrest in both breast cancer stem cells and breast cancer cells. *Br J Cancer, 109*(10), 2587-2596. doi: 10.1038/bjc.2013.642

Sun, J., Wang, B., Liu, Y., Zhang, L., Ma, A., Yang, Z., . . . Liu, Y. (2014). Transcription factor KLF9 suppresses the growth of hepatocellular carcinoma cells in vivo and positively regulates p53 expression. *Cancer Lett, 355*(1), 25-33. doi: 10.1016/j.canlet.2014.09.022

Sundar, S. J., Hsieh, J. K., Manjila, S., Lathia, J. D., & Sloan, A. (2014). The role of cancer stem cells in glioblastoma. *Neurosurg Focus, 37*(6), E6. doi: 10.3171/2014.9.FOCUS14494

Suske, G., Bruford, E., & Philipsen, S. (2005). Mammalian SP/KLF transcription factors: bring in the family. *Genomics, 85*(5), 551-556. doi: 10.1016/j.ygeno.2005.01.005

Swamynathan, S. K., Katz, J. P., Kaestner, K. H., Ashery-Padan, R., Crawford, M. A., & Piatigorsky, J. (2007). Conditional deletion of the mouse Klf4 gene results in corneal epithelial fragility, stromal edema, and loss of conjunctival goblet cells. *Mol Cell Biol, 27*(1), 182-194. doi: 10.1128/MCB.00846-06

Takada, Y., Ye, X., & Simon, S. (2007). The integrins. *Genome Biol, 8*(5), 215. doi: 10.1186/gb-2007-8-5-215

Takahashi, K., & Yamanaka, S. (2006). Induction of pluripotent stem cells from mouse embryonic and adult fibroblast cultures by defined factors. *Cell, 126*(4), 663-676. doi: 10.1016/j.cell.2006.07.024

Takeda, T., Hattori, N., Tokuhara, T., Nishimura, Y., Yokoyama, M., & Miyake, M. (2007). Adenoviral transduction of MRP-1/CD9 and KAI1/CD82 inhibits lymph node metastasis in orthotopic lung cancer model. *Cancer Res, 67*(4), 1744-1749. doi: 10.1158/0008-5472.CAN-06-3090

Takeda, Y., Kazarov, A. R., Butterfield, C. E., Hopkins, B. D., Benjamin, L. E., Kaipainen, A., & Hemler, M. E. (2007). Deletion of tetraspanin Cd151 results in decreased pathologic angiogenesis in vivo and in vitro. *Blood, 109*(4), 1524-1532. doi: 10.1182/blood-2006-08-041970

Tamkun, J. W., DeSimone, D. W., Fonda, D., Patel, R. S., Buck, C., Horwitz, A. F., & Hynes, R. O. (1986). Structure of integrin, a glycoprotein involved in the transmembrane linkage between fibronectin and actin. *Cell, 46*(2), 271-282.

Taverna, D., Moher, H., Crowley, D., Borsig, L., Varki, A., & Hynes, R. O. (2004). Increased primary tumor growth in mice null for beta3- or beta3/beta5-integrins or selectins. *Proc Natl Acad Sci U S A, 101*(3), 763-768. doi: 10.1073/pnas.0307289101

Terpe, H. J., Stark, H., Ruiz, P., & Imhof, B. A. (1994). Alpha 6 integrin distribution in human embryonic and adult tissues. *Histochemistry, 101*(1), 41-49.

Tetreault, M. P., Yang, Y., & Katz, J. P. (2013). Kruppel-like factors in cancer. *Nat Rev Cancer, 13*(10), 701-713. doi: 10.1038/nrc3582

Thomas, S., & Bonchev, D. (2010). A survey of current software for network analysis in molecular biology. *Hum Genomics, 4*(5), 353-360.

Till, J. E., & Mc, C. E. (1961). A direct measurement of the radiation sensitivity of normal mouse bone marrow cells. *Radiat Res, 14*, 213-222.

To, K., Fotovati, A., Reipas, K. M., Law, J. H., Hu, K., Wang, J., . . . Dunn, S. E. (2010). Y-box binding protein-1 induces the expression of CD44 and CD49f leading to enhanced self-

renewal, mammosphere growth, and drug resistance. *Cancer Res, 70*(7), 2840-2851. doi: 10.1158/0008-5472.CAN-09-3155

Tong, X. D., Liu, T. Q., Wang, G. B., Zhang, C. L., & Liu, H. X. (2015). MicroRNA-570 promotes lung carcinoma proliferation through targeting tumor suppressor KLF9. *Int J Clin Exp Pathol, 8*(3), 2829-2834.

Torres, J., & Watt, F. M. (2008). Nanog maintains pluripotency of mouse embryonic stem cells by inhibiting NFkappaB and cooperating with Stat3. *Nat Cell Biol, 10*(2), 194-201. doi: 10.1038/ncb1680

Trapnell, C., Pachter, L., & Salzberg, S. L. (2009). TopHat: discovering splice junctions with RNA-Seq. *Bioinformatics, 25*(9), 1105-1111. doi: 10.1093/bioinformatics/btp120

Uchida, D., Onoue, T., Begum, N. M., Kuribayashi, N., Tomizuka, Y., Tamatani, T., . . . Miyamoto, Y. (2009). Vesnarinone downregulates CXCR4 expression via upregulation of Kruppel-like factor 2 in oral cancer cells. *Mol Cancer, 8*, 62. doi: 10.1186/1476-4598-8-62

Uchida, S., Shimada, Y., Watanabe, G., Li, Z. G., Hong, T., Miyake, M., & Imamura, M. (1999). Motility-related protein (MRP-1/CD9) and KAI1/CD82 expression inversely correlate with lymph node metastasis in oesophageal squamous cell carcinoma. *Br J Cancer, 79*(7-8), 1168-1173. doi: 10.1038/sj.bjc.6690186

Uhrbom, L., Dai, C., Celestino, J. C., Rosenblum, M. K., Fuller, G. N., & Holland, E. C. (2002). Ink4a-Arf loss cooperates with KRas activation in astrocytes and neural progenitors to generate glioblastomas of various morphologies depending on activated Akt. *Cancer Res, 62*(19), 5551-5558.

Urbanska, K., Sokolowska, J., Szmidt, M., & Sysa, P. (2014). Glioblastoma multiforme - an overview. *Contemp Oncol (Pozn), 18*(5), 307-312. doi: 10.5114/wo.2014.40559

Velarde, M. C., Zeng, Z., McQuown, J. R., Simmen, F. A., & Simmen, R. C. (2007). Kruppel-like factor 9 is a negative regulator of ligand-dependent estrogen receptor alpha signaling in Ishikawa endometrial adenocarcinoma cells. *Mol Endocrinol, 21*(12), 2988-3001. doi: 10.1210/me.2007-0242

Verhaak, R. G., Hoadley, K. A., Purdom, E., Wang, V., Qi, Y., Wilkerson, M. D., . . . Cancer Genome Atlas Research, N. (2010). Integrated genomic analysis identifies clinically relevant subtypes of glioblastoma characterized by abnormalities in PDGFRA, IDH1, EGFR, and NF1. *Cancer Cell, 17*(1), 98-110. doi: 10.1016/j.ccr.2009.12.020

Visvader, J. E., & Lindeman, G. J. (2008). Cancer stem cells in solid tumours: accumulating evidence and unresolved questions. *Nat Rev Cancer, 8*(10), 755-768. doi: 10.1038/nrc2499

Voss, M. A., Gordon, N., Maloney, S., Ganesan, R., Ludeman, L., McCarthy, K., . . . Sundar, S. (2011). Tetraspanin CD151 is a novel prognostic marker in poor outcome endometrial cancer. *Br J Cancer, 104*(10), 1611-1618. doi: 10.1038/bjc.2011.80

Wang, J., Rao, S., Chu, J., Shen, X., Levasseur, D. N., Theunissen, T. W., & Orkin, S. H. (2006). A protein interaction network for pluripotency of embryonic stem cells. *Nature, 444*(7117), 364-368. doi: 10.1038/nature05284

Wang, K., Pan, L., Che, X., Cui, D., & Li, C. (2010). Sonic Hedgehog/GLI(1) signaling pathway inhibition restricts cell migration and invasion in human gliomas. *Neurol Res, 32*(9), 975-980. doi: 10.1179/016164110X12681290831360

Wang, X., & Zhao, J. (2007). KLF8 transcription factor participates in oncogenic transformation. *Oncogene, 26*(3), 456-461. doi: 10.1038/sj.onc.1209796

Wang, Y., Yang, J., Zheng, H., Tomasek, G. J., Zhang, P., McKeever, P. E., . . . Zhu, Y. (2009). Expression of mutant p53 proteins implicates a lineage relationship between neural stem

cells and malignant astrocytic glioma in a murine model. *Cancer Cell, 15*(6), 514-526. doi: 10.1016/j.ccr.2009.04.001

Warrier, S., Pavanram, P., Raina, D., & Arvind, M. (2012). Study of chemoresistant CD133+ cancer stem cells from human glioblastoma cell line U138MG using multiple assays. *Cell Biol Int, 36*(12), 1137-1143. doi: 10.1042/CBI20110539

Weng, A. P., Ferrando, A. A., Lee, W., Morris, J. P. t., Silverman, L. B., Sanchez-Irizarry, C., . . . Aster, J. C. (2004). Activating mutations of NOTCH1 in human T cell acute lymphoblastic leukemia. *Science, 306*(5694), 269-271. doi: 10.1126/science.1102160

Wernig, M., Meissner, A., Foreman, R., Brambrink, T., Ku, M., Hochedlinger, K., . . . Jaenisch, R. (2007). In vitro reprogramming of fibroblasts into a pluripotent ES-cell-like state. *Nature, 448*(7151), 318-324. doi: 10.1038/nature05944

Winterwood, N. E., Varzavand, A., Meland, M. N., Ashman, L. K., & Stipp, C. S. (2006). A critical role for tetraspanin CD151 in alpha3beta1 and alpha6beta4 integrin-dependent tumor cell functions on laminin-5. *Mol Biol Cell, 17*(6), 2707-2721. doi: 10.1091/mbc.E05-11-1042

Wong, G. S., & Rustgi, A. K. (2013). Matricellular proteins: priming the tumour microenvironment for cancer development and metastasis. *Br J Cancer, 108*(4), 755-761. doi: 10.1038/bjc.2012.592

Wright, M. D., Geary, S. M., Fitter, S., Moseley, G. W., Lau, L. M., Sheng, K. C., . . . Ashman, L. K. (2004). Characterization of mice lacking the tetraspanin superfamily member CD151. *Mol Cell Biol, 24*(13), 5978-5988. doi: 10.1128/MCB.24.13.5978-5988.2004

Xia, J., & Wishart, D. S. (2010). MetPA: a web-based metabolomics tool for pathway analysis and visualization. *Bioinformatics, 26*(18), 2342-2344. doi: 10.1093/bioinformatics/btq418

Xu, C., Wu, X., & Zhu, J. (2013). VEGF promotes proliferation of human glioblastoma multiforme stem-like cells through VEGF receptor 2. *ScientificWorldJournal, 2013*, 417413. doi: 10.1155/2013/417413

Yamamoto, H., Masters, J. R., Dasgupta, P., Chandra, A., Popert, R., Freeman, A., & Ahmed, A. (2012). CD49f is an efficient marker of monolayer- and spheroid colony-forming cells of the benign and malignant human prostate. *PLoS One, 7*(10), e46979. doi: 10.1371/journal.pone.0046979

Yanagida, A., Sogawa, K., Yasumoto, K. I., & Fujii-Kuriyama, Y. (1990). A novel cis-acting DNA element required for a high level of inducible expression of the rat P-450c gene. *Mol Cell Biol, 10*(4), 1470-1475.

Yang, W., Li, P., Lin, J., Zuo, H., Zuo, P., Zou, Y., & Liu, Z. (2012). CD151 promotes proliferation and migration of PC3 cells via the formation of CD151-integrin alpha3/alpha6 complex. *J Huazhong Univ Sci Technolog Med Sci, 32*(3), 383-388. doi: 10.1007/s11596-012-0066-y

Yang, X., Claas, C., Kraeft, S. K., Chen, L. B., Wang, Z., Kreidberg, J. A., & Hemler, M. E. (2002). Palmitoylation of tetraspanin proteins: modulation of CD151 lateral interactions, subcellular distribution, and integrin-dependent cell morphology. *Molecular Biology of the Cell, 13*(3), 767-781. doi: 10.1091/mbc.01-05-0275

Yang, X. H., Richardson, A. L., Torres-Arzayus, M. I., Zhou, P., Sharma, C., Kazarov, A. R., . . . Hemler, M. E. (2008). CD151 accelerates breast cancer by regulating alpha 6 integrin function, signaling, and molecular organization. *Cancer Res, 68*(9), 3204-3213. doi: 10.1158/0008-5472.CAN-07-2949

Yang, Y. M., Zhang, Z. W., Liu, Q. M., Sun, Y. F., Yu, J. R., & Xu, W. X. (2013). Overexpression of CD151 predicts prognosis in patients with resected gastric cancer. *PLoS One, 8*(3), e58990. doi: 10.1371/journal.pone.0058990

Yauch, R. L., Kazarov, A. R., Desai, B., Lee, R. T., & Hemler, M. E. (2000). Direct extracellular contact between integrin alpha(3)beta(1) and TM4SF protein CD151. *J Biol Chem, 275*(13), 9230-9238.

Ye, J., Wu, D., Shen, J., Wu, P., Ni, C., Chen, J., . . . Huang, J. (2012). Enrichment of colorectal cancer stem cells through epithelial-mesenchymal transition via CDH1 knockdown. *Mol Med Rep, 6*(3), 507-512. doi: 10.3892/mmr.2012.938

Yin, Y., Deng, X., Liu, Z., Baldwin, L. A., Lefringhouse, J., Zhang, J., . . . Yang, X. H. (2014). CD151 represses mammary gland development by maintaining the niches of progenitor cells. *Cell Cycle, 13*(17), 2707-2722. doi: 10.4161/15384101.2015.945823

Ying, M., Sang, Y., Li, Y., Guerrero-Cazares, H., Quinones-Hinojosa, A., Vescovi, A. L., . . . Laterra, J. (2011). Kruppel-like family of transcription factor 9, a differentiation-associated transcription factor, suppresses Notch1 signaling and inhibits glioblastoma-initiating stem cells. *Stem Cells, 29*(1), 20-31. doi: 10.1002/stem.561

Yu, F., Li, J., Chen, H., Fu, J., Ray, S., Huang, S., . . . Ai, W. (2011). Kruppel-like factor 4 (KLF4) is required for maintenance of breast cancer stem cells and for cell migration and invasion. *Oncogene, 30*(18), 2161-2172. doi: 10.1038/onc.2010.591

Yu, K. R., Yang, S. R., Jung, J. W., Kim, H., Ko, K., Han, D. W., . . . Kang, K. S. (2012). CD49f enhances multipotency and maintains stemness through the direct regulation of OCT4 and SOX2. *Stem Cells, 30*(5), 876-887. doi: 10.1002/stem.1052

Zawlik, I., Kita, D., Vaccarella, S., Mittelbronn, M., Franceschi, S., & Ohgaki, H. (2009). Common polymorphisms in the MDM2 and TP53 genes and the relationship between TP53 mutations and patient outcomes in glioblastomas. *Brain Pathol, 19*(2), 188-194. doi: 10.1111/j.1750-3639.2008.00170.x

Zawlik, I., Vaccarella, S., Kita, D., Mittelbronn, M., Franceschi, S., & Ohgaki, H. (2009). Promoter methylation and polymorphisms of the MGMT gene in glioblastomas: a population-based study. *Neuroepidemiology, 32*(1), 21-29. doi: 10.1159/000170088

Zhang, D., Zhang, X. L., Michel, F. J., Blum, J. L., Simmen, F. A., & Simmen, R. C. (2002). Direct interaction of the Kruppel-like family (KLF) member, BTEB1, and PR mediates progesterone-responsive gene expression in endometrial epithelial cells. *Endocrinology, 143*(1), 62-73. doi: 10.1210/endo.143.1.8590

Zhang, J., Espinoza, L. A., Kinders, R. J., Lawrence, S. M., Pfister, T. D., Zhou, M., . . . Jessup, J. M. (2013). NANOG modulates stemness in human colorectal cancer. *Oncogene, 32*(37), 4397-4405. doi: 10.1038/onc.2012.461

Zhang, L., Jiao, M., Li, L., Wu, D., Wu, K., Li, X., . . . He, D. (2012). Tumorspheres derived from prostate cancer cells possess chemoresistant and cancer stem cell properties. *J Cancer Res Clin Oncol, 138*(4), 675-686. doi: 10.1007/s00432-011-1146-2

Zhang, Q. H., Dou, H. T., Tang, Y. J., Su, S., & Liu, P. S. (2015). Lentivirus-mediated knockdown of Kruppel-like factor 9 inhibits the growth of ovarian cancer. *Arch Gynecol Obstet, 291*(2), 377-382. doi: 10.1007/s00404-014-3405-3

Zhang, X. L., Simmen, F. A., Michel, F. J., & Simmen, R. C. (2001). Increased expression of the Zn-finger transcription factor BTEB1 in human endometrial cells is correlated with distinct cell phenotype, gene expression patterns, and proliferative responsiveness to serum and TGF-beta1. *Mol Cell Endocrinol, 181*(1-2), 81-96.

Zheng, Z. Z., & Liu, Z. X. (2007a). Activation of the phosphatidylinositol 3-kinase/protein kinase Akt pathway mediates CD151-induced endothelial cell proliferation and cell migration. *Int J Biochem Cell Biol, 39*(2), 340-348. doi: 10.1016/j.biocel.2006.09.001

Zheng, Z. Z., & Liu, Z. X. (2007b). CD151 gene delivery increases eNOS activity and induces ECV304 migration, proliferation and tube formation. *Acta Pharmacol Sin, 28*(1), 66-72. doi: 10.1111/j.1745-7254.2007.00490.x

Zoller, M. (2009). Tetraspanins: push and pull in suppressing and promoting metastasis. *Nat Rev Cancer, 9*(1), 40-55. doi: 10.1038/nrc2543

Zucker, S. N., Fink, E. E., Bagati, A., Mannava, S., Bianchi-Smiraglia, A., Bogner, P. N., . . . Nikiforov, M. A. (2014). Nrf2 amplifies oxidative stress via induction of Klf9. *Mol Cell, 53*(6), 916-928. doi: 10.1016/j.molcel.2014.01.033

Zuo, H. J., Lin, J. Y., Liu, Z. Y., Liu, W. F., Liu, T., Yang, J., . . . Liu, Z. X. (2010). Activation of the ERK signaling pathway is involved in CD151-induced angiogenic effects on the formation of CD151-integrin complexes. *Acta Pharmacol Sin, 31*(7), 805-812. doi: 10.1038/aps.2010.65

CURRICULUM VITAE FOR PhD. CANDIDATES
The Johns Hopkins University School of Medicine

Jessica Tilghman October 8, 2015

Educational History:

PhD expected 2015 Program in Neuroscience Johns Hopkins School of Medicine
Mentor: John Laterra, MD-PhD

B.S. 2009 Natural Sciences University of Wisconsin-Madison

Other Professional Experience

Technology Transfer Analyst Internship 2013-205 Johns Hopkins Technology Ventures

Fellowships

National Science Foundation Graduate Research Fellowship 2013-2015
Ford Foundation Predoctoral Fellowship 2013-2015

Publications

Tilghman J, Wu H, Sang Y, Shi X, Guerrero-Cazares H, Quinones-Hinojosa A, Eberhart CG, Laterra J, Ying M. (2014) HMMR maintains the stemness and tumorigenicity of glioblastoma stem-like cells. Cancer Res.

Ying M, **Tilghman J**, Wei Y, Guerrero-Cazares H, Quinones-Hinojosa A, Ji, Laterra J. (2014) Kruppel-like factor-9 (KLF9) inhibits glioblastoma stemness through global transcription repression and integrin α6 inhibition. J Biol Chem. 289(47):32742-56.

Sagal J, Zhan X, Xu J, **Tilghman J**, Karuppagounder SS, Chen L, Dawson VL, Dawson TM, Laterra J, Ying M. (2014) Proneural transcription factor Atoh1 drives highly efficient differentiation of human pluripotent stem cells into dopaminergic neurons. Stem Cells Transl Med. 3(8):888-98

Rajpal S, Ahmed M, Sweeney C, Gerovac TA, Allcock B, McChesney S, Patel A, **Tilghman J**, Miranpuri GS, Resnick D. (2010) Cannabinoid subtype-2 receptors modulate the antihyperalgesic effect of WIN 55,212-2 in rats with neuropathic SCI pain. The Spine Journal. 10;(12).

Cramer S, Baggott C, Cain J, **Tilghman J**, Allcock B, Miranpuri G, Rajpal S, Sun D, Resnick D. (2008) The role of cation-dependent chloride transporters in neuropathic pain following spinal cord injury. Molecular Pain. 17;4(36).

Cain J, Baggott C, **Tilghman J**, Rajpal S, Miranpuri G, Resnick D. (2007) Recent Advances in The Study of Spinal Cord Injury and Neuropathic Pain. Annals of Neuroscience. 14:96-107

Rajpal S, Gerovac T, Turner N, **Tilghman J**, Allcock B, McChesney S, Miranpuri G, Park S, Resnick D. (2007) Antihyperalgesic effects of vanilloid-1 and bradykinin-1 receptor antagonists following spinal cord injury in rats. J Neurosurgery:Spine. 6(5):420-4.

Undergraduate Journals

Tilghman J, Cain J, Baggott C, Allcock B, Miranpuri G, Resnick D. (2007) The Effect of Cyclooxygenase 2 Inhibitor Meloxicam on Neuropathic Pain following Spinal Cord Injury. Integrated Biological Sciences-Summer Research Program Journal. 16:111-114

Tilghman J, Miranpuri G, Resnick D. (2006) The Effect of Rolipram and Macrophage Activated Medium on Functional Recovery following Spinal Cord Injury. Integrated Biological Sciences-Summer Research Program Journal.15:101-104

Posters, Abstracts and Presentations

Tilghman J (2013) Regulation of Neural and Neoplastic Stem Cells by Kruppel-like Transcription Factors. 6th Annual Maryland Stem Cell Research Symposium, Johns Hopkins Medical Campus, Baltimore, MD

Tilghman J (2010) The Functional Role of Human Cytomegalovirus protease coiled-coil Domain. Johns Hopkins School of Medicine Graduate Student Association Symposium, Baltimore, MD

Tilghman J (2009) The Effect of MMP Inhibitors on Neuropathic Pain following Spinal Cord Contusion. University of Wisconsin-Madison College of Agriculture and Life Sciences Undergraduate Research Symposium, Madison, WI

Tilghman J (2008) The Effects of TRPV1 Antagonist on Chronic Neuropathic Pain. The 17th Annual National McNair Research Conference, Delavan, WI

Tilghman J (2007) The Effect of Meloxicam on Chronic Neuropathic Pain following Spinal Cord Injury. Integrated Biological Sciences Summer Research Program Symposium, Madison, WI

Tilghman J (2007) The Effect of Rolipram and Macrophage Activated Medium on Functional Recovery following Spinal Cord Injury. University of Wisconsin-Madison Annual Undergraduate Research Symposium, Madison, WI

Tilghman J (2006) The Effects of TRPV1 and B1 Receptor Antagonists on Neuropathic Pain following Spinal Cord Injury: A Rat Model. Integrated Biological Sciences-Summer Research Program Symposium

Tilghman J (2006) The Effects of TRPV1 Antagonist on Chronic Neuropathic Pain following Spinal Cord Injury. University of Wisconsin-Madison Annual Undergraduate Research Symposium, Madison, WI

Tilghman J (2005) New Tools for Studying Neurogenesis. National Institutes of Health Summer Research Poster Day, Bethesda, MD

Service and leadership

2012-2013 **Steering Committee Member**
Alternative Careers in Science Course

- Participated in working group meetings with steering committee to develop course curriculum and discussion topics
- Facilitated panel discussion on diverse careers for graduates
- Contacted and recruited speakers for career panel

2012-2013 **High School Student Teacher Liaison**
Underserved High School Student Mentoring Program
Served as liaison between high school teachers and mentoring program for underserved high school students to collect information on the academic progress of 12 participating students and provide recommendations on educational and behavioral issues on which student mentors should focus on

2011-2012 **High School Student College Visit Coordinator**
College and Career Planning Committee,
Underserved High School Student Mentoring Program

- Conduct surveys of college plans for over 20 high school students, ana lyzed
  findings, and made recommendations on college visit destinations that support the program's mission of 100% college enrollment for program participants
- Coordinated chaperoned college visits to multiple colleges each semest er

2011-2012 **Event Planner**
Neuroscience Department Student Event Planning Committee
Co-organized monthly social events for neuroscience department